

COMMISSIONING OF THE BEAM INSTRUMENTATION SYSTEM OF CSNS

J.L. Sun[#], W.L. Huang, F. Li, P. Li, M. Meng, R.Y. Qiu, J.M. Tian, Z.H. Xu, T. Yang, L. Zeng, T.G. Xu, Institute of High Energy Physics, Chinese Academy of Sciences, China

Abstract

China Spallation Neutron Source (CSNS) accelerator complex consists of a front end, an 80MeV DTL LINAC, and a 1.6GeV Rapid Cycling Synchrotron (RCS). It is designed with a beam power of 100kW in the first phase and reserves upgrade capability to 500kW in the second phase. CSNS has started user operation at 20kW after the initial beam commissioning in 2018, the beam power is quickly up to 50kW and 80kW by two times beam commissioning in between the user beam time 2019, and finally reached 100kW, the design goal, in February 2020. The experiences and most recent status of beam instrumentation system of CSNS during the beam power ramping is introduced.

INTRODUCTION

The CSNS is designed to accelerate proton beam pulses to 1.6 GeV kinetic energy at 25 Hz repetition rate, striking a solid metal target to produce spallation neutrons. The accelerator provides a beam power of 100 kW on the target in the first phase. It will be upgraded to 500kW beam power at the same repetition rate and same output energy in the second phase. A schematic layout of CSNS phase-1 complex is shown in Figure 1. In the phase one, an ion source produces a peak current of 25 mA H- beam. RFQ linac bunches and accelerates it to 3 MeV. DTL linac raises the beam energy to 80 MeV. After H- beam is converted to proton beam via a stripping foil, RCS accumulates and accelerates the proton beam to 1.6 GeV before extracting it to the target [1, 2].

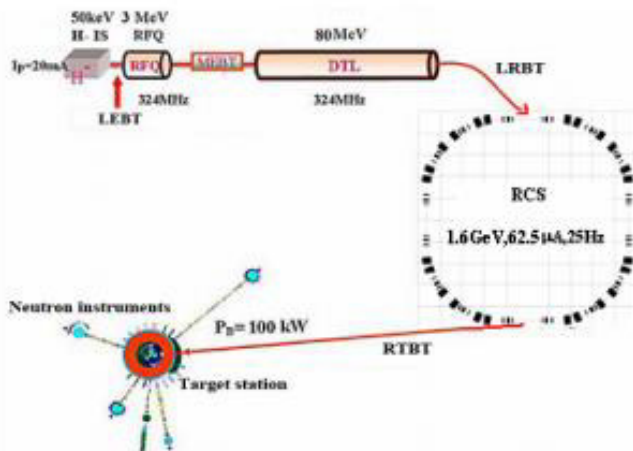


Figure 1: Schematics of the CSNS complex.

[#]sunjl@ihep.ac.cn

BEAM MONITORS

For the entire beam instrumentation system of CSNS, amounts of beam monitors are installed along the beam line, including beam position monitor (BPM), beam current monitor, beam profile monitor, beam loss monitor (BLM) and so on. Layout of the beam instrumentation system as shown in Figure 2 [3].

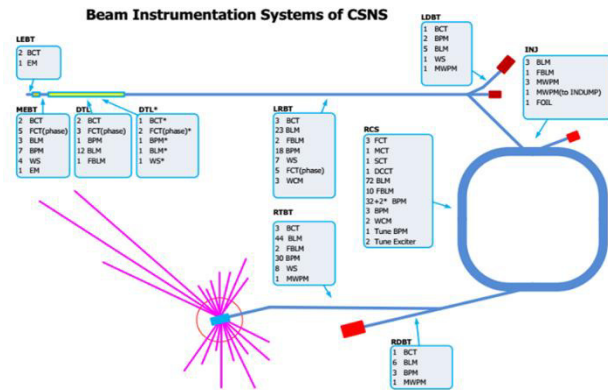


Figure 2: Layout of the beam instrumentation system of CSNS.

Beam Current Monitor

Many current transformer (CT) are used for the current measurement. Part of the magnetic rings of CT purchased from Bergoz and the other developed by our self together with a domestic company. The Cobalt-base alloys with magnetic conductivity around 20,000 to 25,000 at 25 Hz was used for the self-developing ring. Two methods used for the current calculation: 1) Take part of the flat waveform subtract background waveform then averaging; 2) Integrated waveform value as the particle number calculation.

There are two special requests for the current measurement at CSNS. One located at LINAC in front of a beam dump (LDCT), as shown in Figure 3, during normal operation the H- beam goes down to RCS but one of the BLMs along the goes up direction line has an expected high value, which induced by the residual gas stripped proton beam. A new type of electronics for low current measurement was designed for the LDCT and the residual gas stripped proton beam was measured successfully, the H- stripping percentage is ~4%. The other special CT is located at the injection line for the strip foil efficiency measurement. Most of the H- lose two electrons when pass through the strip foil turn to proton beam and cycling in RCS, very tiny part loses only one electron turn to H0, after the second strip foil fully stripped goes to the beam dump, as Figure 4 up shows.

BEAM INSTRUMENTATION PERFORMANCES THROUGH THE ESRF-EBS COMMISSIONING

L. Torino*, ALBA-CELLS, Cerdanyola del Vallès, Spain
N. Benoist, F. Ewald, E. Plouviez, J.L. Pons, B. Roche, K.B. Scheidt, F. Taoutaou, F. Uberto,
European Synchrotron Radiation Facility, Grenoble, France

Abstract

The upgrade of the European Synchrotron Radiation Facility (ESRF) storage ring has led to the construction of a new machine called the Extremely Brilliant Source (EBS). EBS has been successfully commissioned in less than three months and reached the targeted parameters for user mode. The success of the EBS commissioning also depended on the performances and the reliability of the beam instrumentation used to monitor the beam. In this paper a summary of the EBS commissioning is presented with a special focus on the beam instrumentation performances.

INTRODUCTION

After one year of shutdown during which the old ESRF storage ring has been completely dismantled, the new Extremely Brilliant Source (EBS) has been successfully commissioned and it is currently running in user mode.

The innovative Hybrid Multi-Bend Achromate lattice allows to achieve horizontal and vertical emittances of respectively 150 and 5 pm [1]. Thanks to the reduction of emittances, in particular in the horizontal plane, the 6 GeV electron beam is able to produce a more brilliant and coherent synchrotron radiation beam.

User mode beam parameters have been reached in three months.

The commissioning started on November 28th 2019, few days ahead of schedule thanks to the time saved in the installation phase and the quick commissioning of the linac and the booster. The first turn was achieved straight away thanks to the outstanding work done on the machine alignment. The beam was stored for the first time on December 5th with on-axis injection. In this period two obstacles were found and removed and problems related with magnets calibration and cross-talking were spotted and solved. On December 15th off-axis injection was established and accumulation occurred. After one month shutdown on January 17th 2020 the commissioning started again and it ended exactly on time on March 2nd when 200 mA were achieved and the hand was let to the commissioning of beamlines.

The whole commissioning period can be divided into two main phases:

- First turns and storage;
- Accumulation and current ramp-up.

These results have been quickly achieved also thanks to a well functioning beam instrumentation system which has

been able to monitor the beam from day one. Most of the commissioning work for the beam instrumentation in fact was performed on the old ESRF machine, as presented in [2].

In this paper, the performances of the main beam instrumentation systems and their relevance in reaching each of the milestones will be presented.

BEAM POSITION MONITORS

The EBS Beam Position Monitor (BPM) system is composed by 320 BPMs blocks (10 per cells) equipped with a hybrid Libera electronics system for data acquisition and processing [3]. This hybrid readout system is composed by 6 Libera Brilliance, capable to provide stream of data at 10 kHz which are used by the Fast Orbit Feedback, and 4 Libera Spark.

The BPM system was essential during the commissioning not only for orbit measurements and for allowing the machine tuning but also to see the beam during first turns at very low current, thanks to its high sensitivity.

First Turns and Storage

During this phase, BPMs were used mostly in ADC or in Turn-By-Turn (TBT) mode. Liberas Spark naturally work in time domain processing: this makes it rather easy to switch the system to TBT mode. For Liberas Brilliance the anti-smearing algorithm has been used to reduce the effect of the narrow digital filter embedded in the electronics [4].

For the first turns, the most used feature of the BPM system was the the signal “Sum” providing the sum of the signals coming from the four BPM buttons. This signal is proportional to the current and a plot of the its value versus the BPM number provides a clear indication of the presence of the beam along the machine. The intensity of the signal being proportional to the current, a drop of the of intensity represents a drop in current: this feature can clearly reveal the presence of obstacles on the trajectory.

Figure 1 shows one of the first injections in the storage ring during November 28, first day of commissioning. The horizontal axis corresponds to the Libera ADC samples: 304 samples represent one revolution period. On the vertical axis, the BPMs are shown ordered in the direction of the beam propagation: one column represents one machine turn. The data is triggered 7 revolution periods before the beam arrival time. It is clear that the beam was able to perform more than one turn, already at the first injection. Also, it is possible to notice that a drop of beam intensity is present somewhere around 2/3 of the machine (cell 23). This was the first identification of the presence of an obstacle in the

* Itorino@cells.es

BEAM INSTRUMENTATION SYSTEM FOR SHANGHAI SOFT X-RAY FEL TEST FACILITY*

L.W. Lai, L.Y. Yu, Y.B. Leng[†], R.X. Yuan, J. Chen, Y.B. Yan, W.M. Zhou, J. Chen, S.S. Cao, L.H. Hua, B. Gao, N. Zhang, T. Shen, F.Z. Chen, R.T. Jiang, W.C. Fang, C. Feng
 SSRF, Shanghai Advanced Research Institute, Chinese Academy of Sciences, Shanghai, China

Abstract

Shanghai Soft-Xray FEL (SXFEL) test facility was designed and built to demonstrate EEHG and HGHG schemes and verify key technologies for the future hard x-ray FEL facility (SHINE). After three years commissioning 8.8 nm FEL radiation with peak power of 1 MW had been achieved at the end of 2019. The design, fabrication, commissioning and operation of BI system including stripline-BPM, Cavity-BPM, screen monitor, bunch length monitor, beam arrival monitor, bunch energy monitor, will be introduced in this paper. Several lessons learned during design stage and beam commissioning stage, such as radiation damage of CCDs and step-motors, bad choice of CBPM working frequency, thermal drift of BAM and so on, will be addressed as well.

INTRODUCTION

SXFEL Test Facility (SXFEL-TF) was initiated in 2006 and founded in 2014. Its 0.84GeV linac and undulators were installed through 2016 to 2018, it is for testing the cascaded seeding schemes. The main parameters are listed in Table 1. The SXFEL-TF commissioning has completed this year, and the SXFEL user facility (SXFEL-UF) is under construction. The layout of SXFEL-TF and SXFEL-UF are shown in Figure 1.

Table 1: SXFEL-TF Parameters

Parameter	Value
Total length	293m
Electron energy	0.84 GeV
Bunch charge	0.5 nC
Repetition rate	10 Hz
FEL output	8.8 nm
FEL scheme	HGHG/EEHG
FEL pulse	100-200 fs
FEL power	>100 MW

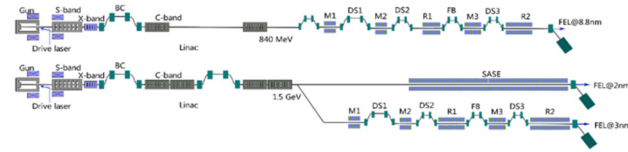


Figure 1: Layout of SXFEL-TF (top) and SXFEL-UF (bottom).

In order to maintain high FEL gain, high performance beam instrumentation system is required for the SXFEL-TF. Measured beam parameters including bunch charge, beam position (BPM), beam profile, beam arrival time (BAM) and bunch length (BLM). Table 2 lists the beam diagnostic devices included and the required resolution.

Table 2: Requirements of SXFEL-TF Diagnostic System

	Quantity	Resolution
Bunch charge	7	1%
Beam position (injector and linac)	28	10μm
Beam position (undulator)	17	1μm
Beam profile	56	20μm
Arrival time	4	100fs
Bunch length (CSR)	1	100fs
Bunch length(deflector)	1	100fs

The system control and data acquisition are based on the EPICS platform, which enables bunch-by-bunch measurement.^[1]

BEAM INSTRUMENTATION SYSTEM DESIGN AND PERFORMANCE

Bunch Charge Measurement

Integrated current transformers (ICT) from Bergoz are adopted to monitor the bunch charge along the accelerator. Instead of using analog integrator BCM-IHR-E from Bergoz and a digitizer to sample the bunch charge result, we using an oscilloscope to sample the signal from ICT directly and perform the integral calculation in the digital zone. The ADC of the oscilloscope is 10 bits, bandwidth is 600 MHz, and maximum sampling rate is 5GSPS. An embedded EPICS soft-IOC has been developed on the oscilloscope to get the sampled data and calculate the charge.

One of the advantages of this solution is avoiding the interference of noise signal to the analog circuit. Another advantage is that digital signal processing algorithms can be

*Work supported by Youth Innovation Promotion Association, CAS (Grant No. 2019290); The National Key Research and Development Program of China (Grant No. 2016YFA0401903).

[†] lengyongbin@zjlab.org.cn

PRECISE BUNCH CHARGE MEASUREMENT USING BPM PICKUP*

J. Chen[†], Y.B. Leng[#], L.W. Lai, B. Gao, S.S. Cao, F.Z. Chen, Y.M. Zhou, T. Wu, X.Y. Xu, R.X. Yuan

Shanghai Advanced Research Institute, CAS, Shanghai, China

Abstract

Precise bunch charge measurement is the fundamental of charge feedback, beam lifetime measurement, beam loss monitor, as well as the basis of the related interlocking work. Beam position monitor (BPM) is often used for high-resolution bunch charge measurement due to its superior performance. In this paper, the pros and cons of Stripline BPM, Button BPM, and Cavity BPM for measurement of bunch charge in storage ring and FEL will be discussed. The related simulations and beam experiment results are also mentioned, the results show that the relative bunch charge resolution of the Button BPM can reach 0.2‰ in SSRF, 0.73‰ and 0.21‰ of the SBPM and CBPM in SXFEL, respectively. Besides, based on the method of beam experiments, we systematically studied the position dependence of BPM pickup for bunch charge measurement and related compensation algorithms.

INTRODUCTION

Shanghai Synchrotron Radiation Facility (SSRF) is a low emittance 3rd-generation light source consisting of a 3.5 GeV storage ring, a full energy booster and a 150 MeV linac, as well as dozens of beam lines and experimental stations. The Shanghai soft X-ray free electron laser (SXFEL) is a test facility for exploring key FEL schemes (EEHG/HGHG) and technologies, which adopt FEL frequency doubling of ultraviolet band seeded laser of 265 nm to achieve output wavelength of 9 nm, 100 fs pulse duration, 10 HZ repetition rate, and 100 MW peak power[1]. The overall length of SXFEL is about 300 meters and the nominal electron beam energy of the linac is 0.84 GeV. And it will be upgrade to a user facility in 2021. In addition, SHINE, a hard X-ray FEL facility with high energy, high repetition rate, is also under pre-research. The total length of the SHINE is about 3.1 Km, located near SSRF and SXFEL, the goal is to build a superconducting linear accelerator with an energy of 8 GeV, 3 undulator lines, 3 light speed lines, and the first batch of 10 experimental stations. Together with SSRF and SXFEL to build a photonic science center in China.

For high quality electron beams, accurate measurement of beam charge and its stability is one of the most important parameters for stable operation of accelerator. For example, for SHINE, so as to avoid damage the cryogenic superconducting undulator caused by beam loss, a requirement that

the beam loss measurement accuracy is better than 0.01% in key areas is proposed. Therefore, research on this topic has great significance to the efficient operation of these facilities.

BPM picks up the electromagnetic field excited when the bunch passes through the vacuum chamber, which carries the information of the bunch, which is widely used in the measurement of a variety of bunch parameters. Its unique characteristics are also one of the methods to achieve high-precision bunch charge measurement.

This paper focuses on the motivation of using BPM probes for high-precision bunch charge measurement, introduces the principle of BPM for bunch charge measurement. The dependence of the horizontal and vertical parameters for high-precision bunch charge measurement is simulated, and some simulation results are verified by beam experiments. In addition, the system signal conditioning and data acquisition schemes and digital signal processing algorithms are also mentioned.

MEASUREMENT PRINCIPLE

For the electrostatic induction BPM, when the beam passes through the vacuum chamber, the electrode generates an induced charge under the action of electrostatic induction, and the induced signal contains the position and charge amount information of the bunch. In electron accelerators, typical probes are SBPM and Button BPM. The output signal can be expressed by Eq.(1) and (2), respectively.

$$V(t) = \frac{\phi Z}{4\pi} \left[e^{\frac{r^2}{2\sigma^2}} - e^{-\frac{(t-2L)^2}{2\sigma^2}} \right] \cdot \frac{Q}{\sqrt{2\pi}\sigma} \quad (1)$$

$$V_B(t) = \frac{Q}{2\pi^{\frac{3}{2}}} \cdot \frac{\phi l R}{\beta_b c} \cdot \frac{t}{\sigma_t^3} \cdot e^{-\frac{r^2}{2\sigma_t^2}} \quad (2)$$

For Cavity BPM, when the bunch passes through the cavity, various characteristic modes of the electromagnetic field will be excited due to the tail field effect. For a standard cylindrical cavity, the excited TM_{010} mode which contains the bunch charge message can be represented by Eq. (3) :

$$V_p^{010} = \frac{q\omega_{010}}{2} \cdot \sqrt{\frac{Z}{Q_{ext}^{010}} \cdot \frac{2LT^2}{\epsilon\omega_{010}\pi a^2 J_1^2(\chi_{01})}} \cdot J_0^2\left(\frac{\chi_{01}}{a}\rho\right) \cdot e^{-\frac{t}{\tau_{010}}} \cdot e^{-\frac{\omega_{010}\sigma_z^2}{2c^2}} \cdot \sin(\omega_{010}t + \varphi) \quad (3)$$

It can be seen from the above expression that the BPM pickups for bunch charge measurement still has the dependent factors such as bunch length, position offset, etc.

*Work supported by National Natural Science Foundation of China (2016YFA0401903) and Ten Thousand Talent Program and Chinese Academy of Sciences Key Technology Talent Program

[†]chenjian@zjlab.org.cn

[#]lengyongbin@sinap.ac.cn

DIAGNOSTICS FOR COLLIMATOR IRRADIATION STUDIES IN THE ADVANCED PHOTON SOURCE STORAGE RING*

J. Dooling[†], M. Borland, W. Berg, J. Calvey, G. Decker, L. Emery, K. Harkay, R. Lindberg, G. Navrotsky, V. Sajaev, J. Stevens, Y. P. Sun, K. P. Wootton, A. Xiao, Argonne National Laboratory, Lemont, USA
A. H. Lumpkin, Argonne Associate of Global Empire, LLC, Argonne National Laboratory, Lemont, USA

Abstract

The Advanced Photon Source (APS) is building a fourth-generation storage ring (4GSR), replacing the present double-bend achromat lattice with a multibend achromat system thereby allowing the production of ultra-bright x-ray beams. The new lattice enables a two-order-of-magnitude reduction in horizontal beam emittance and a factor of two increase in beam current. The result is an electron beam of very high energy- and power-densities. Initial predictions suggest virtually any material struck by the undiluted electron beam will be damaged. Two experimental beam abort studies have been conducted on collimator test pieces in the present APS SR to inform the design of a fully-functional machine protection system for APS 4GSR operations at 200 mA. A comprehensive suite of diagnostics were employed during the studies. The diagnostics used in these experiments are not new, but employed in different ways to obtain unique data sets. With these data sets now in hand, we are developing new numerical tools to guide collimator design.

INTRODUCTION

The Advanced Photon Source Upgrade (APS-U) project centers on the construction of a fourth generation storage ring (4GSR) [1]. The ultra-low emittance lattice operating at 6 GeV and 200 mA will result an electron beam of very high energy- and power-densities. MARS [2] simulations indicated virtually any material struck by the undiluted, primary beam will be damaged. The objective of this work is to conduct experimental studies which informs the design and construction of a robust, fully-functional collimator system for 200 mA APS-U beam operations. A variety of diagnostics play a key role in observing and evaluating the effects of whole beam dumps on candidate collimator materials which is the subject of these studies.

Two beam-loss studies have been performed thus far, the first in May 2019 and the second in January 2020. Conducting these experiments successfully requires a diverse set of diagnostics such as Turn-By-Turn (TBT) Beam Position Monitors (BPMs), cameras, DC Current Transformers (DC-CTs), and beam loss monitors (BLMs). A different set of diagnostic techniques are used after the study to examine the collimator test pieces including microscopy and metallurgy.

* Work supported by the U.S. Department of Energy, Office of Science, Office of Basic Energy Sciences, under Contract No. DE-AC02-06CH11357.

[†] dooling@aps.anl.gov

EXPERIMENTAL METHODS

Both irradiation studies were conducted at the beginning of run periods during start-up machine studies in order to extract the collimator test pieces before user operations began. This approach is somewhat risky since this time may be necessary to condition new vacuum components or other hardware; for example, the collimator/scrapper assembly. A plan view of the assembly is presented in Fig. 1. This location is just downstream of the fourth rf cavity in this Sector 37 (S37) long straight section.

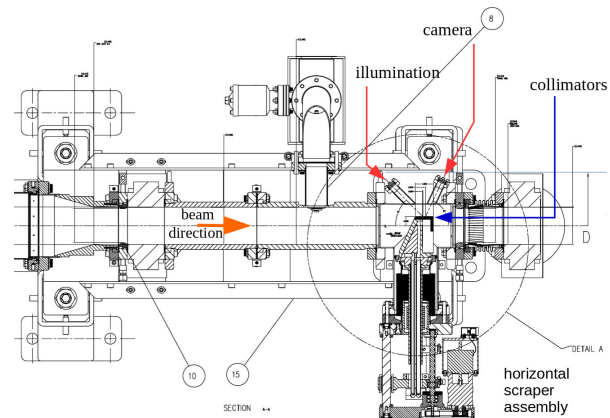


Figure 1: Collimator/scrapper assembly plan view in the APS SR S37 long straight section. The location is just downstream of the fourth rf cavity.

Diagnostic Camera

For both experiments, a diagnostic camera was built in the SR tunnel to view the collimator surfaces. The camera hardware was then disassembled and removed at the end of each study. The collimators are viewed through a 65° port and illuminated through a 45° port as indicated in Fig. 1. The angles are measured from the beam axis. The depth of field (DOF) for the optical system is 2 mm at the collimator surface. The resolution is approximately 50 μm and the field of view is 11 mm. Radiation protection for the camera is provided first by moving the unit approximately 0.5 m below the beam centerline, and second by shielding with Pb bricks. A photograph of the camera assembly and image of the installed collimator pieces prior to the first irradiation experiment are shown in Fig. 2. In the first experiment, two collimator materials were tested: titanium alloy Ti6Al4V and aluminum alloy T6061. In this image the darker titanium

Content from this work may be used under the terms of the CC BY 3.0 licence (© 2020). Any distribution of this work must maintain attribution to the author(s), title of the work, publisher, and DOI

X-RAY BEAM SIZE MONITOR ENCLOSURE FOR THE ADVANCED PHOTON SOURCE UPGRADE*

K. P. Wootton[†], W. Cheng, G. Decker, S. H. Lee, B. X. Yang
 Argonne National Laboratory, Lemont, USA

Abstract

Confirmation of pm rad scale emittances from the Advanced Photon Source Upgrade electron storage ring necessitates direct measurement of the electron beam size. In the present work, we motivate design choices for the X-ray beam size monitor shielding enclosure for the Advanced Photon Source Upgrade. Particular emphasis is given to outlining design choices from the perspectives of safety, overall project construction schedule and eventual beamline operations.

INTRODUCTION

As a high average brightness source of X-ray photons, the storage ring for the Advanced Photon Source Upgrade (APS-U) is designed to operate with ambitious transverse emittances on the order of ~ 42 pm [1, 2]. In order to utilise the high brightness X-ray beams, a range of accelerator diagnostic instruments are planned to provide beam position stability and accelerator control [3]. In particular, to quantify the horizontal and vertical emittances, beam size monitors are planned for APS-U [4].

In the present work, we outline the enclosure design for the APS-U storage ring electron beam size monitor beamline.

BEAM SIZE MONITOR

Hard X-ray synchrotron radiation beam size monitors are planned for APS-U to quantify the transverse emittances of the stored electron beam [4, 5]. For an operating storage ring such as the Advanced Photon Source (APS), this is an important online diagnostic of the beam in the accelerator [6, 7]. A key performance parameter for successful completion of the APS-U project is that the horizontal emittance $\epsilon_x \leq 130$ pm rad [1]. The beam size monitor is the principal instrument for confirming the emittances.

The principal functional requirement for absolute beam size measurement is that the contribution of system resolution σ_r to the measured electron beam size σ_e is not larger than 10% when added in quadrature. For the proposed timing and brightness operating modes of APS-U, the functional requirements of the absolute beam size monitor are summarised in Table 1 [1].

BEAMLINE LOCATION

Measurement of emittance based on the beam size is optimised where the contribution to the beam sizes is dominated by the emittance. For APS-U, the horizontal dispersion η_x

Table 1: APS-U Electron Beam Sizes at Bending Magnet A:M1.1 in Timing and Brightness Operating Modes

Parameter	Value	Units
Timing Mode	–	–
Horizontal beam size	7.2	μm
Vertical beam size	25.1	μm
Brightness Mode	–	–
Horizontal beam size	7.2	μm
Vertical beam size	9.1	μm

is zero by design in the insertion straights, and so the nominal bending magnet source for the beam size monitor is the first longitudinal gradient bending magnet in an arc cell A:M1.1 [1].

The beam size monitor beamline will be located in Sector 38 of the APS-U storage ring. A schematic illustration of the beamline is shown in Fig. 1. This location was selected because the nominated photon source A:M1.1 bending magnet was only available in the radiofrequency cavity insertions. We will extract the bending magnet radiation through an unused insertion device photon beam extraction chamber, because user beamlines will occupy all the APS-U insertion device front ends.

There are several challenges that arise in the construction of a beamline in this location. The storage ring tunnel shield-

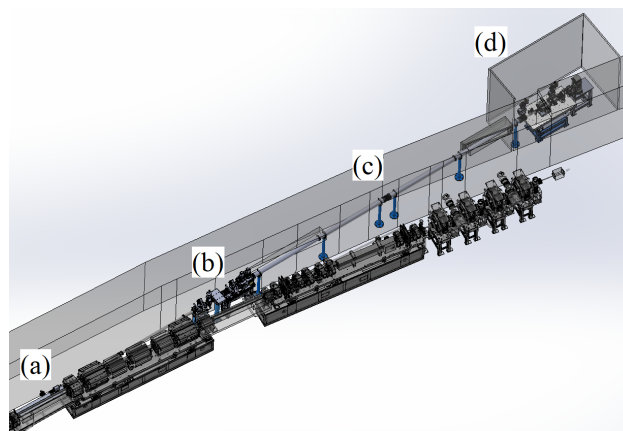


Figure 1: Schematic overview of Sector 38 beam size monitor beamline for APS-U. In this figure, the beam direction is from left to right. (a) Synchrotron radiation absorbers and pinhole mask. (b) Bending magnet beamline front end components (photon shutter, safety shutters and lead collimator). (c) Photon beam vacuum chamber through accelerator shield wall. (d) Endstation instruments and beamline enclosure.

* Work supported by the U.S. Department of Energy, Office of Science, Office of Basic Energy Sciences, under Contract No. DE-AC02-06CH11357.

[†] kwootton@anl.gov

INCLINED X-RAY BEAM POSITION MONITORS TO REDUCE INFLUENCE OF FILLING PATTERN FOR THE SPring-8 PHOTON BEAMLINES

H. Aoyagi[†], Y. Furukawa, S. Takahashi

Japan Synchrotron Radiation Research Institute (JASRI), Hyogo, Japan

Abstract

Influence of bunch filling patterns on X-ray beam position monitors (XBPMs) increased year by year as the bunch current of the storage ring increased. We have performed a systematic evaluation of the influence of the filling patterns. As a result, the cause of the influence was to be found to be suppression of the XBPM current signal due to the space charge effect, and was able to be quantified by observing the behavior of the current signal while changing the applied voltage to a photoelectron collecting electrode. On the other hand, we have designed a new blade-shaped detection element having inclined configuration for the purpose of mitigating the space charge effect. It has been demonstrated that the influence of filling patterns is reduced to a few μm . We also report that, as a result of a series of efforts against the existing XBPMs for all insertion device beamlines, the influence has been reduced to approximately 5 μm RMS.

INTRODUCTION

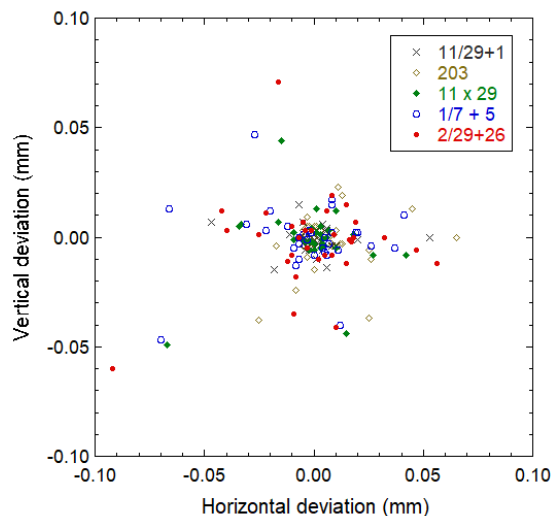
The X-ray beam position monitors (XBPMs) at the SPring-8 storage ring works in a photoemission mode that is equipped with four blade-shaped detection elements made of tungsten as photocathodes [1]. The XBPMs are installed at insertion device beamlines (ID-BLs) and bending magnet beamlines (BM-BLs), and have a stable operation record for over 20 years. Monitoring photon beam axes with the XBPMs, which have been fully evaluated for their performances, ensures the stable supply of the photon beam to beamline users. The rf-BPM of the storage ring excels in global diagnosis of closed orbit distortions, while the XBPM is suitable for accurate diagnosis of photon beams of individual beamlines.

SPring-8 constantly provides various several-bunch mode operations, which combine single bunches (isolated bunches) and train bunches (partial full-filling) [2] to perform the time-division experiment. The bunch current has been gradually increasing, and reached up to 5 mA/bunch in a single bunch and 0.38 mA/bunch in partial full-filling. The bunch current of 1 mA/bunch corresponds to 4.8 nC in the storage ring. As the bunch current increased, the influence of bunch filling patterns on XBPM performance increased year by year.

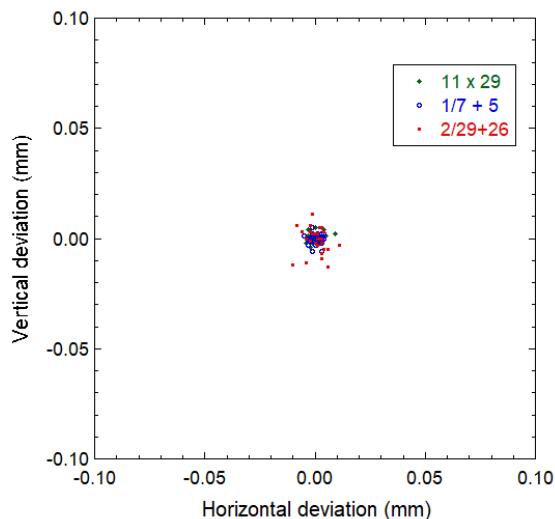
INFLUENCE OF FILLING PATTERN

The XBPM readouts in five types of several-bunch modes systematically were evaluated using the readouts in multi-bunch mode as the reference data to quantitatively

understand the phenomenon that affects the XBPMs by changing the filling pattern. The multi-bunch mode, a type of a filling pattern, has the least impact on the accelerator beam operation. This measurement is performed in the same procedure as for the fixed point observation that is regularly conducted before the beginning of each user operation cycles with setting the ID gap of each ID-BL to a certain fixed value. As shown in Fig. 1 (a), it was found that different filling patterns have different effects on XBPMs.



(a) Before the series of measures



(b) After the series of measures

Figure 1: Deviations of XBPM readouts from the reference positions (multi-bunch) due to variations of five different filling patterns of the storage ring.

[†] aoyagi@spring8.or.jp

MULTIPLEXER SYSTEM FOR THE SPEAR3 BOOSTER BPM UPGRADE*

F. Toufexis[†], L. Campana[‡], P. Boussina, J.J. Sebek, J. Corbett, SLAC, Menlo Park, CA 94025, USA

Abstract

BPM measurements in booster synchrotrons are often only critical during accelerator commissioning or when a problem occurs. As a result, many facilities do not make large investments in booster BPM signal processors; they either have very few BPMs and/or use older generation processors. The SPEAR3 booster BPM processor system, for instance, has operated since 1990 with commercial multiplexers to switch between BPM button signals into a single dated analog BPM processor that was developed at SLAC. This system has reached its end-of-life so we are in the process of upgrading to modern multiplexers that feed a pair of turn-by-turn Libera SPARK-ERXR processors. This low-cost solution gives us the ability to arbitrarily multiplex between BPM signals during the energy ramp with modern BPM processors. The system can either measure 2 BPMs turn-by-turn in parallel during the entire energy ramp, or sequentially measure all BPMs (2 at a time) at different time slices within the ramp. Here we show measurements of the MiniCircuits switch we chose as well as our architecture for the upgrade.

INTRODUCTION

The SPEAR3 injector was commissioned in 1990 [1], and includes a 120 MeV linac injector with a thermionic RF gun [2], the booster synchrotron [3] and the Transport Lines. The entire injector, including the Transport Lines, is equipped with stripline-style Beam Position Monitors (BPMs). The original booster synchrotron BPM electronics used a commercial multiplexer to switch between BPM button signals into an in-house built analog BPM processor [4]. Out of the 40 booster BPMs, 20 are connected to long-haul cables that come out of the ring and are connected to the legacy BPM processor system. In this system, the 20 BPMs are connected to three slow multiplexer modules (referred to as the R10Ts). The output of these three multiplexers is connected to a faster multiplexer. The output of this multiplexer is filtered and then connected to an in-house BPM processor. Two different software systems can obtain the orbit from the booster: one system can get the average position in a number of time slots per booster ramp for one BPM, while the other system can get the position in several time slots for all BPMs in the same ramp.

At the time of this writing two (plus a spare) Instrumentation Technologies Libera SPARK-ERXR Turn-by-Turn (TbT) BPM processors have been installed at the booster and have gone through preliminary testing. We are also building two new multiplexer chassis that will connect the

20 connected booster BPMs into the SPARK processors to measure the orbit on a TbT basis during a booster ramp. We have investigated commercial switch options to replace the R10Ts; there are several option with sub-microsecond switching time but cost upwards of \$7,000 for a 10-input switch that is not financially attractive. The Mini-Circuits USB-1SP16T-83H was the lowest cost option we found, had adequate specifications for our needs, and was readily available to purchase. The specifications are summarized in Table 1.

This work is organized as follows: we begin with time-domain and frequency domain measurements of the switch in the lab. Then we show measurements with the actual BPM signals from the booster. Finally we show the overall architecture of the new system we are building.

TIME-DOMAIN LAB MEASUREMENTS

The MiniCircuits switch provides both a TTL and USB interface. The USB interface can be used for slow switching on the order of milliseconds according to the manual; therefore we use the TTL interface. The unit has a DB9 connector to provide power and TTL signals if USB is not being used. We made a custom cable; one end had a DB9 connector, and the other had two banana plugs to connect ground and power as well as 5 coaxial cables with BNC connectors to connect the TTL signals to a delay generator for testing. The measurement setup is shown in Figure 1.

First we tested with one RF input signal at 400 MHz and -10 dBm. We programmed the delay generator to toggle 1 channel as shown in Figure 2a, switching between the signal and an unconnected input. We noticed that the gating on/off of the output signal jittered with respect to the signal generator. We subsequently connected a second RF input signal, now switching between two inputs. Figure 2b shows the transition of the output. The whole transition itself takes less than 5 μ s as specified; however, the transition time with respect to the delay generator signal again showed jitter of about 10 μ s. We suspect this is due to the microprocessor on the switch that internally controls the switching; most likely the microprocessor periodically checks the input TTL

Table 1: Mini-Circuits USB-1SP16T-83H Switch Specs

Frequency	1 MHz – 8 GHz
Isolation	63 dB Min (0 GHz – 3 GHz)
Transition Time	5 μ s
Power Handling	30 dBm
Insertion Loss	7.5 dB Max (0 GHz – 3 GHz)
Interface	USB & TTL
Inputs	16
Price	\$1,835

* Work sponsored by US Department of Energy Contract DE-AC02-76SF00515.

[†] ftouf@slac.stanford.edu

[‡] Currently at Dipartimento di fisica, Sapienza università di Roma, Rome, Italy

X-RAY BEAM POSITION MONITOR SILICON PHOTODIODE MEASUREMENTS FOR THE ADVANCED PHOTON SOURCE UPGRADE*

K. P. Wootton[†], H. P. Cease, M. J. Erdmann, S. Oprondek, M. Ramanathan, B. X. Yang
Argonne National Laboratory, Lemont, IL, USA

Abstract

To best leverage the orders of magnitude average brightness increase of multi-bend achromat synchrotron radiation storage rings, ambitious beam stability requirements are imposed. One system that will be employed at the Advanced Photon Source Upgrade in support of photon beam stability will be X-ray beam position monitors. In the present work, electrical characterisation of several types of photodiodes are evaluated for potential use in X-ray beam position monitors.

INTRODUCTION

In order to meet demanding photon beam stability requirements of the Advanced Photon Source – Upgrade (APS-U) [1], hard X-ray beam position monitors are planned [2–4]. Several geometries of x-ray beam position monitors for different insertion device beamlines are foreseen, based upon the grazing-incidence insertion device hard x-ray fluorescence BPM (GRID XBPM) detector geometry [2–11].

In the present work, electronic performance testing of silicon photodiodes for X-ray beam position monitors is presented.

PHOTODIODES TESTED

The photodiodes tested in these studies were Luna Opto-Electronics solderable silicon photodiodes. The diodes are intended to be operated either in a photoconductive ('C') or photovoltaic ('V') mode. These solderable photodiodes are compatible with operation in an ultrahigh vacuum environment. Diode types tested in the present work included:

- PDB-C612-2,
- PDB-C613-2,
- PDB-V615-2.

METHOD

We consider here electrical tests that can be performed throughout stages of detector assembly, cleaning and installation. During all measurements in the present work, the photodiode under test was positioned within a light-tight box.

* Work supported by the U.S. Department of Energy, Office of Science, Office of Basic Energy Sciences, under Contract No. DE-AC02-06CH11357.

[†] kwootton@anl.gov

Shunt Resistance

Shunt resistance is defined to be the average slope of the voltage-current $V-I$ curve about 0 V. The accepted practice for the measurement of diodes is to measure the current across the diode at voltages of ± 10 mV [12].

For measurement of shunt resistance, the DC power supply and picoammeter were connected in series with the photodiode. The current through the diode was measured using the picoammeter. The power supply was set to output either +10 mV, 0 mV or –10 mV.

The sequence of measurement was to measure at 0 mV, +10 mV, 0 mV, –10 mV. Three observations of the current at each voltage setpoint were made. It took some time for the picoammeter current measurement to reach equilibrium. During these tests it took approximately 30 s per voltage step for the current measurement to stabilise. In practice, this was the slowest measurement to make.

Two-Wire Resistance

One technique to measure resistance of the diode is to perform a two-wire resistance measurement [13]. The average forward resistance is measured with a digital multimeter (Keysight 34465A 6 1/2 digit multimeter) used as an ohmmeter. The measurement current is 500 nA [14]. Due to the nonlinear $I-V$ curve of the photodiode, this resistance value is expected to change with the measurement current. This measurement only returns a value for the voltage with the leads connected in forward bias across the diode. For a normal diode measured in reverse bias, the multimeter returned an 'overload' response.

Each two-wire resistance measurement took less than one second to measure. Three observations were made at each setting.

Diode Test

A diode test is commonly included on multimeters [13]. It is a voltage measurement at a nominal current. In the present work, the current used was ~ 1 mA.

Each diode test took less than one second to measure. Three observations were made at each setting.

Photocurrent

Photodiodes in the GRID XBPM are illuminated by X-ray fluorescence from a cerium-doped yttrium aluminium garnet (YAG) scintillator crystal. As a performance characteristic, we evaluate the uniformity of DC photocurrent produced by these photodiodes when illuminated by a green LED.

To evaluate the photocurrents of photodiodes, the photodiode was illuminated by a InGaAlP light emitting diode

AUTOMATED MANAGEMENT OF LIBERA SPARK MODULE IOCs IN SPEAR3*

F. Toufexis[†], S. Condamoor, D. A. Morataya Campos, C. S. Ramirez, J. J. Sebek, C. Wermelskirchen, J. Corbett, SLAC, Menlo Park, CA 94025, USA
P. Leban, M. Znidarcic, Instrumentation Technologies, Solkan, Slovenia

Abstract

We are actively upgrading BPM processors in the SPEAR3 accelerator complex as several of the existing systems are reaching end-of-life. To consolidate the resources required for development and maintenance we have evaluated and installed several processors from the Libera SPARK hardware series. We found that two common deployment methods typically used with these modules, micro-SD card and network boot, are either hard to maintain or lack flexibility. Instead we have developed an automated method based on a network boot scheme where an external EPICS soft IOC manages the assignment of specific SPARK modules to physical BPMs in the accelerator. Each module queries the soft IOC at boot time to determine which BPM it is assigned to and then starts its IOC with the appropriate BPM prefix for the PV names. This deployment method allows for quick, seamless swapping of SPARK modules by machine operators or physicists. In addition, it allows us to bring additional modules online for testing, or to move modules to different locations with a different PV prefix for the new location. This method is applicable to other EPICS-enabled devices where the device hardware also hosts an IOC.

INTRODUCTION

SPEAR3 is a 3 GeV, 500 mA, 3rd generation synchrotron light source, commissioned in 2004 [1]. It operates with beam current distributed in four bunch trains and a single isolated timing bunch for pump-probe experiments. Top-up occurs at 5-minute intervals. Each top-up event requires about 50 single-bunch charge pulses into targeted SPEAR3 buckets at a 10 Hz rate. The SPEAR3 storage ring contains 18 lattice cells each with 6 button-style Beam Position Monitors (BPMs). Three BPMs per cell are connected to Bergoz processors for fast orbit control and beam inter-lock purposes. Several more BPMs are connected to the Echotek processors [2] to provide Turn-by-Turn (TbT) orbit information at discrete locations. The Echotek processors were developed in-house and produced commercially when SPEAR3 was commissioned; they are used for accelerator physics programs and not for operations. The Echotek have reached their end of life and we have evaluated commercial alternatives for replacement. A Libera Brilliance+ was first tested in SPEAR3 in 2017 [3]. Since TbT studies for accelerator physics programs do not require the long-term stability capability of the Brilliance+, and additionally the fast or-

bit feedback is implemented in the Bergoz BPM system, a SPARK-ERXR processor [4] was purchased and installed for accelerator physics applications. Additionally we are in the process of installing and testing Beam Loss Monitors (BLMs) for Libera that have the same base hardware and software infrastructure as the SPARKs.

The SPEAR3 injector was commissioned in 1990 [5], and includes the 120 MeV linac injector with a thermionic RF gun [6], the booster synchrotron [7] and the Transport Lines. The entire injector, including the Transport Lines, is equipped with stripline-style BPMs. The original booster synchrotron BPM electronics used a commercial multiplexer to switch between several BPM signals into an in-house built analog BPM processor [8]. In the Linac-To-Booster (LTB) and Booster-To-SPEAR (BTS) Transport Lines 1990's-era Bergoz BPM processors have provided reliable shot-by-shot single-pass data at 10 Hz with limited resolution [8]. As an upgrade to the original Transport Line BPM processors, two smaller-diameter stripline BPMs connected to two SLAC-built uTCA-based BPM processors replaced the last two BPMs at the end of the BTS in 2015 (BTS BPMs 8 and 9). This system has proven hard to maintain and we have evaluated single-pass SPARK-EL processors as a replacement. The units were tested in the BTS and LTB Transport Lines demonstrating comparable position resolution to the uTCA processors at the small-diameter striplines, as well as substantially improved resolution at the large-diameter striplines.

Since these BPM processors, as well as the BLMs, have the same base hardware and software, we wanted a unified architecture of deploying and managing these modules. We aim for an architecture that allows for easy swaps in the event of a module failure, but additionally gives us the flexibility to bring modules online for testing or to relocate modules and change the EPICS Process Variable (PV) prefix they publish appropriately. All these requirements come down to having the ability to dynamically change the EPICS PV prefixes. We perform this through an external EPICS soft Input/Output Controller (IOC) that manages the information for the prefixes and settings. Each module runs a shell script that acquires all this information and starts its IOC with the appropriate prefix and settings. This work is organized as follows: we begin by explaining our considerations for choosing this deployment architecture and then give a high-level description of our solution. Subsequently we describe the infrastructure that is needed to implement this architecture and the details of how a module boots and acquires its PV prefixes. Finally, in the appendix we show certain important code snippets.

* Work sponsored by US Department of Energy Contract DE-AC02-76SF00515.

[†] ftouf@slac.stanford.edu

DIRECT OBSERVATIONS OF SUBMICROPULSE ELECTRON-BEAM EFFECTS FROM SHORT-RANGE WAKEFIELDS IN TESLA-TYPE SUPERCONDUCTING RF CAVITIES *

A. H. Lumpkin[†], R. M. Thurman-Keup, D. R. Edstrom Jr., P. Prieto, J. Ruan,
Fermi National Accelerator Laboratory, Batavia, IL, USA
B. T. Jacobson, A. L. Edelen, J. A. Diaz-Cruz, F. Zhou,
SLAC National Accelerator Laboratory, Menlo Park, CA, USA

Abstract

Experiments were performed at The Fermilab Accelerator Science and Technology (FAST) facility to elucidate the effects of short-range wakefields (SRWs) in TESLA-type rf cavities. FAST has a unique configuration of a photocathode rf gun beam injecting two TESLA-type single cavities (CC1 and CC2) in series prior to the cryomodule. To investigate short-range wakefield effects, we have steered the beam to minimize the signals in the higher-order mode (HOM) detectors of CC1 and CC2 for a baseline, and then used a vertical corrector between the two cavities to steer the beam off axis at an angle into CC2. A Hamamatsu synchroscan streak camera viewing a downstream OTR screen provided an image of y-t effects within the micropulses with ~10-micron spatial resolution and 2-ps temporal resolution. At 500 pC/b, 50 b, and 4 mrad off-axis steering into CC2, we observed an ~100-micron head-tail centroid shift in the streak camera image y(t)-profiles. This centroid shift value is 5 times larger than the observed HOM-driven centroid oscillation within the macropulse, and it is consistent with a calculated short-range wakefield effect using ASTRA simulations.

SUBMISSION OF PAPERS

The preservation of the low emittance of electron beams during transport through the accelerating structures of large facilities is an ongoing challenge. In the cases of the TESLA-type superconducting rf cavities currently used in the European X-ray Free-electron Laser (FEL) [1] and the currently-under-construction Linac Coherent Light Source upgrade (LCLS-II XFEL) [2], off-axis beam transport may result in emittance dilution due to transverse long-range (LRW) and short-range wakefields (SRW) [3-5]. To investigate such effects, experiments were performed at the Fermilab Accelerator Science and Technology (FAST) facility with its unique two-cavity configuration after the photocathode rf gun [6]. We used optical transition radiation (OTR) imaging with a UV-visible synchroscan streak camera to display sub-micropulse y-t effects in the 41-MeV beam.

We report effects on beam transverse position centroids and sizes correlated with off-axis beam steering in TESLA-type cavities. We used a 3-MHz micropulse repetition

rate and targeted diagnostics for these tests. Our initial data from an OTR imaging source indicated our streak camera can provide ~10-micron spatial resolution with 1-2 ps (σ) temporal resolution depending on the bandpass filter employed. Since the observed bunch lengths were 10-20 ps (σ), we had sufficient resolution for up to 20 time slices in the 4σ profile. In this sense we also obtained slice-emittance information (with β -function information). We used the higher-order mode (HOM) detectors and rf BPMs to establish first the desired off-axis steering and then evaluated the short-range wakefield effects on the beam dynamics.

EXPERIMENTAL ASPECTS

The IOTA Electron Injector Linac

The Integrable Optics Test Accelerator (IOTA) electron injector at the FAST facility (Fig. 1) begins with an L-band rf photoinjector gun built around a Cs₂Te photocathode (PC). When the UV component of the drive laser, described elsewhere [7] is incident on the PC, the resulting electron bunch train with 3-MHz micropulse repetition rate exits the gun at <5 MeV. Following a short transport section with a pair of trim dipole magnet packages (H/V100 and H/V101), the beam passes through two superconducting rf (SCRF) capture cavities denoted CC1 and CC2, and then a transport section to the low-energy electron spectrometer, D122. Diagnostics used in these studies include the rf BPMs, the imaging screens at X107, X108, X121, and X124, and HOM couplers at the upstream and downstream ends of each SCRF cavity. The HOM signals were processed by the HOM detector circuits with the Schottky diode output provided online through ACNET, the Fermilab accelerator controls network [4]. The HOM detectors' bandpass filters were optimized for two dipole passbands from 1.6 to 1.9 GHz, and the 1.3-GHz fundamental was reduced with a notch filter. The rf BPMs' electronics were configured for bunch-by-bunch capability with optimized system attenuation. At 2 nC per micropulse, the rms noise was found to be 25 μ m in the horizontal axis (x) and 15 μ m in the vertical axis (y) at B101 in the test with 4.5-MeV beam from the gun. However, for these studies on short-range transverse wakefields, we relied on a streak camera to provide the sub-micropulse spatial information.

* This manuscript has been authored by Fermi Research Alliance, LLC under Contract No. DE-AC02-07CH11359 with the U.S. Department of Energy, Office of Science, Office of High Energy Physics.

[†] lumpkin@fnal.gov

OBSERVATION OF OPTICAL SYNCHROTRON RADIATION FROM ULTRA-LOW CHARGES STORED IN A RING OPERATING AT 425 MeV*

A. H. Lumpkin[†], Argonne Associate, Argonne National Laboratory, Lemont, IL, USA
K. P. Wootton, Argonne National Laboratory, Lemont, IL, USA

Abstract

The initial observations of optical synchrotron radiation (OSR) emitted over millions of passes from a few electrons circulating in the Particle Accumulator Ring (PAR) at the Advanced Photon Source have been done with a digital CMOS camera and a synchroscan streak camera operating at 117.3 MHz. The discrete changes of integrated counts in the CMOS image region of interest are ascribed to single electron steps at ~ 3500 counts per e^- . Circulations of a single electron at 375 MeV and at 425 MeV were demonstrated in the 12 bit digital FLIR USB3 camera images. The Hamamatsu C5680 streak camera operating at the 12th harmonic of the fundamental revolution frequency at 9.77 MHz was used to measure the bunch length from 0.5 nC circulating charge down to tens of electrons or < 10 aC. The latter cases were performed with 6 ps temporal resolution for the first time anywhere, to our knowledge. We report a preliminary effective bunch length of 276 ± 36 ps for 57 electrons (9.1 aC) stored based on a fit to a single Gaussian peak. The results will be compared to the standard zero-current model for the ring.

INTRODUCTION

Investigations into the probability of photon emission via the optical synchrotron radiation (OSR) mechanism from single electrons circulating in small storage rings have been done with spatially-integrating and light-intensity-monitoring photo multiplier tubes (PMTs) or photodiodes in the past [1, 2] and more recently with PMTs and digital CCD cameras [3]. These gave the intensity effect vs stored electron number and transverse size. However, mapping of the longitudinal distribution of photons emitted by a few electrons circulating in a ring has only been done at the 10 ns level [1–4].

We employ for the first time a synchroscan streak camera that is phase locked to 117.3 MHz, the 12th harmonic of the fundamental revolution frequency at 9.77 MHz of the Particle Accumulator Ring (PAR) at the Advanced Photon Source (APS). This provided temporal resolution of about 6 ps on the slowest streak range. In this case electrons circulate at 1/12th the streak camera vertical deflection frequency so no turns are missed, and the phase locking of the instrument to the radiofrequency (rf) means the camera phase is nearly the same to a few ps over hundreds of seconds. The streak camera sees every turn, and its phosphor screen inte-

grates the arrival times of the photo-electron events on the deflection axis (one photon is emitted per electron per 137 turns, the reciprocal of the fine structure constant α). The readout CCD sensor accumulates the phosphor image over 33 ms, and the analogue image is then readout at 30 Hz and digitized.

We also obtained digital CMOS camera images for the single electron emissions averaged over the acquisition range of 0.1–10 s on the chip, as demonstrated by the discrete or quantized steps in the integrated intensity of the OSR-based beam image over 97.7 million turns. These data provided the critical online assessment of the number of stored electrons in the ring in parallel with the streak camera studies.

EXPERIMENTAL ASPECTS

The APS Accelerators

The schematic of the linac and PAR is shown in Fig. 1 [5]. The small ring is designed to accumulate charges injected from the S-band linac which can operate at up to 30 Hz macropulse rate. Usually, the thermionic cathode rf gun is used to generate a short ~ 10 ns pulse train of 28 micropulses at 2.86 GHz. Operations at a 30 Hz rate allow the generation of 1–1.8 nC per macropulse. This is far more than we need, so for the low-charge studies up to 5 beam profile screens were inserted in the beam line to attenuate the number of electrons actually captured in the PAR. As we stepped in the screens, we compensated for the input signal loss in the digital camera with increased exposure times from 100 μ s up to 10 s. We roughly demonstrated an ultra-low charge monitor operating at 6 orders of magnitude below the rf BPM sum signal monitor used normally as a beam intensity monitor. These experiments were done at 375 MeV in the July 2019 injector studies period and 425 MeV in the November 2019 studies period.

The Optical Diagnostics

The OSR was transported from the PAR West dipole magnet source through a quartz window and via Al mirrors out of the accelerator enclosure up to a shrouded optics table on the mezzanine above [6]. This configuration (Fig. 2) provided access to the detectors in use, the digital CMOS camera and the Hamamatsu C5680 streak camera. (The PMT on the East dipole source was not optimized for these tests, but it did provide some medium-intensity level data.) The OSR signal was split by a mirror that was inserted halfway into the light path. Approximately half of the signal went to the digital camera and half to the Hamamatsu C5680 streak camera with an UV-IR transmitting input optics and S20 photocathode. This camera's vertical sweep unit was phase

* Work supported by the U.S. Department of Energy, Office of Science, Office of Basic Energy Sciences, under Contract No. DE-AC02-06CH11357.

[†] lumpkin@anl.gov

STREAK CAMERA MEASUREMENT OF ELECTRON BEAM ENERGY LOSS PER TURN IN THE ADVANCED PHOTON SOURCE PARTICLE ACCUMULATOR RING*

K. P. Wootton[†], J. R. Calvey, J. C. Dooling, K. C. Harkay, Y. Sun, B. X. Yang
 Argonne National Laboratory, Lemont, IL 60439, USA
 A. H. Lumpkin, Argonne Associate of Global Empire, LLC,
 Argonne National Laboratory, Lemont, IL 60439, USA

Abstract

Relativistic electron beams in storage rings radiate a significant fraction of beam energy per turn. As demonstrated in previous experiments, with the radiofrequency accelerating structures off, the turn-by-turn time of arrival of the electron bunch can be observed from the synchrotron radiation that it produces using a streak camera. In the present work, we present measurements of the energy loss per turn of an initially short electron bunch (~1 ps RMS) from a photocathode electron gun in the Advanced Photon Source Particle Accumulator Ring (375 MeV, 102 ns revolution period). With the streak camera synchroscan locked to the twelfth harmonic of the revolution frequency (117.3 MHz), we observe an injection transient in the horizontal direction.

INTRODUCTION

Injecting and accumulating charge in an electron storage ring is a dynamic process. It relies upon the emission of incoherent synchrotron radiation to damp the beam phase space to an equilibrium distribution. The energy loss per turn due to incoherent synchrotron radiation has previously been observed at GeV-scale electron storage rings [1, 2]. In those experiments, the electron beam was injected into the storage ring with the radiofrequency (RF) cavities switched off.

In the present work, dual-sweep streak camera measurements were performed which uniquely show inherent energy spread effects on the bunch length per turn, electron beam energy loss per turn, and the injection transverse transient for the initial ~1 ps duration bunch injected at 375 MeV.

THEORY

Energy Loss per Turn

In the absence of an accelerating RF voltage, an electron loses energy U_0 each turn due to incoherent synchrotron radiation [3]. The energy loss per turn can be calculated using the second synchrotron radiation integral I_0 [4]. Due to the non-zero momentum compaction factor α_c of the ring [4], the electron follows a dispersive orbit and arrives earlier each turn. At a time t following injection, the

change in arrival time of the electron bunch relative to the synchronous arrival time is given by [1]:

$$\Delta T_{\text{tot}} = \frac{1}{2} \frac{f_0}{E} \alpha_c U_0 t^2, \quad (1)$$

where f_0 is the revolution frequency, and E is the electron beam energy.

Injection Transient

Injection transients have previously been observed using turn-by-turn optical measurements at other laboratories [5–10]. For beams injected transversely off-axis for accumulation in a storage ring, the beam centroid is observed to oscillate at the betatron frequency in the plane of the orbit offset. In the Particle Accumulator Ring (PAR), electrons are injected with a horizontal offset from the central beam axis.

Beam centroid oscillations are observed at the betatron frequency if there is a dispersion mismatch, and oscillate at twice the betatron frequency if there is a beta function mismatch [11]. The observation of such transverse effects are deducible from dual-sweep streak camera images.

METHOD

A chain of injectors is used to accelerate electrons at the Advanced Photon Source (APS). The injector chain is illustrated schematically in Fig. 1 [12]. In the present work, we utilise electron beams from the photocathode gun (PCG) [13] and RF thermionic gun 2 (RG2) [14]. These beams are accelerated using the main linac accelerating structures (L2, L4 and L5), and injected into the PAR.

The PAR is operated as an electron damping ring [15]. In normal operation, beams injected from the linac are accumulated over multiple linac cycles and damped before injection as a single bunch into the booster synchrotron. The PAR RF system features two cavities with the fundamental RF cavity operating at the revolution frequency 9.77 MHz, and a 12th harmonic bunch compressing cavity operating at 117.2 MHz [16]. Calculated parameters of the PAR are summarised in Table 1.

To observe the electron beam arrival on a turn-by-turn basis, we used a streak camera installed at the PAR West synchrotron light port: a location in the lattice with non-zero horizontal dispersion [17–19]. The Hamamatsu model C5680 streak camera was operated in the dual-sweep configuration. A synchroscan module was used as the deflector

* Work supported by the U.S. Department of Energy, Office of Science, Office of Basic Energy Sciences, under Contract No. DE-AC02-06CH11357.

[†] kwootton@anl.gov

LOCO CORRECTIONS FOR BEAM TRAJECTORY OPTIMISATION ON THE ISIS ACCELERATOR

E.J. Brookes, H.V. Cavanagh, B. Jones, ISIS, Rutherford Appleton Laboratory, Oxfordshire, UK

Abstract

The ISIS facility at the Rutherford Appleton Laboratory, UK, produces neutron and muon beams for condensed matter research. Its 50 Hz, 800 MeV proton synchrotron delivers a mean beam power of 0.2 MW to two tungsten spallation targets.

The beam optics correction technique implemented in this work is Linear Optics from Closed Orbits (LOCO). LOCO modifies existing accelerator models according to a measured orbit-response matrix (ORM). This correction technique identifies imperfections in the machine lattice, and discrepancies between the machine and model.

The identification of erroneous elements through analysis of the measured ORM is demonstrated in this paper. In comparison to the operational settings achieved through the existing correction techniques, the initial test of the LOCO code demonstrates a 17 % improvement to the RMS trajectory deviation in the horizontal plane. It also shows an 11 % horizontal and 30 % vertical decrease to the standard deviation of trajectory measurements.

INTRODUCTION

The ISIS synchrotron accelerates pulses of 3×10^{13} protons from 70 MeV to 800 MeV at 50 Hz. Particles orbit the ring 12,000 times in the 10 ms acceleration cycle. The 163 m circumference ring contains 32 beam position monitors (BPMs), 14 steering magnets and 20 trim quadrupoles, to measure and adjust the beam optics. Errors in the lattice can result in deviations from the optimal orbit which are difficult to correct empirically. In order to minimise beam loss while maximising beam intensity and use of the available aperture, it is vital to be able to accurately manipulate the beam dynamics throughout the machine.

The Linear Optics from Closed Orbits (LOCO [1]) correction technique, implemented successfully on accelerators worldwide (Fermilab and CERN Boosters [2], Swiss Light Source (SLS) [3]), monitors the behaviour of the beam due to magnet perturbations in an orbit-response matrix (ORM). It then fits perturbations in a simulated version of the ORM, created using existing models in the accelerator design software MAD-X [4] to the measurements. After successful fitting, the resulting matrix is an accurate representation of the machine performance. The modifications made to the model are then reversed and implemented on the machine in order to locate and counteract errors identified by the fitting procedure.

EXISTING CORRECTION PROCEDURE

A model of the accelerator was created in order to predict and study beam optics throughout the machine. This provides the ability to build up a matrix of the ideal responses of all magnets throughout the acceleration cycle.

Originally, the correction technique used was based on the linear equation

$$x_i = R_{ij} \theta_j$$

where x_i is the measured position at monitor i , R_{ij} is the element in the response matrix and θ_j is the kick to magnet j . The matrix was minimised through Singular Value Decomposition in order to determine solutions for θ_j [5].

Later the model was rewritten in MAD-X and its orbit correction capabilities exploited. These corrections directly take measured positions from the machine and vary the N most efficient steering magnets in the model to fit this trajectory. The opposite changes can then be applied to the machine to centre the beam [6].

Though a measured ORM was recorded to aid with steering magnet strength calibration, the MAD-X model and subsequent calculations do not include the ORM in calculations and is therefore not a perfect correction. The constant evolution of real errors on the machine reduces the effectiveness of this method. By measuring a response matrix on the machine and using this in the calculations, the locations of alignment and field errors can be acknowledged and minimised in the correction. Another advantage to the LOCO method is that it uses only response measurements and magnet settings in calculations to determine adjustments to operational magnet settings.

ORBIT-RESPONSE MATRIX

The LOCO method relies on the measurement of the ORM. This is measured by recording the beam position response on the same pulse at all BPMs for a change in current applied to each individual magnet. Each element in the matrix is formed by taking the gradient of three points measured in this fashion. In order to accurately represent the real machine dynamics, the statistical error taken at the 95% confidence level is included in calculations.

The ORM measurements begin with the machine operational setup with a reasonably well-centred beam. The initial measurements from the BPMs are recorded before magnets are individually varied twice, in turn. On each current change, the beam loss was checked around the ring to ensure the beam remained in the vacuum chamber.

During these measurements, it is important to ensure that the current adjustments are large enough to record a measurable change at the BPMs, but small enough that the beam remains within the vacuum chamber. Therefore, the choice of measurement timing and kick strength are important factors. Measurements at ISIS are taken at 4 ms in the acceleration cycle with a total current range of 40 A per magnet. This allows a balance between available aperture and magnetic rigidity.

Since the measured ORM relates to a specific setup of the machine, the response matrix should be re-measured

SIMULATION OF CHERENKOV DIFFRACTION RADIATION FOR VARIOUS RADIATOR DESIGNS

K. Lasocha^{*1}, T. Lefevre, N. Mounet, A. Schloegelhofer², CERN, Geneva, Switzerland
 D. M. Harryman, JAI, Royal Holloway, University of London, Egham, Surrey, UK
¹also at Institute of Physics, Jagiellonian University, Krakow, Poland
²also at TU Wien, Vienna, Austria

Abstract

Studies performed during the last few years at different facilities have indicated that the emission of Cherenkov Diffraction Radiation (ChDR) can be exploited for a range of non-invasive diagnostics. The question remains of how to choose an optimal dielectric material and which radiator shapes give the most promising results. This contribution presents a semi-analytical framework for calculating the electromagnetic field of a charged particle beam, taking into consideration its interaction with surrounding structures. It allows us to directly compute ChDR at arbitrary probe positions inside the radiator. Several configurations will be discussed and presented, including flat and cylindrical radiators of various dimensions and electrical properties, as well as multilayer structures obtained by adding coatings of metallic nanolayers.

INTRODUCTION

A decade after the discovery of Cherenkov radiation [1], Ginzburg and Frank [2] studied the radiation emitted by a particle moving along the axis of an infinitely long evacuated tunnel surrounded by a dielectric medium. During the following decades Linhart [3] and Ulrich [4] described a similar phenomenon associated with a particle moving parallel to the surface of a dielectric half space. These two are the initial examples of Cherenkov Diffraction Radiation (ChDR), which describes the emitted radiation of a charged particle passing in the close vicinity of a dielectric medium and having a velocity greater than the phase velocity of light in that medium.

Recently, the possibilities which ChDR brings to non-invasive beam diagnostics have been extensively investigated, with the first observation of incoherent radiation, using GeV electrons and positrons at Cornell [5, 6]. What followed were designs of beam position monitors [7] as well as bunch length monitors [8] based on the coherent radiation from short bunches. In parallel more refined radiation models have been developed [9, 10]. In addition, several accelerator facilities across the world have confirmed the feasibility of observing ChDR [11–13].

All this interest motivates the need of developing a tool for quantitative description of ChDR for real case scenarios. Most analytic models serve well only in a limited spectrum of cases, due to the simplicity of the considered radiators. On the other hand, more flexible numerical simulations are

very time consuming, especially if the radiator components differ significantly in size. The aim of this contribution is to present a semi-analytical approach, which is based on numerical calculations of the beam field propagating across surrounding materials, according to constraints set by the Maxwell equations. The presented procedure describes radiators infinite in the direction of beam propagation, but gives the possibility of studying complex multilayer structures orthogonal to the direction of beam propagation. The proposed method should be treated as a natural extension of a framework for beam impedance calculations, developed at CERN [14].

CYLINDRICAL GEOMETRY

We shall start by considering the geometry presented in Fig. 1 which is described using cylindrical coordinates r , θ and s . A charged particle travels with the velocity $v = \beta c$ along the s axis in the centre of an axisymmetric structure, consisting of an arbitrary number of layers. Each layer has its own permittivity ϵ_i and permeability μ_i , which may be frequency dependent. The central layer is constrained to be vacuum, but the subsequent layers may be any material, with the outermost layer extending to infinity.

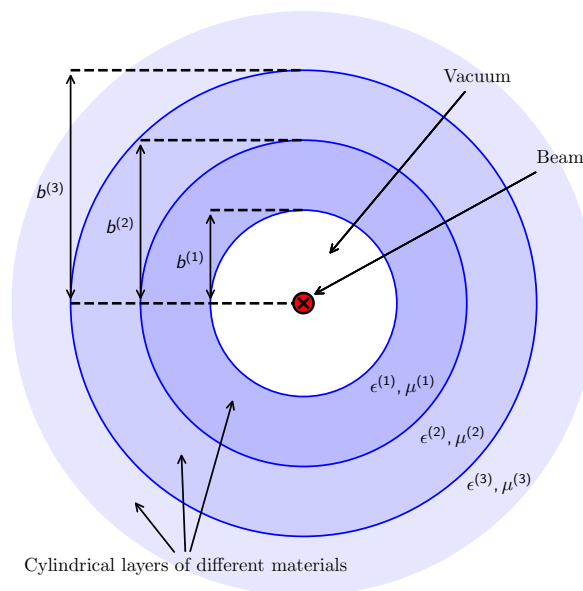


Figure 1: Cylindrical geometry with concentric layers of different materials. The beam travels along the axis perpendicular to the page.

* kacper.lasocha@cern.ch

DEVELOPMENT OF NOVEL NON-DESTRUCTIVE 2D AND 3D BEAM MONITORING DETECTORS AT THE BERN MEDICAL CYCLOTRON*

C. Belver-Aguilar[†], T. S. Carzaniga, A. Gsponer, P. Häffner, P. Scampoli¹,
M. Schmid, S. Braccini, Albert Einstein Center for Fundamental Physics (AEC),
Laboratory of High Energy Physics (LHEP), University of Bern, Bern, Switzerland
G. Molinari, TERA Foundation, Novara, Italy

¹also at Department of Physics "Ettore Pancini", University of Napoli Federico II, Naples, Italy

Abstract

The Laboratory for High Energy Physics (LHEP) at the University of Bern is developing novel beam monitoring detectors for the 18 MeV medical cyclotron in operation at the Bern University Hospital (Inselspital). A 2D non-destructive beam monitor — named π^2 — was developed, based on a thin aluminium foil coated with P47 scintillating material and a camera. It measures the transverse position, shape, and intensity of the beams for several applications, as radiation hardness or radioisotope production studies. This detector allows the processing of data in real time and a reconstruction of the transverse phase space. Based on the π^2 , a first prototype of a 3D beam monitoring detector — named π^3 — was conceived, constructed, and tested. It is based on the same scintillating foil mounted on a movable support with a miniaturized camera. The π^3 detector allows for the study of the beam evolution along a beam line, even inside a magnet, and the reconstruction of the beam envelope. In this paper, we report about the design, construction and beam tests performed with these two detectors. Further developments will be also presented and discussed.

INTRODUCTION

Beam monitoring plays a crucial role in both the commissioning and operation of particle accelerators. For some medical cyclotron applications, like the irradiation of small and expensive solid targets [1], non-destructive beam monitors are essential.

At the Bern medical cyclotron, three different beam monitors have been developed by the LHEP. The first one, named UniBEaM [2], is used to measure the beam transverse profile by means of a moving scintillating fiber. The second one is the π^2 , a detector based on a fixed scintillating foil and a camera, which allows to measure the beam spot in 2D. The third one is the first prototype of an evolution of the π^2 detector, called π^3 , where both the scintillating foil and the camera are mounted in a moving support to allow assessing the beam evolution along the beam path.

In this paper, the main features and beam tests of the π^2 and π^3 beam monitors are reported. Beam tests were performed using the 6 m long Beam Transfer Line (BTL) [3] and the 18 MeV proton beam delivered by the Bern medical cyclotron.

* Work partially supported by the Swiss National Science Foundation (SNSF). Grants: 200021_175749, CRSII5_180352, CR2312_156852

[†] carolina.belver@lhep.unibe.ch

THE π^2 BEAM MONITOR

The π^2 hardware, based on a phosphor screen and a camera, is a common design which was already used in some other accelerator facilities, for example at the Korean Institute of Radiological and Medical Sciences [4]. However, the pre-processing and analysis software that has been implemented in our detector represents a step forward in the analysis of the images provided by this type of detectors: it is being developed to perform real-time measurements of beam position, size and current, but also phase space representation and beam emittance measurement, as well as tuning of the BTL magnet currents.

The π^2 detector, as shown in Fig. 1, consists of a cerium- and terbium-doped yttrium orthosilicate ($Y_2SiO_5:Ce,Tb$) phosphor screen (P47) and a camera, to control the beam position and beam size during a proton irradiation. This detector can monitor beam currents in the range between pA and several μA .

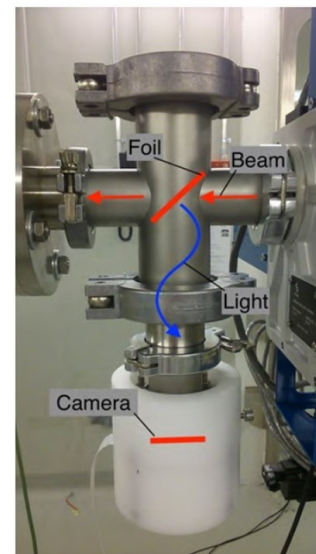


Figure 1: The KF40 four way pipe that supports the π^2 detector. The positions of the scintillating foil and camera are shown in red.

The scintillating screen is placed at the center of a KF40 four way pipe with a tilt angle of 45° with respect to the beam path. It has a diameter of 20 mm, and consists of a $0.8 \mu m$ aluminum foil coated with a $1 \mu m$ layer of P47. An optimal heat dissipation is achieved by gluing the thin

DEVELOPMENT OF A THERMAL RESPONSE MODEL FOR WIRE GRID PROFILE MONITORS AND BENCHMARKING TO CERN LINAC4 EXPERIMENTS

A. Navarro*, F. Roncarolo, CERN, Geneva, Switzerland
M. Sapinski, TERA Foundation

Abstract

The operation of wire grids as beam profile monitors, both in terms of measurement accuracy and wire integrity, can be heavily affected by the thermal response of the wires to the energy deposited by the charged particles. A comprehensive model to describe such interaction has been implemented including beam induced heating, all relevant cooling processes and the various phenomena contributing to the wire signal such as secondary emission and H^- electron scattering. The output from this model gives a prediction of the wire signal and temperature evolution under different beam conditions. The model has been applied to the wire grids of the CERN LINAC4 160 MeV H^- beam and compared to experimental measurements. This successful benchmarking allowed the model to be used to review the beam power limits for operating wire grids in LINAC4.

INTRODUCTION

Wire Grid Profile monitors [1] are extensively used for transverse beam profile measurements in linacs and transfer lines. They consist of a series of thin wires supported on a frame, as shown in Fig. 1. The signal on each wire, used to reconstruct the beam profile, is generated by a combination of different phenomena occurring after the beam-wire interaction, such as direct charge deposition (e.g. stripped electrons stopped in the wire in the case of H^- beams), secondary emission of electrons, thermionic emission of electrons, etc. In most cases these wire grids are movable devices that are inserted into the beam line only when needed.

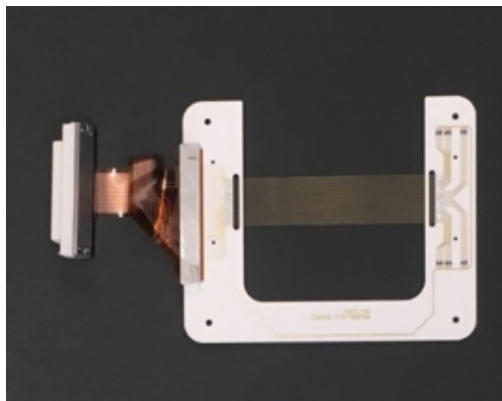


Figure 1: Example of a Wire Grid recently installed in the CERN LINAC4, featuring $40\ \mu\text{m}$ tungsten wires separated by $0.5\ \text{mm}$.

* araceli.navarro.fernandez@cern.ch

For a given wire grid detector design and materials, the beam power density, defined by beam intensity, transverse size and longitudinal structure, can generate high wire temperatures, which may perturb the measurement accuracy or even damage the detector. An example of such an issue is shown in Fig. 2, where a LINAC4 grid suffered overheating of the wires after operation at 160 MeV. This prompted the need for a thorough understanding of the wire temperature evolution in order to correctly retrieve the transverse beam characteristics and set operational limits on the beam power allowed for grid use.

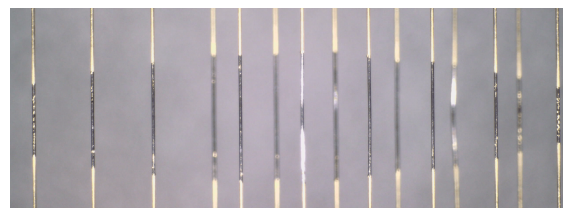


Figure 2: Effect of wire grid heating as observed with an optical microscope, with the individual wires visible over the grey background. The evaporation of the gold coating (dark central area on each wire) is clearly visible, from which one can even infer the beam density profile in the plane of measurement.

The original LINAC4 wire grid design was already supported by theoretical calculations of the thermal response [2, 3]. However, the operational limits defined by this approach clearly did not take into account all phenomena. We therefore adopted and applied another model, initially developed for fast wire scanners [4], with the aim of benchmarking dedicated beam measurements and defining operational limits.

Measuring the temperature evolution of thin wires as they interact with particle beams is challenging. Firstly, the temperature range is broad, from 300 K up to 3000 K, which excludes the use of contact thermometers [5]. Secondly, the small wire diameters makes the use of optical methods [6] very difficult. Benchmarking of the simulations is therefore based on the observation of thermionic currents, occurring at well known temperatures, similar to the studies presented in [7] for measuring stripping foil temperatures.

HEATING MODEL

During operation, the wire temperature increase due to particles energy deposition is accompanied by various cooling processes occurring both during and after the beam passage.

A BEAM PROFILE MONITOR FOR HIGH ENERGY PROTON BEAMS USING MICROFABRICATION TECHNIQUES*

Wilfrid Farabolini, Antonio Gilardi, Blerina Gkotse, Alessandro Mapelli, Isidre Mateu[†],
Viktoria Meskova^{†,1}, Giuseppe Pezzullo, Federico Ravotti, Ourania Sidiropoulou,
European Organization for Nuclear Research (CERN), Geneva, Switzerland
Didier Bouvet, Jean-Michel Sallese,
École Polytechnique Fédérale de Lausanne (EPFL), Lausanne, Switzerland
¹also at École Polytechnique Fédérale de Lausanne (EPFL), Lausanne, Switzerland

Abstract

In High Energy Physics (HEP) experiments it is a common practice to expose electronic components and systems to particle beams, in order to assess their level of radiation tolerance and reliability when operating in a radiation environment. One of the facilities used for such tests is the Proton Irradiation Facility (IRRAD) at the European Organization for Nuclear Research (CERN). In order to properly control the 24 GeV/c proton beam and guarantee reliable results during the irradiation tests, Beam Profile Monitor (BPM) devices are used. The current BPMs are fabricated as standard flexible PCBs featuring a matrix of metallic sensing pads. When exposed to the beam, secondary electrons are emitted from each pad, thus generating a charge proportional to the particle flux crossing the pads. The charge is measured individually for each pad using a dedicated readout system, and so the shape, the position and the intensity of the beam are obtained. The beam profile determination with this technique requires thus the usage of non-invasive and radiation tolerant ($\sim 10^{18}$ p/cm²/y) sensing elements. This study proposes a new fabrication method using microfabrication techniques in order to improve the BPMs performance while greatly reducing the device thickness, thus making them also appropriate for the monitoring of lower energy and intensity particle beams. The fabricated prototypes were tested at the CERN CLEAR facility with 200 MeV electrons.

INTRODUCTION

Beam monitoring instrumentation is essential for the IRRAD proton facility, where about a thousand samples are irradiated every year, with a total accumulated proton fluence typically exceeding 10^{18} p/cm². To successfully perform these tests, a precise monitoring of the proton beam profile is essential. Therefore, flexible Printed Circuit Boards (PCBs) patterned with a matrix of sensing pixels, have been used as Secondary Electron Emission (SEE) Beam Profile Monitors (BPMs) since several years [1]. These devices were manufactured with a standard flex-PCB technology, composed of multiple copper layers sandwiched with epoxy glue. These stacked layers were origi-

nally considered to multiply the signal, but had the drawback of making a rather thick device (~ 0.6 mm). Moreover, radiation-induced damage effects were observed in the sensing region of the device and, sometimes, induced its failure during operation. These effects were attributed to the epoxy not resisting the levels of radiation at which the BPMs are exposed.

This article presents a series of working prototypes based on a newly developed microfabrication process with nanometre aluminium (Al) layers on thin polymeric substrates. Compared to the old BPMs, the new prototypes are thinner (20 times the substrate, and one order of magnitude the metal), and therefore less invasive when interacting with the beam. They are expected to present an enhanced radiation tolerance thanks to the employed microfabrication technology (which avoids gluing) and have a higher sensitivity because of the usage of Aluminium (Al) as sensing material which has, intrinsically, higher secondary electron yield (SEY) than copper.

The validation of their functionality with experiments in dedicated test-benches and a particle beam, is also presented in this paper. These experiments are the prerequisite to have operational BPM devices for the IRRAD facility after the CERN Long Shutdown 2, as well as, to investigate their usability in very low energy beams as of interest for more general-purpose applications (e.g. industry, medicine).

STATE OF THE ART

The standard beam instrumentation for secondary beam area at CERN is generally not designed to be used in an irradiation beam-line. To cope with this problem, custom-made standard BPM devices consisting on rectangular-shaped, flexible PCBs, patterned with a matrix of metallic sensing pads on the one end, and a multi-pin connector on the opposite one, have been developed for the IRRAD facility at CERN (see Fig. 1(left)).

Secondary Electron Emission (SEE), on which the BPMs working principle is based, occurs when a high-intensity beam impinges on a metallic foil and electrons of the energy below 50 eV (Secondary Electrons (SE)) are produced. The number of SEs ejected from the foil is proportional to the local beam intensity [2]. The SEs are then converted into an electrical signal, which is measured and recorded by a dedicated electronics. An online web application, finally displays the current from every metallic pad resulting in two-dimensional beam profiles.

*Work supported by the European Union's Horizon 2020 research and innovation programme under grant agreement No 777222 (ATTRACT Phase-1 project).

[†]e-mail address: isidre.mateu@cern.ch, viktoria.meskova@cern.ch.

THz DETECTION TECHNIQUES OVERVIEW

F. Mazzocchi, D. Strauß, T. Scherer, KIT IAM-AWP, Eggenstein Leopoldshafen, Germany
A. S. Müller, E. Bründermann, KIT IBPT, Eggenstein Leopoldshafen, Germany

Abstract

In the following work, we present a general overview of the various techniques that can be employed to detect and characterize THz waves. The overview will take into consideration several technologies based on different physical principia, capable of both broadband and narrowband detection.

INTRODUCTION

In recent years, the THz part of the electromagnetic spectrum has attracted special attention due to the broad range of possible applications deriving from it and its presence in multiple natural phenomena. T-rays are able to pass almost unobstructed through a wide range of non-polar materials such as fabrics, paper, wood, ceramics, plastics and plasma. Radioastronomy, spectroscopy, molecular sensing, plasma diagnostics, security and biomedical imaging are only a few possible uses of the THz spectrum. Such wide range of applications demands a similarly wide range of detection techniques and devices. The methods presented in this overview have been organized in four groups, based on the physical principia they rely on: thermal, direct, heterodyne and sampling detection. For each of the techniques, the operational limits and the most frequent applications are also presented.

THERMAL DETECTORS

Conceptually speaking, thermal detectors represent the simplest sensors employed for power measurements in the THz region, and can be thought as composed by three distinct parts: the radiation absorber, the heat sink and the thermal link between them (Fig. 1).

Radiation impinging on the absorber determines a rise in temperature $\Theta(T)$ given by [1]

$$\Theta = \frac{\eta P_{\omega}}{\sqrt{\omega^2 C^2 + G^2}} \quad (1)$$

where C and G are, respectively, the thermal capacity and conductivity. η is the detection efficiency and P_{ω} the power related to the incoming radiation. We can define the response time of the detector as

$$\tau = C/G \quad (2)$$

that is minimized for small thermal masses and high conductivities. For room temperature detectors, we can expect response time ranging from as few seconds to a few milliseconds. Examples of thermal detectors include pyroelectrics, thermopiles, Golay cells and bolometers. Nowadays, bolometers are the most widespread of these kind of

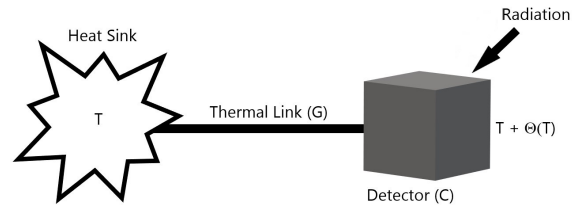


Figure 1: Schematic representation of a thermal detector main elements.

detectors, and will be the main subject of the section. The reader interested in the other aforementioned devices can refer to [1] for a more extensive treatment. In 1961 Low [2] described a popular bolometer based on germanium, that consisted in a doped semiconductor absorber suspended in vacuum by wires that function as both thermal and electrical contacts. The semiconductor is biased with a constant current, and the change in temperature induced by the absorbed radiation determines a detectable change in the electrical resistance of the device. We can introduce the generalized resistance temperature coefficient α as:

$$\alpha = R^{-1} (dR/dT) \quad (3)$$

where R and T are the resistance and temperature. α represents the steepness of the R/T curve. Of course the higher the voltage response of the detector to a given signal, the better. This is achieved by cooling the device down to liquid helium temperatures or lower. The obtained reduced thermal capacitance determines therefore a faster and more sensitive detector. Given that bolometers are operated with a current bias, there is an additional varying electrical power that leads to an effective thermal time constant $G_{Eff} = G - \alpha P_E = G - I^2 R \alpha$. Semiconductor bolometers typically require heavy doping, in order for them to have a more metal like behaviour of the resistance, avoiding thermal runaways. The main conduction mechanism is, in this case, performed by charge carriers passing from one donor atom to the other. The resistance temperature coefficient takes the explicit form of

$$\alpha = -\frac{1}{2} \sqrt{\frac{T_0}{T^3}} \quad (4)$$

with T_0 in the order of 2–10 K. Semiconductor bolometers can reach Noise Equivalent Power (NEP) in the order of 10^{-12} – 10^{-13} W/Hz^{1/2} in a 0.15–15 THz frequency range and response times of roughly 10 μ s. Applications in astrophysics are the most widespread, with notable instru-

Content from this work may be used under the terms of the CC BY 3.0 licence (© 2020). Any distribution of this work must maintain attribution to the author(s), title of the work, publisher, and DOI

FILLING PATTERN MEASUREMENT USING A 500 MHz DIGITIZER AT SOLEIL AND APS STORAGE RINGS

D. Bisiach, M. Cargnelutti, P. Leban, M. Žnidarčič, Instrumentation Technologies doo, Solkan, Slovenia

N. Hubert, D. Pedeau, SOLEIL, Gif-sur-Yvette, Paris, France

A. Brill, N. Sereno, ANL, Lemont-Illinois, USA

Abstract

Filling pattern was measured at SOLEIL and APS storage ring using a 500 MHz digitizer. Various filling patterns were measured: from a single bunch to a multi-bunch hybrid fill. The digitizer has 14-bit granularity and locks the sampling clock to exact RF frequency (352 MHz). Signals were sampled from the standard BPM pickup and APD diode. Data were retrieved using Matlab and Labview interfaces and compared to existing systems.

INTRODUCTION

An essential part of the synchrotron diagnostics system involves the investigation of the bucket distribution during the operation.

Modern light sources allow to operate with different filling pattern modes (e.g. single bunch, multi-bunch, hybrid patterns), and knowledge of the real-time bunch charge longitudinal distribution can help to tune the beam stability and performance [1].

Digitizers with high ADC resolution and wide dynamic range are an alternative to the existing high sampling rate oscilloscopes that are commonly used in combination with BPM pick-up or APD diode detectors.

The total dynamic range is 90 dB which is achieved with the use of the 0-31 dB frontend attenuators. The instrument is triggerable with a maximum trigger frequency of 1kHz (see Fig. 1).

The Libera Digit 500 DC version has an analog bandwidth of 0-250 MHz, the Libera Digit 500 AC version used during the testing at Soleil, and APS has a 250 MHz-2 GHz analog bandwidth.

The purpose of these measurements was to confirm that the Libera Digit 500 could be used as a filling pattern monitoring device in case of BPM pickups and to evaluate its behavior also using diode detectors [3].

Access to the interface can be performed using a TANGO client, Labview, or the SSH interface.

MEASUREMENTS – SOLEIL

The fill pattern monitoring testing consisted of testing two setups, the first using a BPM pickup as a bunch detector and the second using an APD diode setup.

Fill Pattern Monitor Using BPM

The original filling pattern monitoring instrumentation at Soleil consists of an Agilent Digitizer with 8 GS/s-8 bit resolution.

The setup with the Libera Digit 500 AC is illustrated in Fig.2 and it was implemented to retrieve the signal directly from a pickup using attenuators and phase shifters to tune the signal delays and the bunch flat top.

The pickup outputs (A, B, C, and D) were connected to fixed attenuators. Each attenuator output entered a mechanical phase shifter (API Technologies – Weinschel, bandwidth DC-3GHz). Since the signal power was still too high some additional attenuators were placed before the signal splitter-combiner (Mini-Circuits ZFRSC-4-842-S+, DC-8400 MHz). The combined signal then entered an additional mechanical phase shifter (4428C from ARRA, bandwidth DC-4 GHz).

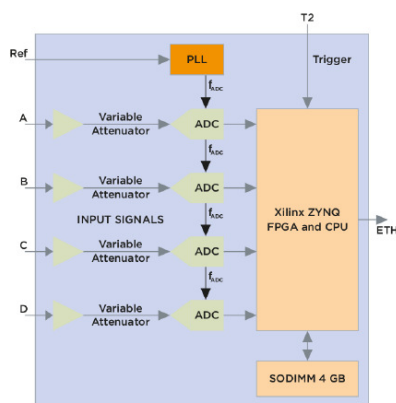


Figure 1: Libera Digit 500 block schematics.

The Libera Digit 500 is a 500 MHz/14-bit ADC digitizer based on the CavityBPM hardware [2] with the possibility to customize the frontend (e.g. input bandwidth, additional filters...). The sampling clock is locked to an external reference input to lock the internal PLL (maximum jitter 10 ps) on the machine RF clock. Data from the ADC are directly sent to a Xilinx Zynq 7035 based SOC which runs both the signal processing and the OS.

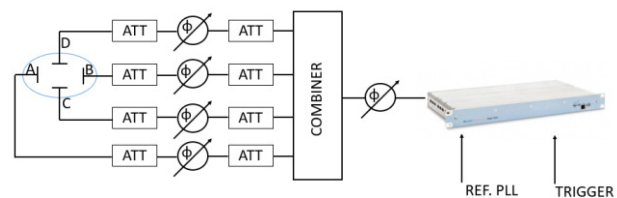


Figure 2: Setup schematics.

BUNCH PURITY MEASUREMENT FOR SSRF*

B.Gao, L.W.Lai[†], X.Q.Liu, S.S.Cao, Y.B.Leng

Shanghai Advanced Research Institute, Chinese Academy of Sciences, Shanghai, China

Abstract

SSRF is currently working on the beam line phase-II project, which has moved toward laser/X-ray pump-probe experiments. To quantify the bunch filling pattern and purity of the timing bunch, high precision beam charge measurement is necessary. Therefore, a bunch purity monitor based on the time-correlated single-photon counting techniques has been installed. A series of tests to evaluate the system have been carried out, according to these results, it is able to predict the system performance. The system has exceptionally good time resolution (a few pico seconds) and high dynamic range (more than seven orders of magnitude).

INTRODUCTION

Shanghai synchrotron radiation facility (SSRF) is a third-generation synchrotron radiation light source. It has completed a lot of research work in the 11 years since its establishment. The ongoing SSRF beamline phase-II project, the main construction content includes the construction of 16 beam lines and experimental stations, experimental auxiliary systems, light source performance expansion, etc. The project focuses on major scientific and technical issues in the fields of energy, environment, materials, condensed matter physics, earth sciences, chemistry and life sciences, with the goal of greatly improving the overall experimental capabilities of SSRF. It also has a lot of technology goals. To realize the third-generation synchrotron radiation light source experimental technology with near-limit resolution (time/space/energy/momentum), realize the innovative combination of photon energy regions and ultra-long station hall experimental technology, and realize online/offline comprehensive experimental capabilities [1].

At SSRF storage ring 720 RF buckets are available be populated with electrons. At the primary operational mode, 200 buckets are left empty, only 520 bunches in 4 bunch trains are injected to the storage ring. During the construction of the SSRF beamline phase-II project, the requirements for time-resolved experiments and special time structure filling modes are proposed. In order to meet this requirement, SSRF will be operated in hybrid mode. In the future, one of the buckets in the dark place will be populated with the timing bunch.

For the time-resolved experiment, in the detection window, there expects no other interference except for the synchronization light emitted by the probe bunch, that is, it is

necessary to ensure that there are no electrons in the buckets around the timing bunch. These experiments typically require the pattern to be as exact as possible, with ideally no electrons in unwanted bucket/bunch positions: a typical ratio of $10^5:1$ between wanted/unwanted populations is desired this ratio often being referred to as the bunch purity [2]. However, in actual operation after the bunch is excited from the electron gun, due to acceleration errors during acceleration, part of the electrons will be captured by the RF buckets adjacent to the timing bunch, resulting in poor bunch purity; In addition, due to the effect of intra-beam scattering, there will also has a small amount of electrons in the adjacent buckets. Therefore, the users want to get more accurate bunch pattern, the purity measurement concept is born from this. Therefore, the injector and X-Y kicker magnets must be optimized to eliminate unwanted charges. At this time, the measurement of the bunch pattern provides a very important basis.

Historically, a dedicated BPM was used to monitor the filling pattern at SSRF and other light sources [3-6]. Although the beam charge monitor based on the BPM provides a rough monitoring of the bunch pattern, the resolution can reach to 0.02% (average measurement), this method is far from the requirement of purity measurement. Therefore, a more precise system is needed to measure the bunch purity of the timing bunch.

A bunch purity measurement system based on the photomultiplier tube and time-correlated single photon counter has been established at SSRF. This article introduces the construction of this system, the verification and optimization of system performance, and the related beam experiment results.

TIME-CORRELATED SINGLE PHOTON COUNTING

Time-correlated single photon counting (TCSPC) has the advantages of good time resolution, high sensitivity, high measurement accuracy, and large dynamic range. Photon counting technology is a digital technology that measures discrete photon pulses [7,8]. The intensity of the detected photocurrent is lower than the thermal noise level ($10^{-14}W$) of the photodetector itself at room temperature. It is difficult to use the usual DC detection method Extract it out. The photon counting method takes advantage of the natural discrete characteristics of the photon detector's output electrical signals under weak light irradiation, and uses pulse discrimination technology and digital counting technology to identify and extract extremely weak signals. The photomultiplier tube (PMT) outputs a fluctuating direct current when the input light intensity is relatively strong, and when the light is weak, the output photocurrent is no longer continuous, and when the input light is extremely

* Work supported by Youth Innovation Promotion Association, CAS (Grant No. 2019290); SSRF-II beamline project

[†] lailongwei@zjlab.org.cn

MODERNIZATION AND OPERATION OF IONIZATION-PROPORTIONAL GAS COUNTER AT INR RAS PROTON LINAC

A. Melnikov[†], S. Gavrilov¹

Institute for Nuclear Research of the Russian Academy of Sciences, Troitsk, Moscow, Russia
¹also at Moscow Institute of Physics and Technology (National Research University), Moscow, Russia

Abstract

Multinode gas counter is used as a detector for low intensity proton beam diagnostics at INR RAS linac. The device consists of ionization chamber to measure beam current and two proportional chambers, based on stripe geometry, to measure beam profiles. The data is processed with Labview software. The models and methods predicting operational characteristics of the counter in ionization and proportional mode are presented. An analytical model of recombination was tested to predict the saturation voltage for ionization mode. Beam test results and operational characteristics of the counter are presented as well as results of investigations of counter degradation under the beam. A new design of a gas filled counter is also discussed.

INTRODUCTION

A proton irradiation facility (PIF) at INR RAS linac is used to study radiation effects in electronic components. This facility is characterized with operational parameters: proton energy - 20÷210 MeV; particles per pulse - $10^7 \div 10^{12}$; pulse duration - 0.3÷180 μ s; pulse repetition rate - 1÷50 Hz.

Partially diagnostics is realized with a beam current transformer (BCT) installed in the beam pipe. The BCT provides absolute nondestructive measurements of beam pulse current with the amplitude > 25 μ A. To measure beam current and profiles for less intensive beams MGC based on gas ionization is foreseen.

MULTIANODE GAS COUNTER

Multinode gas counter (MGC) [1] consists of 5 plates (Fig. 1) which are printed-circuit boards made of FR4 with 0.5 mm width. The metal covering is 18 μ m nickel, plated with 0.05 μ m immersive gold.

Three central plates form a dual gap ionization chamber. Electrons of primary ionization are collected at the middle anode plate by a quasi-uniform electrostatic field. This part of the detector allows to measure beam current in an ionization mode.

Lateral regions are proportional chambers for beam position and profile measurements. Electrons are collected at the multichannel anode structure, which consists of 25 stripes with 100 μ m width, 100 mm length and 4 mm spacing. Strong nonuniform field around stripes leads to electron avalanches, increasing the signal.

[†] alexei.a.melnikov@gmail.com

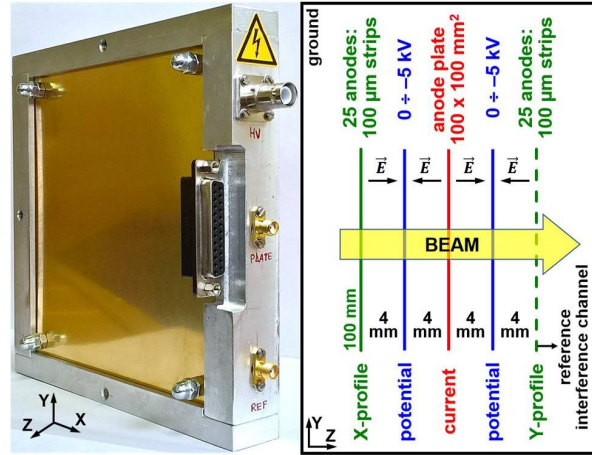


Figure 1: MGC photo and layout.

The total assembly of the counter is not sealed. The filling gas is atmospheric air.

The information about readout electronics and data acquisition system can be found elsewhere [2].

IONIZATION MODE

The number of primary ionization electrons defines the plateau level of ionization mode. The computed signal level based on dE/dx agrees with experimental results with 10% precision [2]. The gas composition was assumed as 80% N_2 and 20% O_2 molecules at standard conditions.

The measured signal from ionization chamber electrodes is caused by induced currents due to the moving electrons and ions: $i^{e,+,-}$ [3].

$$i^e(t) = \frac{Q_0}{t_{de}} \left(1 - \frac{t}{t_{de}} \right) \exp\left(-\frac{t}{T_a}\right).$$

$$i^+(t) = \frac{Q_0}{t_{d+}} \left(1 - \frac{t}{t_{d+}} \right).$$

$$i^-(t) = \frac{Q_0}{t_{d-}} \left[1 - \frac{t}{t_{d-}} - \frac{T_a}{t_{de}} \left\{ 1 - \exp\left(-\frac{t_{de}}{T_a} \left(1 - \frac{t}{t_{d-}} \right)\right) \right\} \right],$$

where Q_0 is the total charge of primary particles, $t_{de,+,-}$ is the drift time of electrons or ions of corresponding sign, T_a is an attachment time.

REENTRANT CAVITY RESONATOR AS A BEAM CURRENT MONITOR (BCM) FOR A MEDICAL CYCLOTRON FACILITY*

S. Srinivasan[†], P.-A. Duperrex, J. M. Schippers
 Paul Scherrer Institut, 5232 Villigen PSI, Switzerland

Abstract

At PSI, a dedicated proton therapy facility, with a superconducting cyclotron, delivers 250 MeV beam energy, pulsed at 72.85 MHz. The measurement of beam currents (0.1-10 nA) is generally performed by ionisation chambers (ICs), but at the expense of reduced beam quality, and scattering issues. There is a strong demand to have accurate signal with a minimal beam disturbance. A cavity resonator, on fundamental resonance mode, has been built for this purpose. The cavity, coupled to the second harmonic of the pulse rate, provides signals proportional to the beam current. It is installed in a beamline to measure for the energy range 238-70 MeV. Good agreement is reached between the expected and measured sensitivity of the cavity. The cavity delivers information for currents down to 0.15 nA with a resolution of 0.05 nA when integrated over one second. Its application is limited to a machine-safety monitor to trigger interlocks, within the existing domain of the proton therapy due to the low beam current limits. With new advancements in proton therapy, especially FLASH, the cavity resonator's application as an online beam-monitoring device is feasible.

INTRODUCTION

In proton radiation therapy at PSI, proton beams of low intensities (0.1-10 nA) are traditionally measured with ICs [1]. We face a strict regulation of their use due to scattering issues.

A non-invasive BCM, is modelled as a lumped element LC circuit, such that its fundamental mode of resonance is at 145.7 MHz as described in [2]. The induced electric and magnetic fields are concentrated in the capacitive (region 2) and the inductive zones (region 3) of the BCM, as shown in Figure 1. Here, we report on its beamline measurements for the energy range 238-70 MeV.

BCM LOCATION

The proton therapy facility, PROSCAN, is a temperature-controlled environment (28.5 ± 0.5 °C), to have stable operating conditions for its beamline elements. The energy degradation (238-70 MeV), is achieved with the help of a degrader [3], which results in growth of emittance and energy spread [4-6]. An Energy Selection System (ESS), along with a pair of collimators, maintains the beam quality at patient location by limiting the energy spread. An elongation of the proton bunch length and an energy dependent decrease in the bunch amplitude downstream of the degrader is the consequence. This affects the BCM's sensitivity as it is coupled to the second harmonic of the pulse repetition rate, which is located at sixteen meters from the degrader exit as shown in Figure 2.

A Sinc function normalised to average beam current and at multiple energies is given in Table 1, represents the BCM's expected second harmonic amplitude factor, A_2 , proportional to the sensitivity.

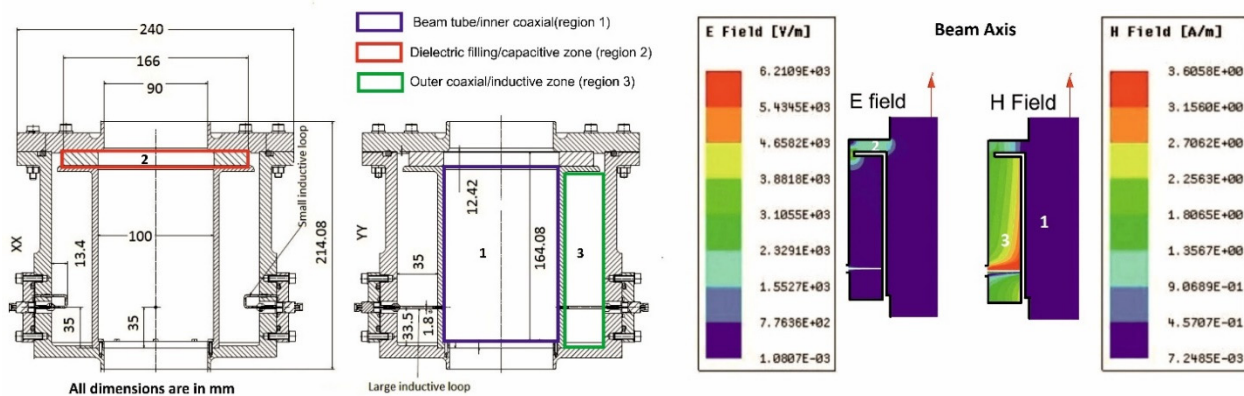


Figure 1: Cut-section of the reentrant cavity resonator (XX and YY) with dimensions corresponding to TM_{010} frequency at 145.7 MHz. Region 1, 2 and 3 represent the inner coaxial (or beam tube), dielectric filling in the reentrant gap (capacitive zone), and the outer coaxial (inductive zone). The E fields and H fields excited within the resonator shows the separation of the capacitive (marked as 2) and inductive zones (marked as 3) in this resonator (right).

* This project has received funding from the European Union's Horizon 2020 research and innovation programme under the Marie Skłodowska-Curie grant agreement No 675265.

[†] sudharsan.srinivasan@psi.ch

INVESTIGATION OF AN OPTICAL-FIBER BASED BEAM LOSS MONITOR AT THE J-PARC EXTRACTION NEUTRINO BEAMLINE*

S. Cao[†], M. Friend, High Energy Accelerator Research Organization (KEK), Tsukuba, Japan

Abstract

Optical fibers, which at once generate and guide Cherenkov light when charged particles pass through them, are widely used to monitor the beam loss at accelerator facilities. We investigate this application at the J-PARC extraction neutrino beamline, where a 30 GeV proton beam with eight bunches of ~ 13 ns (1σ) bunch width and 581 ns bunch interval, is extracted from the Main Ring, transported, and hit onto a graphite target to produce a highly intense beam of neutrinos. Three 30 m-length 200 μ m-core-diameter optical fibers, which are arranged flexibly to form 60 m- or 90 m-length fibers, were installed in the beamline. The beam loss signal was observed with the Muti-Pixel Photon Counters. We discuss the result and prospects of using optical fibers for monitoring and locating the beam loss source.

J-PARC EXTRACTION NEUTRINO BEAMLINE

J-PARC extraction neutrino beamline, detailed in [1], provides one of the most intense beams of $\nu_\mu(\bar{\nu}_\mu)$ for the research concerning neutrino particles, whose its massiveness is the only experimental evidence so far beyond the description of the Standard Model of elementary particles. To extract the 30 GeV proton beam from Main Ring and transport it toward a graphite target for neutrino production, the 238 m-length beamline is instrumented with 21 normal magnets (eight steering, four dipole, and nine quadrupole magnets) and 14 doublets of superconducting combined function magnets. The neutrino beamline receives a beam in a so-called fast-extraction mode, where each beam spill consists of eight bunches of ~ 13 ns (1σ) bunch width and 581 ns bunch interval. In 2020, J-PARC operates stably at around 515 kW with an intensity of 2.65×10^{14} protons-per-pulse (ppp). J-PARC accelerator and neutrino beamline [2] plan to upgrade to MW-power beam by reducing the cycle repetition from 2.48 s to 1.16 s and increasing the beam intensity to 3.2×10^{14} ppp. To realize the MW beam, equipment robustness against high intensity, beam loss tolerability, handling the radioactive waste, and precisely and continuously monitoring the beam profile are essential. This work concerns merely the beam loss monitor (BLM), including the experience of operating the gas-based BLM system and investigation of using optical fiber-based BLM (O-BLM) as a complementary option for monitoring the beam loss.

GAS-BASED BLM

Proportional counter with a mixture of Ar and CO₂ (Canon Electron Tubes & Devices E6876-400) [3] was cho-

sen to monitor the spill-by-spill beam loss. There are 50 BLMs distributed along 238 m-length beamline, one shown in Fig. 1, and they are integrated into the Machine Protection System (MPS), allowing us to abort the next beam spill in case the spill-integrated BLM signal with the latest spill is higher than a pre-defined threshold.

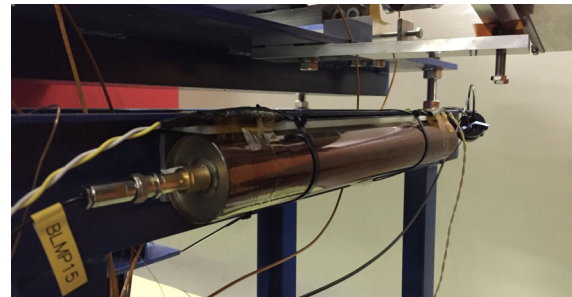


Figure 1: A gas-based BLM installed under the magnet.

Figure 2 shows the beam loss distribution along the beamline. The beam loss is high near the extraction point (at ~ 0 m position), a collimator (at ~ 45 m position), and at the most downstream due to backscattering of proton beams on the beam window, production target, and intercepting beam profile monitor. The beam loss is quiet along the superconducting magnet section (from 54 m to 201 m positions).

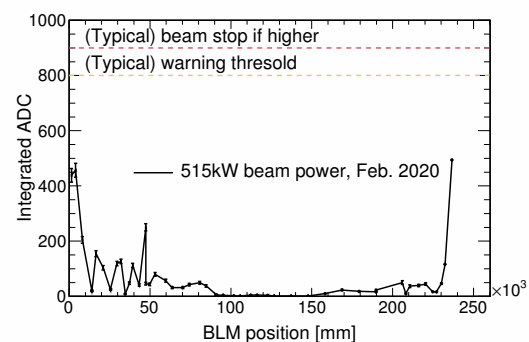


Figure 2: Beam loss distribution with the gas-based BLMs along the 238 m-length extraction neutrino beamline.

With more than ten year operation of BLM, it is well-established that the gas-based BLM functions stably and reliably. The most downstream BLM placed in the highest radioactive area comparing to other BLMs, has signals linearly proportional to the beam power, providing us a useful beam-based calibration to check BLM response regularly and no degrading indication observed. For semi-offline monitoring and analysis, the BLM signal is sampled 30 MHz with

* Work supported by the J-PARC/KEK Neutrino Group
[†] cvson@post.kek.jp

THE INSERTABLE BEAM STOP IN THE ESS SPK SECTION

E. M. Donegani*, T. Grandsaert, T. Shea, C. A. Thomas
European Spallation Source ERIC, Lund, Sweden

Abstract

This paper deals with the Insertable Beam Stop (IBS) to be installed at the transition between the normal conducting and superconducting sections of the ESS linac. The IBS will be used to avoid beam losses in the cryogenic cavities during tuning and commissioning of the ESS linac. The IBS will stop protons in the energy range from 73 MeV to 92 MeV. The proton beam has a current up to 62.5 mA, and 5 and 50 μ s long pulses at a rate of 14 or 1 Hz, respectively. Firstly, the IBS was designed in MCNPX/ANSYS to withstand thermal and structural stresses, while minimizing neutron production and limiting the deposited power in the cryogenic cavities below 0.2 W/m. Secondly, the prompt background and residual dose in the vicinity of the IBS were computed, as well as the activation of the IBS components themselves. Finally, a feasibility study was performed to determine if the IBS can be profitably used as a beam-profile monitor. The results will serve as input for calculations of the expected signal in beam loss monitors. Moreover, they will enable the design of the nearby shielding limiting the activation of surrounding structures and allowing maintenance works.

INTRODUCTION

The European Spallation Source (ESS) in Lund (Sweden) is currently one of the largest science and technology infrastructure projects being built today. The facility will rely on the most powerful linear proton accelerator ever built, a rotating spallation target, 22 state-of-the-art neutron instruments, a suite of laboratories, and a supercomputing data management and software development centre [1].

The ESS accelerator high-level requirements are to provide a 2.86 ms long proton pulse at 2 GeV at repetition rate of 14 Hz. This represents 5 MW of average beam power with a 4% duty cycle on the spallation target [2].

A comprehensive suite of beam instrumentation and diagnostics [3] has started to support the commissioning and operation of the normal-conducting linac (NCL) section of the ESS linac. Additional devices are going to be deployed in the superconducting linac (SCL) section, and in the transport lines to the tuning dump and to the spallation target.

At the transition between the NCL and the SCL sections, an Insertable Beam Stop (IBS) will be installed in order to avoid beam losses in the cold cavities during tuning up and commissioning of the ESS linac.

In the following three paragraphs, the main studies that are ongoing and devoted to the design of the IBS will be summarized:

1. MCNPX/ANSYS studies to perform thermo-mechanical simulations,
2. MCNPX/CINDER'90 studies for activation calculation and shielding design,
3. Feasibility studies of utilizing the IBS as a beam-profile monitor.

THERMO-MECHANICAL ANALYSIS

The IBS must guarantee that the proton beam is fully stopped and the beam power is safely dissipated as waste heat. The maximum proton beam current is 62.5 mA and the maximum beam energy is 92 MeV, leading to a peak power of 5.75 MW.

In order to withstand the high power, to minimize the heat transfer to the cold linac section and also the residual radioactivity, the only possible choice for the IBS core is graphite (with a density of 1.8 g/cm³). Further challenges are posed by the limited space available in the Linac Warm Unit (LWU, see Fig. 1), and its particle-free environment. Therefore, the graphite core is embedded in a tungsten shielding, surrounded in turn by a 3 mm thick layer of titanium, allowing vacuum cleaning and avoiding particle generation.

The outer IBS radius is 5.5 cm and the total IBS length is 8 cm. The IBS is water cooled and the pipes of the circuit system are made of SSL. Energy deposition calculations

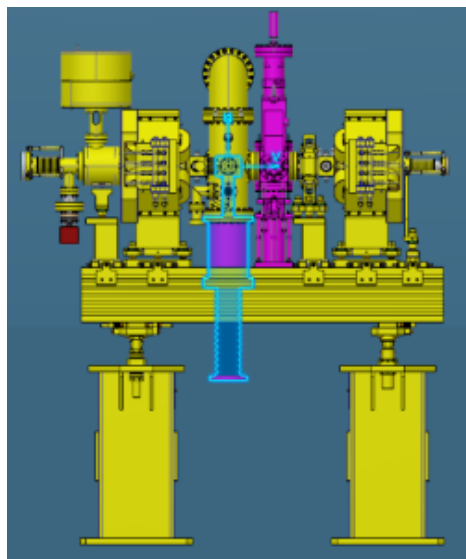


Figure 1: The Linac Warm Unit (LWU) in the ESS spoke (SPK) section, holding the IBS (highlighted in blue). The beam goes from right to left. (Courtesy of STFC and the ESS Vacuum section).

* elena.donegani@ess.eu

PROTON-INDUCED SEY FROM BEAM INTERCEPTIVE DEVICES IN THE ESS LINAC

E. M. Donegani*

European Spallation Source ERIC, Lund, Sweden

Abstract

During the ESS linac commissioning, a wealth of beam-interceptive devices will be exposed to protons with nominal and non-nominal energies spanning from 75 keV to 2 GeV. Therefore, a database of proton-induced Secondary Emission Yield (SEY) values was prepared for the structural materials of devices insertable into the ESS linac. The database relies on calculations of collision stopping powers in MCNPX and the Sternglass theory applied to protons in the [0.001, 2000] MeV energy range. Results are reported for relevant materials to wire scanners, bunch shape monitors and target imaging systems: Cu, Ti, Ni, W, SiC, TZM and graphite. In the future, the novel method can be used also for determining the impact of secondaries on emittance or beam-current measurements with Emittance Monitor Units or Faraday cups of the ESS linac, respectively. Moreover, the database can be extended to critical structural materials of the ESS linac itself, in order to estimate the impact of secondary electrons on the overall beam quality.

INTRODUCTION

The European Spallation Source (ESS) in Lund (Sweden) is currently one of the largest science and technology infrastructure projects being built today. The facility will rely on the most powerful linear proton accelerator ever built, a rotating spallation target, 22 state-of-the-art neutron instruments, a suite of laboratories, and a supercomputing data management and software development centre [1]. The ESS accelerator high-level requirements are to provide a 2.86 ms long proton pulse at 2 GeV at repetition rate of 14 Hz. This represents 5 MW of average beam power with a 4% duty cycle on the spallation target [2].

A comprehensive suite of beam instrumentation and diagnostics [3] has started to support the commissioning and operation of the normal-conducting linac (NCL) section of the ESS linac. Additional devices are going to be deployed in the superconducting linac (SCL) section, and finally in the transport lines to the tuning dump and to the spallation target. Therefore, a wealth of beam-interceptive devices will be exposed to protons with nominal and non-nominal energies, spanning from 75 keV to 2 GeV:

- Wire Scanners (WS) [4] and Bunch Shape Monitors (BSM) [3] to determine the transverse and the longitudinal charge distribution, respectively;
- Target imaging systems [5] to detect small fractions of the proton beam that are outside a defined aperture, and to measure the horizontal and vertical beam profiles.

The WS, BSM and target imaging systems rely on secondary emission from thin wires or grids, from which a current proportional to the beam intensity is measured. The structural materials of such wires and grids are reported in Table 1.

Table 1: List of beam-interceptive devices in the ESS linac, with the corresponding main structural materials and the proton energy range E_P they are exposed to.

Device	E_P [MeV]	Material
EMU	[0.075, 3.6]	TZM, Cu, W
FC	[0.075, 74]	C, Cu, TZM
BSM	[3.6, 90]	C, W
WS	[3.6, 2000]	C, W
IBS	[73, 360]	Ti
Target imaging	[800, 2000]	Ni, SiC, W

There is another set of beam-interceptive devices whose performance can be severely limited by secondary electrons:

- Faraday cups (FC) [6] whose ability to measure the beam current depends on the capability of recapturing the ejected electrons;
- Emittance Monitor Units (EMU) for measuring the emittance, which can rely either on an internal FC [7] or on slit and grid combination [8];
- Insertable Beam Stops (IBS) [9] which is used to safely stop the beam in a particle-free vacuum environment.

Therefore, a database of SEY values was developed for all the structural materials relevant to the beam-interceptive devices in the ESS linac. The newly developed method for calculating Secondary Emission Yields (SEY), induced by protons in the [0.001, 2000] MeV range, is described in the following paragraph.

METHOD

The novel method for calculating the SEY is based on quick calculations of stopping powers in MCNPX [10] and the Sternglass theory [11]. As a first step, a cylindrical rod of the material of interest is simulated in MCNPX; the radius is set equal to two Molière radius, while the length is set long enough to fully contain a beam of 2 GeV protons.

The proton beam is defined as a monoenergetic source of 2 GeV protons, with a Gaussian distribution having $\sigma=0.6$ cm. The beam is perpendicularly impinging on the base of the cylindrical rod. In addition to protons, also electrons, neutrons and photons are transported. One single run

* elena.donegani@ess.eu

SIMULATION OF THE SIGNAL PROCESSING FOR THE NEW INTERACTION REGION BPMs OF THE HIGH LUMONENSITY LHC

D. R. Bett*, University of Oxford, UK
 M. Wendt, M. Krupa, A. Boccardi, CERN, Geneva, Switzerland

Abstract

New stripline beam position monitors (BPMs) will be installed at the Interaction Regions of the ATLAS and CMS experiments as part of the High-Luminosity upgrade to the LHC. These BPMs will be located in sections of the beamline where the two counter-propagating proton beams co-exist within a single pipe, such that the signal observed on each output port is a combination of the signals generated by each beam. The use of the BPMs as the input for a possible luminosity feedback system places a demanding requirement on the long-term accuracy of the BPMs. Accurate measurement of the position of each beam requires a method for isolating the individual beam signals. A simulation framework has been developed covering all stages of the measurement process, from generation of the signals expected for beams of a given intensity and orbit through to digitization, and has been used to evaluate several candidate methods for extracting the position of each beam in the presence of the unwanted signal from the other.

INTRODUCTION

The High Luminosity LHC is an upgrade of the LHC with a target luminosity five times larger than the current nominal value of $10^{34} \text{ cm}^{-2}\text{s}^{-1}$. As part of this upgrade, the beam position monitors (BPMs) in interaction region (IR) 1 and 5 will be replaced, corresponding to the vicinity of the ATLAS and CMS detectors respectively.

The layout of the right side of IR1 and IR5 is illustrated in Fig. 1. Far from the interaction point (IP) the proton beams exist in their own individual pipes and the BPMs need only measure the position of the one beam. Close to the IP, the two beams travel within the same pipe and the BPMs in that region are required to measure the position of both beams. Six new octagonal stripline BPMs of two different types will be installed either side of each of the two IPs, with the BPM closest to the IP being of type A and the remainder of type B. The two types have slightly different apertures and will be installed with different orientations of the electrodes; type A BPMs will have the electrodes oriented at 0° and 90° in the lab frame and the type B BPMs will be rotated by 45° due to the tungsten shielding at those locations. The longitudinal location of each BPM, s , determines the difference in arrival time of the two beams, Δt (Table 1).

BPM MODEL

The CST Microwave Studio [1] model of the type A BPM is shown in Fig. 2. I_1 and I_2 represent beams entering the

* douglas.bett@physics.ox.ac.uk

Table 1: BPM distance from the IP (s) and difference in the arrival time of the two beams (Δt).

BPM Type	s [m]	Δt [ns]
A	21.853	3.92
B	33.073	3.92
B	43.858	6.82
B	54.643	9.72
B	65.743	10.52
B	73.697	7.36

BPM from opposite directions and V_1 to V_8 the signals observed at each end of the four striplines designated right (R), top (T), left (L) and bottom (B). Stripline BPMs are highly directive [2]; in the ideal case, there is perfect cancellation at the downstream ports between the signal induced in the direction of the beam as the beam enters the BPM, and the signal induced as the beam exits the BPM. The resulting bipolar signal is therefore only observed at the upstream port. This allows such a BPM to be used to distinguish the signal generated by beams travelling in opposite directions.

In practice the cancellation is not total and a small amount of signal is observed at the downstream end, combining with main signal from the opposite beam. Figure 3 shows the voltages calculated at each end of each stripline when a simulated beam with the indicated current profile travels along the BPM axis. The first beam to arrive is designated “beam 1” and induces a large (“coupled”) signal at upstream ports 1-4 and a much smaller (“isolated”) signal at downstream ports 5-8, while the reverse is true for “beam 2” which enters the other end of the BPM after time Δt . Each beam distorts the signals that will be used to measure the position of the other beam, and this distortion must be taken into account in order to obtain accurate measurements of the position of each individual beam.

SIMULATION

The numerical computation software GNU Octave [3] was used to simulate the process of obtaining beam position measurements from the stripline signals. The CST predictions of the signals induced at each end of the stripline are scaled according to the position and charge of each beam and the signals from beam 2 are delayed as appropriate in order to form the set of stripline waveforms V_1 to V_8 . As the BPMs are located in a very high-radiation environment, long (> 100 m) cables will be used to transport the signals to a digital processor able to operate at a sample frequency of ~ 4 GHz. Given the pulses themselves are only a few

DESIGN AND TEST OF CBPM PROTOTYPES FOR SHINE*

S. S. Cao[†], Y. B. Leng^{*}, R. X. Yuan, R. T. Jiang

Shanghai Advanced Research Institute, Chinese Academy of Sciences, Shanghai, China

Abstract

SHINE (Shanghai High repetition rate XFEL aNd Extreme light facility) is designed to be an extremely high performance hard X-ray free electron laser facility located at Zhangjiang, Shanghai. As one of the key parameters of the facility, the resolution of the beam position measurement in the undulator section is required to be under 200 nm at a low bunch charge of 100 pC and better than 10 μm at 10 pC. To achieve this, a pre-study based on cavity beam position monitors is under development. Four sets of cavity monitors with different frequencies or load quality factors have been designed and are now manufactured by four different companies. It aims to select the cavity with the best performance and select the most capable company. This paper will briefly introduce the motivation, cavity design considerations, and cold test results.

INTRODUCTION

SHINE is a newly proposed high-repetition-rate X-ray FEL facility, which is designed to become one of the most efficient and advanced free electron laser user facilities in the world, providing a tool for cutting-edge research subjects. The facility includes a superconducting linear accelerator with an energy of 8 GeV, 3 underlines, 3 optical beam lines, and the first 10 experimental stations [1,2]. The fundamental parameters of SHINE are presented in Table 1.

Table 1: The Fundamental Parameters of SHINE

Parameters	Values	Units
Beam energy	8	GeV
Bunch charge	100	pC
Max rep-rate	1	MHz
Pulse length	20-50	fs
Peak brightness	5×10^{32}	~

The construction of such a high-level FEL facility has strict requirements for each subsystem. Beam position as one of the key parameters can be used to monitor the electron beam orbital changes. For SHINE, the position resolution requirement at the undulator is better than 200 nm. To achieve that, the high-resolution and high-sensitivity cavity beam position monitor (CBPM) is utilized to extract the beam position [3,4]. The principle is that the intensity of the TM₁₁₀ mode excited by the beam is proportional to the beam position. By extracting the signal of TM₁₁₀ mode, the beam position can be ob-

tained. Moreover, the signal of TM₁₁₀ mode is also related to the bunch charge, thus it is essential to use a reference cavity to normalize the bunch charge.

Four different types of CBPM are currently under development. The reason for developing four types of CBPM is based on the following considerations. Firstly, the higher the cavity frequency, the more compact the cavity, and the higher sensitivity and higher the ratio of signal-to-noise (SNR) of the output signal is expected. Thus the C-band and X-band CBPM are proposed. Secondly, the higher the Q_{load} , the longer the signal length, the higher the signal processing gain and the greater the crosstalk between the bunches. Thus the cavities with different Q_{load} are also proposed. Thirdly, it is also necessary to cooperate with several manufacturers and evaluate the processing capabilities so as to select the most capable one. At present, some CBPMs have been fabricated and are awaiting acceptance checks, while others are still under development.

The following subsections will introduce this in detail.

DEVELOPMENT OF FEEDTHROUGH

As an indispensable part of all beam position monitors (BPMs), feedthrough is used to couple the energy stored inside the cavity to the outside to the cavity and convert it to an electrical signal for subsequent electronic processing. Previously, the feedthroughs are purchased from companies. However, the bandwidth of purchased feedthrough is only about 8 GHz, which cannot meet the requirements of X-band CBPM, while the customized feedthroughs are too expensive. Therefore, we decided to independently develop high-bandwidth feedthroughs. Since Dr. Yuan has successfully completed the design of the high-bandwidth N-type feedthrough, we decided complete the design of the SMA-type feedthrough based on the N-type feedthrough.

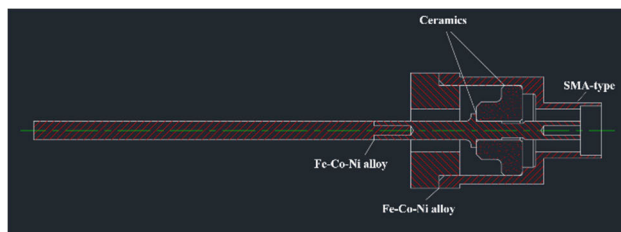


Figure 1: Structure of the SMA-type feedthrough.

The structure of the SMA-type feedthrough is shown in Fig. 1. The first batch of 20 prototypes have been developed, as shown in Fig. 2, including 8 dual-port SMA prototypes and 12 SMA-type feedthroughs. The dual-port SMA prototypes are used to evaluate the bandwidth of the feedthrough and the processing consistency. To improve the connection stability of the SMA interface, a gold-

* Work supported by National Key Research and Development Program of China under Grant 2016YFA0401903.

[†] lengyongbin@sinap.ac.cn

EXPERIMENTS WITH A QUADRATED DIELECTRIC-FILLED REENTRANT CAVITY RESONATOR AS A BEAM POSITION MONITOR (BPM) FOR A MEDICAL CYCLOTRON FACILITY*

S. Srinivasan[†], P.-A. Duperrex, J. M. Schippers
 Paul Scherrer Institut, 5232 Villigen PSI, Switzerland

Content from this work may be used under the terms of the CC BY 3.0 licence (© 2020). Any distribution of this work must maintain attribution to the author(s), title of the work, publisher, and DOI

Abstract

Low beam currents (0.1-10 nA) are used for tumour treatment in the proton radiation therapy facility at PSI. The facility houses a superconducting cyclotron with an extraction energy of 250 MeV pulsed at 72.85 MHz. Online measurement of the beam position is traditionally performed with the help of ionisation chambers (ICs), however, at the expense of reduced beam quality and scattering issues. There is a strong demand to have this measurement performed with minimal beam disturbance, since the beam position is directly associated with the dose-rate applied. A cavity resonator, working on the principle of an electric dipole mode resonance, whose frequency is coupled to the second harmonic of the pulse rate, has been built to measure beam position in a purely non-invasive manner. Followed by a reasonable agreement between the test-bench and the simulation results, the cavity is installed in one of the beamlines. Here, we report on the measurement of the cavity BPM as a function of beam current and position and its shortcomings. When measured with a spectrum analyser, the cavity BPM can deliver position information within the accuracy and resolution demands of 0.50 mm.

INTRODUCTION

Proton beams of low beam currents (0.1-10 nA) are used for radiation therapy at PSI, and its position is traditionally measured with multi-strip ionisation chambers (ICs) [1]. Due to a strict demand for minimal disturbance of the beam, a non-invasive BPM, modelled as four LC cavities within a ground cylinder with a common dielectric is described in [2] as a potential replacement to ICs. It is designed to work on the dipole mode (TM_{110}) of resonance at 145.7 MHz for off-centered beams. The BPM prototype is characterised on a test-bench and its position dependence is in good agreement with the simulation expectation as seen in [2]. The TM_{110} mode frequencies of the horizontal and the vertical polarisations, localised in horizontal and vertical cavities, are at 146.0 MHz and 148.1 MHz due to cavity asymmetries from reassembling to correct for sensitivities as described in [2]. Hence, for validation of the BPM prototype with beam measurements, only horizontal plane cavities are studied due to its proximity to the design TM_{110} mode frequency demand.

* This project has received funding from the European Union's Horizon 2020 research and innovation programme under the Marie Skłodowska-Curie grant agreement No 675265.

[†] sudharsan.srinivasan@psi.ch

BEAMLINE MEASUREMENTS

The BPM, as shown in Figure 1 [3], is installed in the temperature-controlled (28.5 ± 0.5 °C) proton therapy facility, PROSCAN, at six meters from the degrader exit (Figure 2).

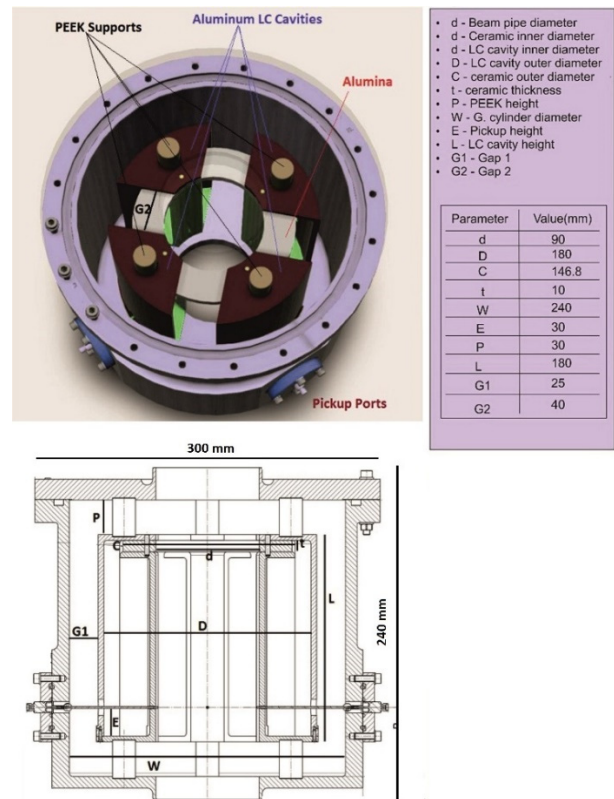


Figure 1: Geometry of the four-quadrant reentrant cavity BPM with its design TM_{110} mode frequency at 145.7 MHz and its design monopole mode frequency (TM_{010}) at 127.1 MHz.

The sensitivity of the BPM is expected to be nearly constant for different energies since the influence of energy spread from the degrader on bunch length elongation at the BPM location will be minimal unlike for the BCM location as described in [4].

The measurement reference is an IC located within a meter behind the BPM. The measurement chain, as shown in Figure 2, consists of a single stage amplification of 36 dB each for the horizontal plane cavities and a spectrum analyser. The pickups of the vertical plane cavities of the BPM are terminated with 50 Ω. The beam position response of the BPM prototype is verified at different beam currents and energies.

ADVANCED LIGHT SOURCE HIGH SPEED DIGITIZER*

J. Weber[†], J. Bell, M. Chin, E. Norum, G. Portmann
Lawrence Berkeley National Laboratory, Berkeley, CA, USA

Abstract

The Advanced Light Source (ALS) is developing the High Speed Digitizer (HSD), a data acquisition system based on the latest Radio Frequency System-on-Chip (RFSoc) technology. The system includes 8 channels of 4GHz 4Gbps analog input, programmable gain, self-calibration, and flexible data processing in firmware. The initial motivation for the HSD project was to develop a replacement for aging ZTEC oscilloscopes that would be more tightly integrated with the ALS Control System and Timing System than any available commercial oscilloscope. However, a general approach to the design makes the HSD system useful for other applications, including a Bunch Current Monitor, as well as for other facilities beyond ALS.

INTRODUCTION

The ALS currently uses mostly ZTEC digital oscilloscopes and a few in-house designed hardware systems to monitor fast signals around the accelerator, including integrating current transformers (ICTs), wall current monitors, traveling wave electrodes, and fast magnet pulsers. The ZTEC scopes were desirable because they have no local display, so they are compact (up to two 4-channel units per 1U rack slot), and each unit runs an EPICS IOC to integrate with the ALS control system. Over time, some of these scopes have proven unreliable. Recently the ALS has experienced some failures of these units that cannot be repaired, leaving the facility with few or no spares of some of the models in production use.

A few years ago, Xilinx introduced RFSoc technology that integrates high speed data converters (DACs and ADCs) with programmable logic and dedicated CPUs in a single chip [1]. By including the ADCs, this architecture simplifies the rest of the analog/RF front end hardware design for fast analog signals. The high channel density makes the cost per channel of a full system design competitive with an equivalent commercial oscilloscope.

The High Speed Digitizer (HSD) is a new design being developed for ALS based on the Xilinx ZCU111 RFSoc evaluation kit [2]. The kit includes 8 ADCs with 12-bit 4 GSps 4 GHz performance, which are sufficient to meet the ALS fast signal channel density and performance requirements. An SFP interface to a high speed serial transceiver receives the 2.5 Gbps timing event stream into an embedded event receiver (EVR), enabling synchronous sampling with the accelerator RF frequency, and integrated triggering. The Ethernet interface allows integration with

the ALS control system. A controlled impedance RFMC expansion connector provides direct access to the RFSoc analog inputs.

At ALS, the existing Bunch Current Monitor (BCM) system is already based on the ZCU111 with a different front end, and will be replaced with an HSD unit so it is on a common hardware platform with other HSD units. APS is also using the existing ALS BCM hardware, and is evaluating the HSD as an upgrade to the BCM and a potential solution for monitoring fast signals as well. Other accelerators have also expressed interest in evaluating this system for similar applications.

ARCHITECTURE

The HSD system architecture is consistent with the network-attached device (NAD) model used for ALS in-house designed instrumentation systems, as shown in Fig. 1. The architecture is flexible in that the number of soft IOCs required to support devices and how they are connected can be adjusted to trade off network bandwidth, CPU performance, and maintenance complexity. In the case of ALS, the small number of HSD units and low average data transfer rate make it suitable for a single soft IOC. Each HSD unit communicates with the EPICS soft IOC via a clean and simple UDP interface, which allows either side to be upgraded independently. Each unit also receives the timing event link from the timing distribution infrastructure.

The HSD design is intended to be general purpose to accommodate multiple applications, including as a Fast Scope and Bunch Current Monitor, and others that fit the specifications. The firmware can be modified to achieve this with the same hardware configuration.

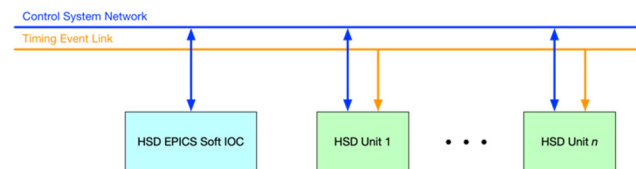


Figure 1: High Speed Digitizer (HSD) units in a network-attached device (NAD) architecture.

HARDWARE

The HSD hardware consists of a ZCU111 board with an analog front end board (HSDAFE) connected to the RFMC mezzanine interface, and a front panel board (HSDFP) containing an LCD display and connectors for front panel pushbuttons. Panel mount SMA patch cables connect the 8 analog input channels from the front panel to the HSDAFE. Different cable lengths compensate for differences in trace lengths on the board, so the input path length matches across all channels. A split ribbon cable harness connects the HSDFP to two PMOD connectors on the

* Work supported by the Director, Office of Science, Office of Basic Energy Sciences, of the U.S. Department of Energy under Contract No. DE-AC02-05CH11231

[†] jmweber@lbl.gov

Content from this work may be used under the terms of the CC BY 3.0 licence (© 2020). Any distribution of this work must maintain attribution to the author(s), title of the work, publisher, and DOI

Content from this work may be used under the terms of the CC BY 3.0 licence (© 2020). Any distribution of this work must maintain attribution to the author(s), title of the work, publisher, and DOI

UPGRADE AND FIRST COMMISSIONING OF TRANSVERSE FEEDBACK SYSTEM FOR SSRF*

N. Zhang[†], B. Gao, L. Lai, R. Yuan, Shanghai Synchrotron Radiation Facility, Shanghai, China

Abstract

To be a part of the transverse feedback system upgrade plan in SSRF PHASE II project, a set of Dimtel feedback processors [1] was installed to replace the previous set. In the commissioning, the ability of suppressing the transverse oscillation was tested and evaluated, also, beam diagnostics and control tools of the processors was used for injection transient analysis, tune tracking and bunch cleaning. The results of the commissioning and data analysis will be presented in this paper.

INTRODUCTION

SSRF is a third generation 3.5 GeV synchrotron light source with 720 bucket in the storage ring and a RF frequency of 499.654 MHz. The transverse feedback (TFB) system was started in 2010, and the feedback kicker consists of one vertical electrode and one horizontal electrode, one feedback processor designed by Spring-8 to produce 2 independent channel of feedback signal for both planes. In SSRF PHASE II project, 16 more beam line will be built before 2022, and more IUVs are planned to be installed in the storage ring, which would lead impedance of the whole ring increase from 4M Ohm to 8M Ohm. Another challenge for beam transverse motion control is a newly introduced hybrid operation mode, which consists of about 500 filled buckets of 0.5mA and one high current bucket of 20mA. It is evaluated that the feedback system could suppress the transverse instability even when the product of impedance and beam current increases to 3 times, but the limitation of individual bunch current is 10mA. If only one electrode is used for each plane, the dynamic range for each channel is required to reach 32dB, it would be very difficult for TFB processors and power amplifier configuration. So a 3-electrodes kicker scheme was designed, compared with the 2-electrodes kicker, one more vertical electrode was specialized for controlling the hybrid bunch. 2 TFB processors were also to be added to fit the new kicker plan, one for normal buckets in both planes, the other for the big bunch in vertical plane. Since the 3-electrodes kicker is planned to install one year later, the commissioning only refers to the normal operation mode processor.

FEEDBACK SETUP

A stripline kicker with 3 electrodes talked above is going to operate as a transverse feedback actuator in all modes. Normal operation mode is driving when driving a horizontal electrode and a vertical one, Hybrid mode is driving when driving all the 3 electrodes. The designed kicker is shown in Figure 1.

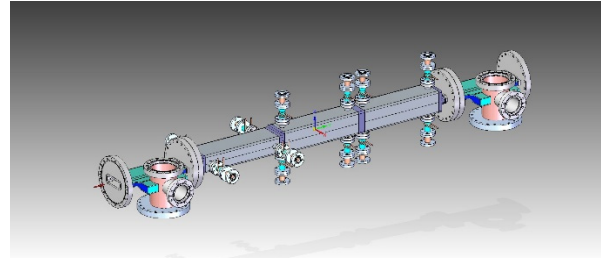


Figure 1: Transverse feedback kicker with 3 electrodes, the first electrode is horizontal electrode, and the 2 and 3 are vertical electrodes.

The feedback electronics includes one hybrid network, one FBE-500LT front-end, and 2 iGp-12 processors. The hybrid signal of differential horizontal and differential vertical ($\Delta x + \Delta y$), and the differential vertical (Δy) of the beam motion are created from BPM signals in the hybrid network (Fig. 2). The 2 channel signals would be processed by FBE-500LT and then fed to iGp-12 separately.

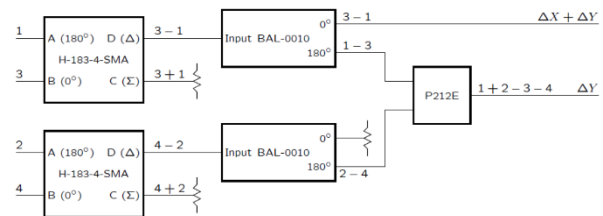


Figure 2: Layout of hybrid network.

Since one iGp-12 only have only one pair of differential input channels, the 16-step FIR filter was specially designed to provide feedback signals in both X and Y plane simultaneously, which is shown in Figure 3. And the differential output is divided into 2 way to fed X and Y kickers.

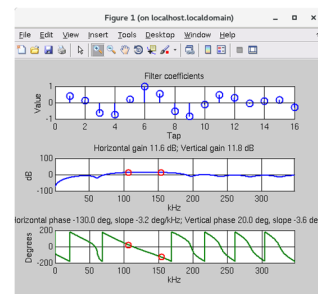


Figure 3: 16 step FIR design of feedback for both X and Y plane.

[†] zhangning@zjlab.org.cn.

Content from this work may be used under the terms of the CC BY 3.0 licence (© 2020). Any distribution of this work must maintain attribution to the author(s), title of the work, publisher, and DOI

MEASUREMENTS OF ULTRAVIOLET FEL SEED LASER PULSE WIDTH BROADENING IN THIN β -BBO CRYSTALS*

Chunlei Li¹, Xingtao Wang, Wenyan Zhang, Lie Feng, Bo Liu[†]

Shanghai Advanced Research Institute, Chinese Academy of Science, Shanghai, China

¹ also at Shanghai Institute of Applied Physics, Chinese Academy of Science, Shanghai, China

Abstract

Short pulse, high power seed lasers have been implemented to improve the longitudinal coherence and shot-to-shot reproducibility of Free Electron Lasers (FEL). The laser pulse duration is typically 100 - 200 fs with wavelengths in the 260 nm range produced from third harmonic generation of a Ti:sapphire laser. The pulse duration must be measured accurately for seeded FEL operation. The Ultraviolet (UV) pulse width measurement can be carried out with intensity cross-correlation based on the difference frequency generation (DFG) in ultrathin β -Barium Borate (BBO) crystals. The DFG output pulse broadened due to group velocity mismatch between the 266.7 nm and 800 nm components. The broadening effect depends on the BBO crystal thickness so we explored 0.015 mm, 0.055 mm and 0.1 mm thick samples. To the best of our knowledge, this is the first time that β -BBO crystal with thickness of only 0.015 mm has been used to measure the UV seed laser pulse width. Experiment results show the measured pulse width broadens with increased BBO thickness in agreement with a theoretical model.

INTRODUCTION

Particle accelerator and laser technologies are effectively combined in FEL facilities, with the latter being a key factor determining the ultimate performance [1]. Laser technology is used at many strategic points: (1) cathode drive laser (257-267 nm, 5-30 ps) to create the electron bunch, (2) laser heater (400-1030 nm, 15-20 ps) to increase beam energy spread [2], and (3) seed laser (210-280 nm, 90-300 fs) to improve longitudinal coherence and reproducibility of the FEL output [3].

Two-beam cross correlation can be used to characterize the temporal structure of photocathode drive laser pulse [4-7] and the resulting electron bunch length [8]. The drive laser pulse width is in a range of 5-50 ps, so pulse broadening caused by the group velocity mismatch (GVM) in ultrathin (<0.1 mm) BBO crystal is negligible. However, pulse broadening has to be understood when measuring the seed laser pulse in the range of 100-300 fs.

In this paper, pulse broadening was experimentally investigated using β -BBO crystals with three different thicknesses to experimentally determine the effect of GVM on the measurement. Ultrathin crystals with thickness of only 0.015 mm were found to have the least broadening effect.

*This study was sponsored by Shanghai Sailing Program (18YF1428700).

[†]Corresponding author: liubo@zjlab.org.cn

SEED LASER SYSTEM

Figure 1 shows a schematic for Shanghai soft X-ray free electron laser (SXFEL) seed laser system. The laser consists of 4 main stages: (1) Oscillator, (2) Amplifier, (3) third harmonic generation (THG), and (4) beam transport line. The oscillator (Vitara-T, Coherent Inc.) is pumped by a 4.88 W green CW Verdi laser (Coherent Inc.) to deliver a 0.7 W stream of 79.33 MHz pulses at 800 nm with horizontal polarization to a synchronized regenerative Ti:Sapphire amplifier (Elite Duo, Coherent Inc.). The pre-amplified oscillator pulses have 7nJ energy and are stretched to 200 ps using a grating pair, then amplified by the regen and recompressed (CPA system). The output has 3 mJ in 100 fs (FWHM). The infrared (IR) pulses are then tripled to 266.7 nm with 300 μ J and a bandwidth of 0.8 nm. The UV light is then transported to the main FEL undulator through vacuum beam transport lines.

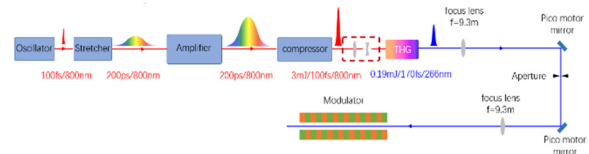


Figure 1: Schematic of SXFEL seed laser system.

The structure of THG optics is shown in Fig. 2. Here the compressed IR pulse is frequency-doubled to 400 nm in a β -BBO crystal (type I, $o + o = e$, 0.5 mm, $\theta = 29.2^\circ$), and subsequently undergoes sum-frequency generation when re-mixed with 800 nm in a second β -BBO crystal (type I, 0.5 mm, $\theta = 44.4^\circ$). The conversion efficiency from 800 nm to 266 nm was about 10%. The 266.7 nm UV pulse width was measured by co-linear cross correlation as presented in the following section.

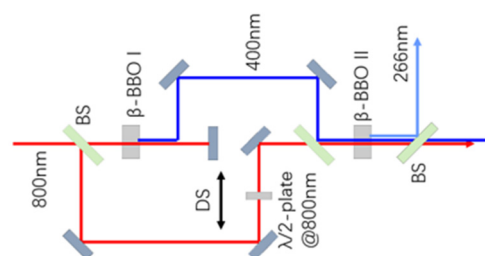


Figure 2: Structure of third harmonic generation (THG) device. BS-beam splitter; DS-delay stage.

EVALUATION OF A NOVEL PICKUP CONCEPT FOR ULTRA-LOW CHARGED SHORT BUNCHES IN X-RAY FREE-ELECTRON LASERS*

B. Scheible[†], A. Penirschke, Technische Hochschule Mittelhessen (THM), Friedberg, Germany
M. K. Czwalińska, H. Schlarb, Deutsches Elektronen-Synchrotron (DESY), Hamburg, Germany
W. Ackermann, H. De Gerssem, Technische Universität Darmstadt (TUDa), Darmstadt, Germany

Abstract

The all-optical synchronization systems used in various X-ray free-electron lasers (XFEL) such as the European XFEL depend on transient fields of passing electron bunches coupled into one or more pickups in the Bunch Arrival Time Monitors (BAM). The extracted signal is then amplitude modulated on reference laser pulses in a Mach-Zehnder type electro-optical modulator. With the emerging demand of the experimenters for future experiments with ultra-short FEL shots, fs precision is required for the synchronization systems even with 1 pC bunches. Since the sensitivity of the BAM depends in particular on the slope of the bipolar signal at the zero crossing and thus, also on the bunch charge, a redesign with the aim of a significant increase by optimized geometry and bandwidth is inevitable. In this contribution a possible new pickup concept is simulated and its performance is compared to the previous concept. A significant improvement of slope and voltage is found. The improvement is mainly achieved by the reduced distance to the beam and a higher bandwidth.

INTRODUCTION

Free-electron lasers (FEL) became an important light source for experiments in various fields since they provide ultra-short pulses with extreme brilliance in atomic length and time scales [1]. FEL are well suited for applications in pump-probe experiments [1], where the timing jitter is specifically critical [2], as well as for capturing image sequences with atomic resolution on fs-time-scales, even below the FEL repetition rate [1, 3, 4].

For the generation of ultra-short X-ray pulses, FEL with short and ultra-low charge electron bunches (≤ 1 pC) have been found as a favorable option [5, 6]. Short bunches may shorten the X-ray pulse, reduce timing jitter and lead to single-spike operation, if sufficiently small compared to the cooperation length of the SASE process [2, 5, 6]. The European XFEL (EuXFEL) was upgraded from initially 1 nC electron bunches to cover a range from 0.02 nC to 1 nC [7] with a possible bunch length below 3 fs in the undulator section [8]. Moreover, a decrease to ultra-low charges of 1 pC is targeted.

The application in time-resolved experiments entails tight requirements for the overall machine synchronization in order to reduce the timing jitter [2]. The timing information is

also used for post-processing experimental data [1]. The synchronization concerns all critical subsystems, specifically in the injector and if present the seeding and the pump laser [1]. Furthermore, the instrumentation must be suited for a broad spectrum of operation modes with different bunch properties even in a single bunch train [9, 10]. Besides, bunch arrival time monitors (BAM) are installed throughout the whole facility, thus experiencing different bunch properties.

A tremendous improvement in synchronization, exceeding RF techniques, and reduction of arrival time as well as energy jitter was achieved by the implementation of an all-optical synchronization system with two different feedback loops [11]. Though some updates have been introduced [12, 13], the basic scheme in use by the Deutsches Elektronen-Synchrotron (DESY) remained unchanged.

In this contribution the all-optical synchronization system will be briefly introduced with special attention on the state-of-the-art cone-shaped pickups, followed by an analytical discussion of the principal parameters determining the BAM resolution. These are the basis for three designs, which are presented at the end of this paper.

ALL-OPTICAL SYNCHRONIZATION SYSTEM

The all-optical synchronization system, as successfully tested at the free-electron laser in Hamburg (FLASH) by Löhl [11], mainly comprises of a mode-locked reference laser, length stabilized fiber links and different end-stations for synchronization and arrival time measurement [10–15]. The arrival time is non-destructively measured with respect to the reference laser in the BAM, which include high-bandwidth pickup electrodes in the RF unit, a Mach-Zehnder type electro-optical modulator (EOM) and the data acquisition system (DAQ) [10, 15].

Basic Working Principle of BAM

The transient electric fields of passing electron bunches are extracted in the RF unit and, if foreseen, initially processed with analogue components like RF combiners, limiters or attenuators [11, 12]. The received bipolar signal is transmitted over radiation hard silicon dioxide coaxial cables to the EOM [12], there it is probed at its zero-crossing by the reference laser [11]. Any temporal deviation will lead to an additional voltage, which the EOM turns into an amplitude modulation of the laser pulse. Therefore, the laser amplitude holds the timing information, which can be retrieved in the DAQ [11]. The signal slope at its zero crossing strongly influences the BAMs temporal resolution.

* This work is supported by the German Federal Ministry of Education and Research (BMBF) under contract no. 05K19RO1

[†] bernhard.scheible@iem.thm.de

SUBMICROPULSE ENERGY-TIME CORRELATIONS OF 40-MeV ELECTRON BEAMS AT FAST*

R. Thurman-Keup†, A. H. Lumpkin, Fermi National Accelerator Laboratory, Batavia, IL, USA

Abstract

We have recently extended our ability to explore submicropulse effects in relativistic electron beams to energy-time (E-t) correlations. The Fermilab Accelerator Science and Technology (FAST) facility consists of a photoinjector, two superconducting TESLA-type capture cavities, one superconducting ILC-style cryomodule, and a small ring for studying non-linear, integrable beam optics called IOTA. The linac contains, as part of its instrumentation, an optical transport system that directs optical transition radiation (OTR) from an Al-coated Si surface to an externally located streak camera for bunch length measurements. For the first time, an OTR screen after the spectrometer magnet was used for measurements of submicropulse E-t correlations. The projected, micropulse time profile was fit to a single Gaussian peak with $\sigma = 11.5 \pm 0.5$ ps for 500 pC/micropulse and with a 200-micropulse synchronous sum, in agreement with the upstream bunch-length measurement at a non-energy-dispersive location. The submicropulse E-t images were explored for four rf phases of CC1, and the E vs. t effects will be presented.

INTRODUCTION

The Fermilab Accelerator Science and Technology (FAST) facility was constructed for advanced accelerator research [1]. It consists of a photoinjector-based electron linac followed by an ILC-type cryomodule and a small ring called IOTA (Integrable Optics Test Accelerator) for studying non-linear optics among other things [2]. Presently under construction, is an RFQ-based proton injector to supply protons to the IOTA ring. To support operations in the electron linac, an optical transport system was installed to take light from various sources (synchrotron radiation, transition radiation) and send it to various instruments including a Hamamatsu streak camera located outside the en-

closure [3]. In this paper, we present the first measurements from a newly installed optical transport line that takes optical transition radiation (OTR) from an Al-coated Si surface after the spectrometer magnet to the streak camera. The transport is arranged in such a way as to map the energy direction of the OTR screen to the spatial direction in the streak camera, allowing for a measurement of the energy-time (E vs. t) phase space of a micropulse.

FAST FACILITY

The FAST facility (Fig. 1) begins with a 1.3 GHz normal-conducting rf photocathode gun with a Cs₂Te-coated cathode. The photoelectrons are generated by irradiation with a YLF laser at 263 nm that can provide several μ J per pulse [4]. Following the gun are two superconducting 1.3 GHz capture cavities (CC1 and CC2) that accelerate the beam to its design energy of around 50 MeV. After acceleration, there is a section for doing round-to-flat beam transforms, followed by a magnetic bunch compressor and a short section that can accommodate small beam experiments. At the end of the experimental section is a spectrometer dipole which can direct the beam to the low energy dump. If the beam is not sent to the dump, it enters the ILC-type cryomodule where it receives up to 250 MeV of additional energy and is sent to either a high-energy dump or the IOTA ring. Table 1 lists the typical beam parameters.

Table 1: Beam Parameters for FAST

Parameter	Value
Energy	20 – 300 MeV
Micropulse Charge	< 10 fC – 3.2 nC
Micropulse Frequency	0.5 – 9 MHz
Macropulse Duration	≤ 1 ms
Macropulse Frequency	1 – 5 Hz
Transverse Emittance	> 1 μ m
Micropulse Length	0.9 – 70 ps

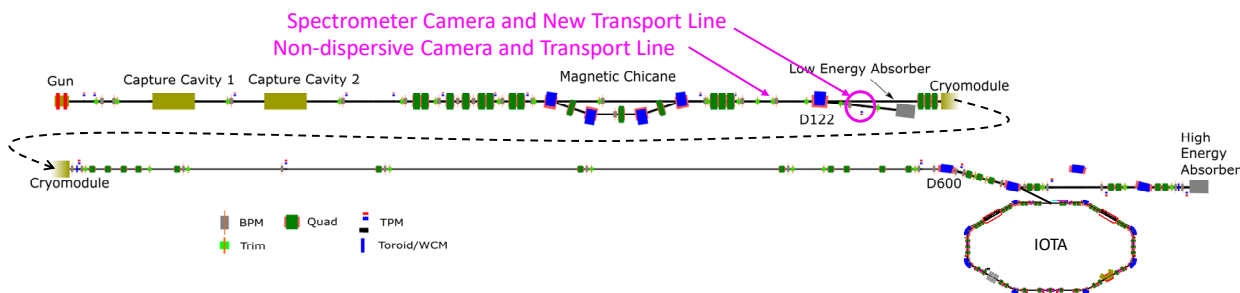


Figure 1: Layout of the FAST facility. D122 is the spectrometer magnet, after which is the OTR source for the new optical transport line.

* This manuscript has been authored by Fermi Research Alliance, LLC under Contract No. DE-AC02-07CH11359 with the U.S. Department of Energy, Office of Science, Office of High Energy Physics.

† keup@fnal.gov

PROTOTYPE DESIGN OF BUNCH ARRIVAL TIME MEASUREMENT SYSTEM BASED ON CAVITY MONITOR FOR SHINE*

Y.M. Zhou[†], S.S. Cao, J. Chen, Y.B. Leng[#]

Shanghai Advanced Research Institute, CAS, Shanghai, China

Abstract

The Shanghai high repetition rate XFEL and extreme light facility (SHINE) is planned to be built into one of the most efficient and advanced free-electron laser user facilities over the world to provide a unique tool for kinds of cutting-edge scientific research. The measurement of bunch arrival time is one of the key issues to optimize system performance. This is because the FEL facility relies on the synchronization of electron bunch and seeded lasers. Currently, there are mainly two methods to measure the bunch arrival time: the electro-optical sampling method and the RF cavity-based method. Considering the latter one has a simpler system and lower cost, the method has been adopted by SXFEL. The previous results show that the measurement uncertainty of bunch arrival time has achieved to be 45 fs, which can be further optimized. For SHINE, the bunch arrival time resolution is required to be better than 25 fs@100pC, and 200 fs@10 pC. The RF cavity-based method will also be applied. This paper will present the system prototype design and related simulation results.

INTRODUCTION

To achieve high-intensity and ultra-fast short wavelength radiation, several X-ray FEL facilities have been completed or under construction around the world[1-3]. Shanghai High repetition rate XFEL and Extreme light facility (SHINE) is the first hard X-ray FEL light source in China, which constructed began in April of 2018. The total length of the entire device reached 3.1 km. It will build an 8GeV superconducting linear accelerator, 3 undulator lines, 3 beamlines, and 10 experiment stations in phase-I. It can provide the XFEL radiation in the photon energy range of 0.4-25keV. The main parameters are presented in Table 1[4]. The SHINE has many excellent characteristics such as ultra-high brightness (up to 109 times that of the third-generation synchrotron radiation), high repetition frequency (1MHz), femtosecond ultra-fast pulse (pulse width < 100fs), and strong spatial and temporal coherence. Moreover, it also possesses nano-level ultra-high spatial resolution capabilities and femtosecond-level ultrafast time resolution. Therefore, the establishment of the SHINE will provide cutting-edge research methods such as high-resolution imaging, ultra-fast process exploration, and advanced

structural analysis for physics, chemistry, life sciences, materials science, energy science, and other disciplines, forming a unique and multidisciplinary interdisciplinary advanced scientific research platform.

High precision bunch arrival time is one of the key technologies because it is the foundation for the synchronization of electron bunches and seeded lasers. At present, two main detection methods, the electro-optical sampling method and the RF cavity-based method, are widely used. Since the system of the latter method is very simple and economical, it has been successfully applied to SXFEL. The measurement uncertainty of bunch arrival time has reached 45fs[5, 6]. However, DESY conducted a theoretical analysis on this and found that the theoretical limit of this method is 1-3fs[7], and the best result obtained by the LCLS experiment is 13fs[8]. Therefore, we consider further optimizing the system to improve the measurement accuracy. It is hoped that the RF cavity-based method can be applied to the SHINE and achieve 25fs@100pC, 200fs@10pC measurement uncertainty of bunch arrival time.

This paper will focus on the prototype design of the bunch arrival time measurement system (BAM) based on the cavity monitor in the SHINE. The system mainly includes four modules: cavity probe, RF front-end, local oscillator, and signal acquisition system. A detailed introduction and experimental simulation results have been presented.

Table 1: Main Parameters of the SHINE

Parameter	Value
Beam energy	8GeV
Energy spread	0.01%
Photon energy	0.4-25keV
Repetition rate	1MHz
Wavelength	0.05-3.0mm
Pulse length	20-50fs
Bunch Charge	10-300pC

SYSTEM FRAMEWORK

A typical framework of the bunch arrival time system is shown in Figure 1. The main method is to perform digital acquisition after down-converting the signal to an intermediate frequency (IF) signal. A cavity probe used to measure the bunch arrival time is installed at a specific position in the accelerator, and the signal of the probe is led out via a long/short cable as the RF input of the RF front-end. The

*Work supported by National Natural Science Foundation of China (2016YFA0401903) and Ten Thousand Talent Program and Chinese Academy of Sciences Key Technology Talent Program

[†]zhouyimei@zjlab.org.cn

[#]lengyongbin@sinap.ac.cn

EFFECT OF PHASE MODULATION ON THE TRANSVERSE BEAM SIZE AND EMITTANCE OF THE HLS-II RING*

Yunkun Zhao, Baogen Sun[†], Jigang Wang, Fangfang Wu, Sanshuang Jin
National Synchrotron Radiation Laboratory (NSRL),
University of Science and Technology of China (USTC)

Abstract

In this paper, the radio-frequency (RF) phase modulation method is exploited to investigate the variations in the transverse beam size and emittance at Hefei Light Source (HLS-II). Meanwhile, a certain quantitative analysis was performed on the stability and practicability of the beam transverse profile measurement systems. The experiments show that the RF phase modulation method can effectively explore the robustness and stability of beam transverse profile measurement systems over the range of 20.0–22.5 kHz, which is close to the first-harmonic of the synchrotron frequency. It is concluded that when the modulation amplitude of the external phase perturbation is less than 0.04 rad, this optical system can be capable of maintaining reliable and stable working status. This is also useful for analyzing the influence of RF phase noise on the subsequent beam measurement and diagnostics, which including the deterioration of beam quality, emittance blowup, beam jitter, and beam loss.

INTRODUCTION

In the synchrotron radiation (SR) storage ring light sources, it is crucial to real-time high-accuracy monitor the variations of the transverse beam size and emittance. With this in mind, HLS-II is equipped with two transverse beam profile measurement systems as that of the synchrotron light imaging system and interferometric system to precisely measure the beam size, emittance, and energy spread on the basis of the actual measurement requirement [1, 2]. In previous machine experiments, a RF phase modulation method is developed to improve beam lifetime and explore longitudinal beam characteristics in the HLS-II storage ring. However, we found that the transverse beam size and emittance are affected by the parametric resonances resulting from the introduced phase perturbation [3, 4]. Therefore, it is necessary to deeply research and elaborate the variations of beam transverse profile and beam emittance subjected to the external RF phase modulation. It has considerable physical and engineering guiding significance in the operation, commissioning, and beam manipulation of the HLS-II storage ring and our future Hefei Advanced Light Facility (HALF) [5]. Considering that the preliminary machine measurement are

carried out in the single-bunch operation mode, we mainly focused on investigating the stability and feasibility of the beam transverse profile measurement systems by use of the changes on the transverse beam size and emittance. Furthermore, the dependence curve of the beam energy spread as a function of the RF phase modulation frequency is further analyzed under different modulation amplitudes.

THE MEASUREMENT PRINCIPLE

As for the HLS-II storage ring, it is noted that the interferometer and imaging system are installed on the dedicated diagnostic beamlines B7 and B8, respectively. Correspondingly, the underlying equations for the transverse beam emittance and energy spread can be separately expressed as

$$\begin{cases} \varepsilon_x = \frac{\sigma_{x,B7}^2 \eta_{x,B8}^2 - \sigma_{x,B8}^2 \eta_{x,B7}^2}{\beta_{x,B7} \eta_{x,B8}^2 - \beta_{x,B8} \eta_{x,B7}^2} \\ \delta = \left(\frac{\sigma_{x,B8}^2 \beta_{x,B7} - \sigma_{x,B7}^2 \beta_{x,B8}}{\beta_{x,B7} \eta_{x,B8}^2 - \beta_{x,B8} \eta_{x,B7}^2} \right)^{1/2} \end{cases} \quad (1)$$

Where the subscripts B7 and B8 represent the parameters at the light source points respectively, ε_x for the horizontal beam emittance, δ for the beam energy spread, η_x for the dispersion function in the horizontal direction, σ_x for the horizontal beam size, and β_x for the beta function in the horizontal plane, x . Similarly, the vertical beam emittance can be obtained by

$$\varepsilon_y = \sigma_y^2 / \beta_y \quad (2)$$

Here, σ_y and β_y indicate the beam size and beta function in the vertical direction y , respectively. To the best of our knowledge, the applied external RF phase modulation will bring about the obvious parametric resonances in the case that the modulation frequency is close to an integral multiple of the synchrotron oscillation frequency. In the case that the modulation frequency of the RF system approaches to a single harmonic of the synchrotron frequency, which corresponding to the standard Hamiltonian equation related to the charged particle motion can be described by [3, 4]

$$\langle H_1 \rangle_t = (\omega_s - \omega_m) J - \frac{\omega_s J^2}{16} - \frac{\omega_s a_m}{2} (2J)^{\frac{1}{2}} \cos \psi - \omega_s \quad (3)$$

In Eq. (3), it is worth pointing out that the systematic Hamiltonian formalism is an invariant. ω_s denotes the synchrotron oscillation angular frequency, which is equal to $\omega_s = 2\pi f_s$, where f_s represents the synchrotron frequency. Whereas ω_m denotes the modulation angular frequency of the external RF noise that is equivalent to $\omega_m = 2\pi f_m$, in which f_m represents the modulation frequency, and a_m represents the phase

* Work supported by the National Natural Science Foundation of China under Grant 11575181, Grant 51627901 and Grant 11705203, the Anhui Provincial Natural Science Foundation under Grant 1808085QA24, and the Fundamental Research Funds for the Central Universities under Grant WK2310000080

[†] bgsun@ustc.edu.cn

AN ALTERNATIVE PROCESSING ALGORITHM FOR THE TUNE MEASUREMENT SYSTEM IN THE LHC

L. Grech*, G. Valentino

Department of Communications and Computer Engineering, University of Malta, Msida, Malta
D. Alves, M. Gasior, S. Jackson, R. Jones, T. Levens, J. Wenninger
Beams Department, CERN, Geneva, Switzerland

Abstract

The betatron tune in the Large Hadron Collider (LHC) is measured using a Base-Band-Tune (BBQ) system. Processing of these BBQ signals is often perturbed by 50 Hz noise harmonics present in the beam. This causes the tune measurement algorithm, currently based on peak detection, to provide tune estimates during the acceleration cycle with values that clearly oscillate between neighbouring harmonics. The LHC tune feedback cannot be used to its full extent in these conditions as it relies on stable and reliable tune estimates. In this work we present two alternative tune measurement algorithms, designed to mitigate this problem by ignoring small frequency bands around the 50 Hz harmonics and estimating the tune from spectra with gaps. One is based on Gaussian Processes and the other is based on a weighted moving average. We compare the tune estimates of the new and present algorithms and put forward a proposal that can be implemented during the renovation of the BBQ system for the next physics run of the LHC.

INTRODUCTION

The tune (Q) of a circular accelerator is defined as the number of betatron oscillations per turn [1]. This is a critical parameter in the Large Hadron Collider (LHC) which has to be monitored and corrected in order to ensure stable operations [2] and adequate beam lifetime. The Base-Band Q (BBQ) system in the LHC is used to measure the tune. It essentially consists of an electromagnetic pickup followed by a diode-based detection and acquisition system [3]. The diode detectors pick-up a small modulation caused by betatron motion on the large beam intensity pulses and converts it to baseband, which for the LHC is in the audible frequency range. The BBQ system in the LHC is sensitive enough to not require that the beam is externally excited in order to measure the tune, picking-up the residual beam oscillations. This normally results in a frequency spectrum where the tune is the dominant peak [3,4].

Since the start of the LHC, spectral components at harmonics of the 50 Hz mains frequency have been observed with several different diagnostic systems [5]. Studies have shown that these modulations are on the beam itself, although their source is unclear. These harmonics are clearly visible in the BBQ system, resulting in a frequency spectrum polluted with periodic lines every 50 Hz (Fig. 1). Since these harmonics are also present around the betatron tune, they are

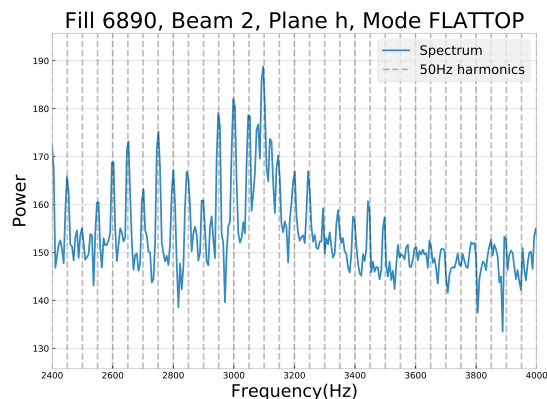


Figure 1: Example of 50 Hz harmonics present in the BBQ spectrum.

a potential source of error for the tune estimation algorithm. The current tune estimation algorithm applies a series of filters and averaging techniques which have been developed in order to mitigate the impact of the 50 Hz harmonics on the final measured value. However, it is not uncommon to have the estimated tunes oscillate between neighbouring 50 Hz harmonics. The fact that the tune estimate locks-in to a particular ~ 50 Hz harmonic is clearly not desirable. On top of that, having the tune jump from one line to another affects the tune feedback system, causing it to switch off as a protective measure against unstable behaviour.

In this paper, we present a study on alternative approaches for the tune estimation algorithm. The common underlying idea is to mask-out the 50 Hz harmonics from the frequency spectrum of the BBQ signal. Following this, a polynomial fit, a weighted moving average and Gaussian Processes have been selected for comparison in terms of tune estimation performance.

We begin by describing the presently implemented tune estimation algorithm and then proceed to describe the proposed alternatives. We then perform a thorough comparison of all methods by simulating numerous plausible BBQ spectra for different tune values and widths. Finally we show two examples with comparisons between all three methods applied to recorded BBQ data and finish with concluding remarks.

* leander.grech@um.edu.mt

Content from this work may be used under the terms of the CC BY 3.0 licence © 2020. Any distribution of this work must maintain attribution to the author(s), title of the work, publisher, and DOI

HIGH-ACCURACY DIAGNOSTIC TOOL FOR BEAM POSITION MONITOR TROUBLESHOOTING IN SSRF BASED ON CLUSTERING ANALYSIS *

R. T. Jiang^{†1}, Y. B. Leng^{†1}, C. Jian¹

¹ Shanghai Advanced Research Institute, Chinese Academy of Sciences, Shanghai, 201204, China

Abstract

Beam position monitors (BPMs) are important to monitor the beam moving steadily. In spite of some data is viewed and analysed, a large fraction of data has never been effectively analysed in accelerator operation. It lead to some useful information not coming to the surface during the beam position monitor troubleshooting processing.

We will describe in this paper our efforts to use clustering analysis techniques to pull out new information from existing beam data. Our focus has been to look at malfunction of BPM, associating basic running data that is β oscillation of X and Y directions, energy oscillation and doing predictive analysis. Clustering analysis results showed that 140 BPMs could be classified into normal group and fault group and abnormal BPM could be separated. Based on the results, the algorithm could locate fault BPM and it could be an effective supplement for data analysis in accelerator physics.

INTRODUCTION

The storage ring in SSRF is equipped with 140 BPMs located at 20 cells of the storage ring to monitor the beam dynamics[1]. Each one can give a specific signal that can indicate some properties of the beams at its position individually. Usually, these BPMs are used to inform the accelerator physicists and operators the local status of the beams, such as the beam position and (relative) beam current or lifetime. Meanwhile, the BPM also serve as the orbit feedback system to ensure stability of the beam dynamics[2]. Comparing the measured and computed values of the beam dynamics at each position, one can tell how well the state of runtime accelerator. It could literally see that the BPMs are the eyes and ears for the SSRF. However, a typical BPM system consists of the probe (button-type or stripline-type), electronics (Libra Electronics/ Brilliance in SSRF) and transferring component (cables and such), and complex composition parts easily lead lots of failure. Ever since the SSRF commissioning in 2009, the BPM have occurred all kinds of malfunction. They were permanently damage of individual probe or corresponding cable, misaligned (position/angle) probes, high-frequency vibrations, electronics noise, and others. These faults mean useless of the signals from the BPM and seriously affect the light

source supply time. Hence, it is essential to find an effective tool to detect the faulty BPM for operation of the storage ring.

In our study, we put much effort into real-time processing of data, in order to present to operators results that allow them to either diagnose the health of the system or have a signal on which to perform some optimization process. With development in machine learning methods, a series of powerful analysis approaches make it possible for detecting beam position monitor's stability. Cluster analysis is one of machine learning methods. It is aimed at classifying elements into categories on the basis of their similarity[3]. Its applications range from astronomy to bioinformatics, bibliometric, and pattern recognition. Clustering by fast search and find of density peaks is a new approach based on the idea that cluster centres are characterized by a higher density than their neighbours and by a relatively large distance from points with higher densities[4]. This idea forms the basis of a clustering procedure in which the number of clusters arises intuitively, outliers are automatically spotted and excluded from the analysis. It is able to detect non-spherical clusters and automatically find the correct number of clusters. Based on the advantage of clustering by fast search and find of density peaks, this study establish a multi-dimensional clustering analysis model and monitor the running status of accelerator malfunction.

EXPERIMENTAL DATA AND ANALYSIS METHOD

In this study, the experimental data were collected from the BPM turn-by-turn (TBT) data under the different beam intensity, respectively, are 69 mA 73 mA 78 mA 88 mA 90 mA 96 mA 100mA 104mA 108 mA 111 mA 115 mA 120 mA 124 mA 130 mA 134 mA 140 mA 144 mA 157 mA. By analysing the raw data, we extracted the data of transverse oscillation of X and Y direction, energy oscillation data to judge the faulty BPM. A multi-dimensional clustering analysis model was established and the three characteristic factors were the input variables to locate the BPM malfunctions at different beam intensity. The model has a assumptions that cluster centres are surrounded by neighbours with lower local density and that they are at a relatively large distance from any points with a higher local density. For each data point i , it will compute two quantities: its local density ρ_i and its distance δ_i from points of higher density. Both these quantities depend only on the distances d_{ij} between data points, which are assumed to satisfy the triangular inequality. The local density ρ_i of data point i is defined as

* Work supported by Chinese Academy of Sciences Key Technology Talent Program

[†] jiangruitao@sinap.ac.cn

[†] lengyongbin@sinap.ac.cn

ENERGY GAIN MEASUREMENT FOR ELECTRONS ACCELERATED IN A SINGLE-CYCLE THz STRUCTURE*

Sergey Kuzikov[†], Sergey Antipov, Pavel Avrakhov, Euclid Techlabs LLC, Bolingbrook, IL, USA
 Sergey Bodrov, Alexey Fedotov, Andrey Stepanov, Alexander Vikharev
 Institute of Applied Physics of Russian Academy of Sciences, Nizhny Novgorod, Russia

Abstract

Gradients on the order of 1 GV/m have been obtained via single cycle (~1 ps) THz pulses produced by the conversion of a high peak power laser radiation in nonlinear crystals (~1 mJ, 1 ps, up to 3% conversion efficiency). For electron beam acceleration with such broadband (0.1-5 THz) pulses, we propose arrays of parabolic focusing micro-mirrors with common central. To measure energy gain of electrons in the THz structure we propose applying a voltage (up to 400 kV) to the structure respecting the cathode and anode. Electrons become preliminary accelerated at the entrance that makes design of the structure simpler, because velocity of particles is near to be constant and almost equals the speed of light. On the other hand, the anode can be reached only by the electrons accelerated in the THz field so that one can directly measure the resulting energy gain at the anode.

SINGLE-CYCLE THz STRUCTURES

High-field single cycle THz pulses are now produced by means of laser light rectification in a nonlinear crystal [1-2]. Such pulses can potentially provide ~1 GV/m acceleration of sub-picosecond bunches. In [3-8], a new accelerating structure design was proposed, which introduces a set of waveguides with different adjusted lengths.

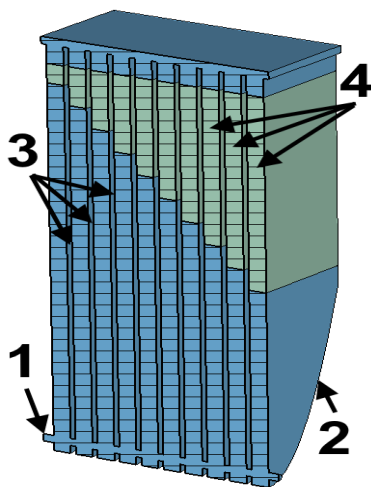


Figure 1: Sketch of broad band THz structure based on dielectric delay waveguides: 1 – beam channel, 2 – mirrors of the parabolic shape, 3 – oversized vacuum waveguides, 4 – delay waveguides filled with dielectrics.

Accelerating structure design is based on waveguide array with different adjusted delays, in which the synchronism of accelerated particles with transversely propagating picosecond THz pulse is to be sustained (Figure 1). Inserted dielectric slabs of the different lengths provide the synchronism of the accelerated particles with transversely propagating single-cycle THz pulse (Figure 2). In the transverse direction, the accelerating structure introduces focusing parabolic mirrors. These mirrors enhance the accelerating field seen by electrons by several times. Such design allows for an overall reduction of losses and mitigation of the negative action of frequency dispersion in the waveguide, because most pathway of THz pulse propagation lies in a wide oversized waveguide. The THz pulse is focused in at the very end of the structure.

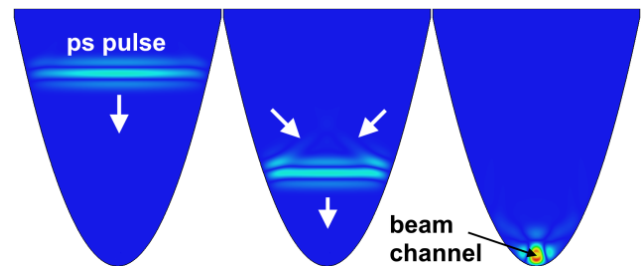


Figure 2: E-field distributions at the parabolic mirror while focusing the short THz pulse, for the time correspondent to beginning of focusing at $t=3.6$ ps (left), for time when focusing is close to maximum at $t=7.6$ ps (center), and in maximum of focusing (right) at $t=11.6$ ps.

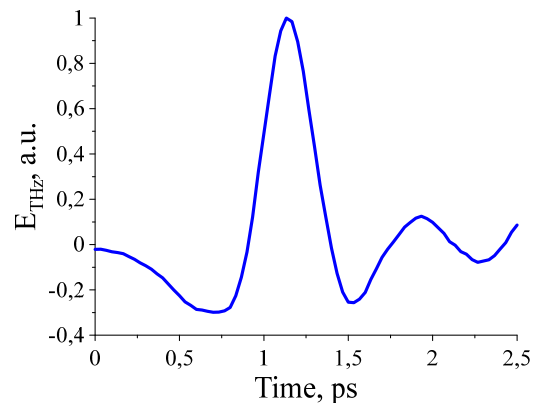


Figure 3: Experimental oscillogram of the single cycle THz pulse shape.

The structure in Figure 2 consists of the identical parabolic mirrors described above. The structure is fed by a single-cycle THz pulse propagating in parallel to metallic blades where the E-field is perpendicular to these blades.

* This work was supported by the Russian Science Foundation under Grant 19-42-04133.

[†] s.kuzikov@euclidtechlabs.com

DESIGN OF THE BEAM DIAGNOSTIC SYSTEM FOR THE NEW 3 GeV LIGHT SOURCE IN JAPAN

H. Maesaka[†], T. Fukui, RIKEN SPring-8 Center, Kouto, Sayo, Hyogo, Japan
H. Dewa, T. Fujita¹, M. Masaki¹, S. Takano^{1,2}, JASRI, Kouto, Sayo, Hyogo, Japan
K. Ueshima, QST Harima District, Kouto, Sayo, Hyogo, Japan
¹also at QST Harima District, Kouto, Sayo, Hyogo, Japan
²also at RIKEN SPring-8 Center, Kouto, Sayo, Hyogo, Japan

Abstract

We designed and developed the beam diagnostic system for the new 3 GeV light source project in Japan. To achieve the performance goals of the light source, we need to precisely measure various beam parameters of the storage ring, such as beam position, stored current, beam size, betatron tune, etc. We developed a button-type beam position monitor (BPM) with a single-pass resolution of less than 0.1 mm for a 0.1 nC injected bunch and with sub- μm closed-orbit distortion resolution for more than 100 mA stored current. The BPM stability was evaluated to be 5 μm for more than one month. The stored current is monitored by two DC current-transformers, which are attached to a vacuum chamber designed to have small beam impedance and small temperature rise. The beam size is measured by an X-ray pinhole camera with a 10 μm resolution. We will install a 3-pole wiggler as a radiator for the X-ray pinhole camera and diagnostics with visible light. Since the resistive wall impedance is expected to be high in the storage ring, we developed a bunch-by-bunch feedback (BBF) system to suppress the beam instability. We tested FPGA-based high-speed electronics for BBF and confirmed sufficient damping performance. A realtime betatron-tune monitor is also implemented in the BBF system. Thus, the beam diagnostic system is ready for the construction of the new light source.

INTRODUCTION

A new 3 GeV light source is now being constructed in Sendai, Japan [1], and will be completed in 2023. It will generate highly brilliant X-rays more than 10^{21} photons/s/mm²/mrad²/0.1%BW around 1 keV photon energy. These X-rays are emitted from a brilliant electron beam having a small natural emittance of 1.1 nm rad and a high beam current of 400 mA. This electron beam performance will be realized with a double double-bend achromat lattice on a 16-cell storage ring with a circumference of 349 m.

To provide the brilliant and stable X-rays to users, the electron beam needs to be stored stably with the design performance. Therefore, the various beam parameters, such as the beam orbit, current, size, etc. have to be monitored precisely and stably. Since a low-emittance storage ring has a narrow dynamic and physical aperture, the electron beam should be precisely steered within the aperture in the commissioning stage by using beam monitors and by tuning

various magnets. Consequently, we have designed a precise and stable beam diagnostic system based on the development results of the beam monitors for the SPring-8 upgrade project [2]. In the following sections, we describe the design and test results of the beam monitors for the new 3 GeV light source.

OVERVIEW OF THE BEAM DIAGNOSTIC SYSTEM

In the commissioning of the storage ring of the new light source, the trajectories of a 0.1 nC bunch from the injector linac need to be measured with a resolution of 0.1 mm std. by the single-pass (SP) mode BPM. To adjust and keep the beam orbit to the ideal one in the user operation, a sub- μm resolution is necessary for the closed-orbit distortion (COD) mode BPM for a stored beam of more than 100 mA. The BPM should also be stable within 5 μm in one operation cycle (~ 1 month). The total stored beam current and each bunch current must be precisely monitored to keep the stored current and the bunch filling pattern constantly in the top-up injection mode. The bunch phase should also be monitored to inject a beam at an appropriate timing in the RF bucket. A precise realtime betatron-tune monitor is necessary to correct the tune shift caused by the gap changes of the insertion devices. Since the storage ring is equipped with narrow aperture vacuum chambers, the beam impedance will excite the beam instability. Therefore, a bunch-by-bunch feedback control system is also required to cure the beam instability.

Based on the above requirements, we designed a beam diagnostic system for the 3 GeV storage ring, as listed in Table 1. We use button-type BPMs for the beam orbit measurement. Seven BPMs are distributed in a unit cell and 112 BPMs are used in total. The stored beam current is measured by two DC current transformers (DCCTs), which are installed into a short straight section (SSS) for beam monitors (SSS-MON1). A 3-pole wiggler is also installed in SSS-MON1 for an X-ray pinhole camera to monitor the beam size. Visible light from the wiggler is also extracted

Table 1: List of Beam Monitors

Diagnostic instruments	Number of units
Beam position monitor (BPM)	112 (7 per cell)
Beam current monitor (DCCT)	2
Stripline BPM	2
Beam size monitor	1
Betatron tune monitor	1 (in BBF)
Beam instability control (BBF)	1

[†] maesaka@spring8.or.jp

PROGRESS OF PROFILE MEASUREMENT REFURBISHMENT ACTIVITIES AT HIPA

R. Dölling[†], E. Johansen, M. Roggli, M. Rohrer
Paul Scherrer Institut, 5232 Villigen PSI, Switzerland

Abstract

At PSI's High Intensity Proton Accelerator (HIPA) facility some 180 profile monitors and 10 radial probes are in use to measure transverse beam profiles in beam lines and cyclotrons at energies of 0.87 to 590 MeV. Mechanical malfunctions and increased noise in some devices, a lack of spare parts and the obsolescence of most of the driver and read-out electronics as well as extended requirements to the measurement, necessitate the development of improved versions of the electronics and of several monitors. We give an update on the status of three projects in this regard: A long radial probe in the Ring Cyclotron, a profile monitor and BPM at 590 MeV in high radiation environment and new loss monitor electronics, which should also serve as a basis for the profile monitor readout.

INTRODUCTION

Operation of HIPA started more than 40 years ago [1]. Meanwhile, a majority of HIPA beam diagnostics has reached an age of 20 to 35 years. Some twenty years ago, the focus of development resources shifted to PSI's newer accelerator facilities SLS, Proscan and SwissFEL. With the aging hardware, we have over the years, gravitated towards an increasingly critical situation. Many diagnostics need to be renewed or refurbished in the next decade.

Since HIPA is a user facility, accelerator development today proceeds at a much slower pace than in the initial years. Nevertheless, the approach based on Joho's N^{-3} scaling law [2, 3] is followed, where increased acceleration voltages in the RF cavities of the cyclotrons result in decreased beam losses and allow higher beam currents. A complementary approach [4, 5], based on a more detailed knowledge of beam and beam loss in the machine, would profit from profile measurements with high dynamic range or more than one dimension, as reported, e.g., in [6].

The replacement of components is a rare opportunity to adapt, improve or extend the functionality of diagnostics, which can support operation and development of the accelerator facility. At IBIC'19 and Cyclotrons'19 we reported on the start of the above mentioned three projects in this regard. For all three, we choose a design which allows later changes and improvements and already implements a number of concrete improvements. These projects will also generate expertise for the production of spares or the replacement of other similar monitors, respectively will serve as a basis for the replacement of the CAMAC profile monitor electronics. In the following, we give an update on the status and further steps of these projects.

[†] rudolf.doelling@psi.ch

RADIAL PROBE IN RING CYCLOTRON

We detailed the design of the basic version of the probe proposed in [7]. The downstream probe head will carry a vertical and two diagonal wires to determine the radial projected profiles of all turns and, to a certain degree [8], of most of the vertical profiles. Shielding electrodes at both sides along the probe carrier [7], which can be biased, will, hopefully, help to prevent disturbances by plasma clouds.

Realization of the hardware has progressed. The long service vacuum chamber including support, turbo pump and vacuum valves, as well as the mechanism to move the probe carrier into the cyclotron (Fig. 1) are ready. Fabrication of the rail guiding the carrier inside the cyclotron and of the 3-wire probe head (Fig. 2) is underway. The design of electrical feedthroughs and details of wiring nears completion. Wiring and lab testing of the complete assembly is still pending. We hope to be able to install the probe in the Ring Cyclotron in the coming, exceptionally short shutdown in February to replace the defect probe and to gain experience with the new design.

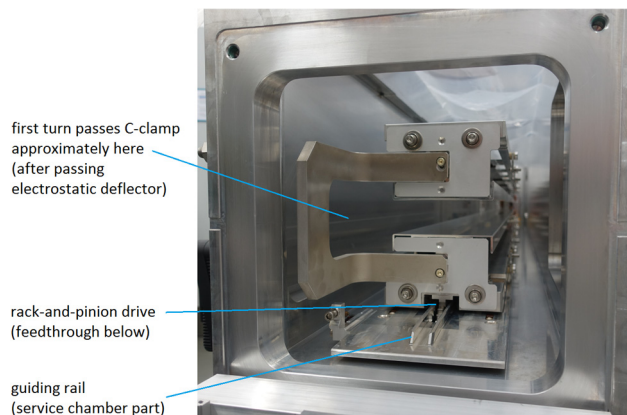


Figure 1: Probe carrier in parking position in the service chamber (in the lab, seen from cyclotron centre).

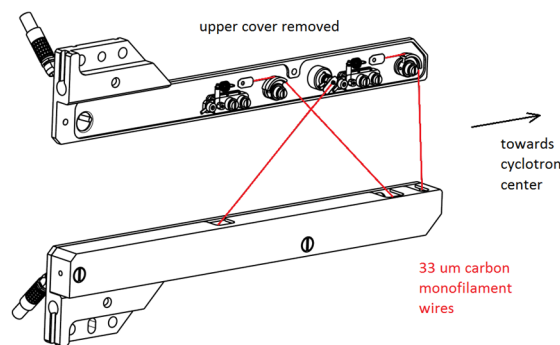


Figure 2: 3-wire probe head (seen from cyclotron side).

FIRST BEAM PROFILE MEASUREMENTS BY BEAM INDUCED FLUORESCENCE AT THE J-PARC NEUTRINO EXTRACTION BEAMLINE

S. Cao, M. Friend*, K. Nakayoshi, K. Sakashita

High Energy Accelerator Research Organization (KEK), Tsukuba, Japan

M. Hartz, Kavli IPMU (WPI), University of Tokyo, Tokyo, Japan and TRIUMF, Vancouver, Canada

Y. Koshio, A. Nakamura, Okayama University, Okayama, Japan

Abstract

A Beam Induced Fluorescence (BIF) profile monitor is under development at the J-PARC neutrino extraction beamline, where neutrinos are produced using 30 GeV protons from the J-PARC MR accelerator. Towards the goal of continuously and non-destructively measuring the 1.3 MW proton beam profile spill-by-spill using fluorescence from proton interactions with injected gas, a full working prototype monitor was installed in the beamline in 2019. The prototype includes a scheme for pulsed injection of N₂ gas into the ultra-high vacuum beampipe and two optical readout arms, a conventional one using an Image Intensifier coupled to a CID camera, along with an array of optical fibers coupled to a Multi-Pixel Photon Counter array. Initial beam tests of the system were carried out in early 2020, and BIF light was successfully observed in both optical systems. Details of the prototype monitor, along with first proton beam profile measurement results, will be shown. Improvement plans towards continuous operation of the new profile monitor will also be discussed.

J-PARC AND THE NEUTRINO EXTRACTION BEAMLINE

The J-PARC Main Ring (MR) accelerator currently provides a 515 kW 30 GeV beam to the J-PARC neutrino extraction beamline for the T2K experiment [1]. The beam structure consists of eight ~ 13 ns (1σ) bunches with a bunch spacing of 581 ns. Currently, $\sim 2.65 \times 10^{14}$ protons per spill are supplied with a spill repetition rate of 2.48 s, while upgrades are planned to increase the number of protons per spill to 3.2×10^{14} and decrease the repetition rate to 1.16 s.

The position and profile of the proton beam extracted into and propagated through the neutrino extraction beamline must be continuously monitored to prevent any damage to equipment due to mis-steered beam, as well as to understand the proton beam properties as inputs into physics analyses.

Currently, the beam profile is measured by a suite of 19 Segmented Secondary Emission Monitors (SSEMs), 18 of which can only be used periodically or during beam tuning. This is because each SSEM causes 0.005% beam loss, which is enough to cause radio-activation of and possibly even damage to beamline equipment. Of course, this loss is proportional to the beam power, and the total induced loss

will increase as the number of protons per pulse and beam spill repetition rate are increased.

Development towards a continuous, non-destructive beam profile monitor is therefore underway. Due to the large number of protons per bunch, and therefore the relatively high beam-induced space-charge field in the J-PARC neutrino extraction beamline, a Beam Induced Fluorescence (BIF) monitor [2] was chosen as a suitable profile monitor candidate. The BIF monitor detects light induced by de-excitation of gas which has been excited or ionized by interactions with incident protons. The longitudinal and transverse pattern of the induced fluorescence should match that of the original proton beam, allowing for an indirect measurement of the proton beam position and profile.

J-PARC NEUTRINO BEAMLINE BEAM INDUCED FLUORESCENCE MONITOR

Development of the J-PARC neutrino extraction beamline BIF monitor has been underway since 2015, with a full working prototype installed in the beamline in 2019 [3]. A photograph of the installed prototype is shown in Fig. 1.

The monitor includes a series of valves for gas injection into the beam pipe, as well as transparent fused quartz windows mounted on the bottom and side of the beam pipe to allow fluorescence light to escape. The inner surface of the beampipe near the interaction region is coated with a 1- μ m-thick coating of Diamond Like Carbon in order to minimize reflections within the beampipe. As shown in Fig. 2, two separate optical focusing and transport systems are used – one mounted on the side of the beam pipe to make a measurement of the vertical transverse beam position and profile, and one mounted on the bottom of the beam pipe to make a measurement of the horizontal beam properties.

The vertical beam measurement arm consists of a series of lenses and mirrors to focus the light downwards onto an array of silica core optical fibers. These optical fibers are used to transport the fluorescence light away from the high-radiation area near the beamline and into a lower-radiation environment inside a subtunnel ~ 30 meters away, where an array of Multi-Pixel Photon Counters (MPPCs) is used to detect the light.

The horizontal beam measurement arm consists of a more conventional light detection system – two lenses focus the induced fluorescence light onto a gated Micro-Channel Plate (MCP) based Image Intensifier, which is coupled to a

* mfriend@post.kek.jp

RECENT PROGRESS ON THE COMMISSIONING OF A GAS CURTAIN BEAM PROFILE MONITOR USING BEAM INDUCED FLUORESCENCE FOR HIGH LUMINOSITY LHC

M. Ady, O. R. Jones, S. Mazzoni[†], I. Papazoglou, C. Pasquino, A. Rossi,
S. Sadovich, G. Schneider, R. Veness, CERN, Geneva, Switzerland
P. Forck, S. Udrea, GSI, Darmstadt, Germany
N. Kumar, A. Salehilashkajani, C. P. Welsch, H. D. Zhang
University of Liverpool and Cockcroft Institute, Warrington, UK

Abstract

For the high-luminosity upgrade of the Large Hadron Collider (“HL-LHC”), active control of proton beam halo will be essential for safe and reliable operation. Hollow Electron Lenses can provide such active control by enhancing the depletion of halo particles, and are now an integral part of the high luminosity LHC collimation system. The centring of the proton beam within the hollow electron beam will be monitored through imaging the fluorescence from a curtain of supersonic gas. In this contribution we report on the recent progress with this monitor and its subsystems, including the development of an LHC compatible gas-jet injection system, the fluorescence imaging setup and preliminary test measurement in the LHC.

INTRODUCTION

The high-luminosity upgrade of the Large Hadron Collider (“HL-LHC”) is a major upgrade of LHC that aims at extending its operability by a decade by increasing its instantaneous luminosity by a factor five beyond its present design value [1]. At the core of the HL-LHC is the upgrade of the focusing triplets to allow for a smaller β^* in the interaction region, combined with compact superconducting radio frequency crab cavities for bunch rotation. These are advanced technical solutions that require a substantial modification of a number of LHC subsystems. The collimation system for HL-LHC, for instance, will require an improved cleaning performance to cope with the increased stored beam energy. To achieve this, is it envisaged to control the diffusion of halo particles by means of a Hollow Electron Lens (HEL) [2]. This will enclose the circulating proton beam with a low energy electron beam, deflecting any halo protons that drift into the electron beam, while leaving the proton beam core unaffected. Key to a correct operation of the HEL is the centring of the circulating proton beam within the hollow electron beam to guarantee that the core will propagate in a region of negligible electromagnetic field. To monitor the HEL alignment, a beam gas curtain (BGC) profile monitor using fluorescence is under development in the framework of the HL-LHC project through a collaborative effort between CERN, GSI and the Cockcroft Institute / University of Liverpool. In this contribution we report on recent progress with the development of the

BGC and its subsystems and on the installation of a prototype that will be operated during the next LHC physics run.

BGC PRELIMINARY STUDIES

Beam Gas Curtain Models and Simulations

Gas curtain generation in the BGC consists of several stages between the gas injection point and the beam interaction chamber. These stages are separated by skimmers, selecting only the central, co-linear part of the gas jet while rejecting the rest. The resulting pressure drop is approximately 2 orders of magnitude per stage. The Monte Carlo code Molflow+ was used to simulate the pressure distribution after the final skimmer, assuming a free molecular flow regime after the first skimmer. Skimmer sizes were therefore calculated so that the expanding gas curtain achieves a width of 20 mm at the interaction point, which is sufficiently wide to cover the hollow electron beam and allow a margin for beam position changes.

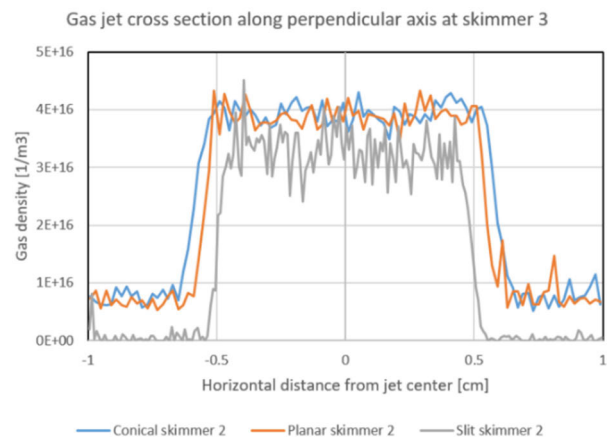


Figure 1: Density profiles for different second skimmer shapes before the interaction point.

Given the skimmer positions (determined by mechanical constraints) and the required sizes, a series of simulations were carried out to verify the gas density in the system to optimize the density within the jet and low contaminations outside of the stream. Figure 1 shows the density profiles at skimmer 3 for different second skimmer shapes before the interaction point. The planar con-

TRANSVERSE PHASE PORTRAIT TOMOGRAPHY OF PROTON BEAMS AT INR RAS LINAC

A. I. Titov^{1†}, S. A. Gavrilov¹

Institute for Nuclear Research of the Russian Academy of Sciences, Moscow, Russia
¹also at Moscow Institute of Physics and Technology (State University), Moscow, Russia

Abstract

Measuring of the parameters of the transverse phase portraits is crucial for beam dynamics. A method of tomographic reconstruction is implemented at INR RAS linac as an alternative to already existing quadrupole variation method. In this work new feature of disturbing online measurements of phase portrait parameters and important experimental results are discussed. Comparison of tomographic method with quadrupole variation method is presented.

INTRODUCTION

Measuring of the parameters of the transverse phase space is crucial for beam dynamics. For low-energy beams these measurements can be made with slit-grid or pepper pot devices. However, for high-energy beams another method is applied – a quadrupole variation method (QVM). A typical layout of components, required for QVM measurements, is presented on Fig. 1.

Another way of measuring beam transverse phase portrait parameters, which can be attributed to QVM, is a tomographic reconstruction. It can be implemented with the same layout as QVM and differs only in processing of obtained information. Feasibility of tomographic reconstruction method is based on Radon transform and was firstly implemented in 70s [1].

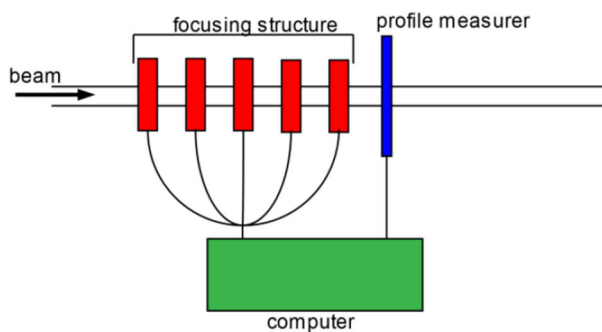


Figure 1: Typical layout of components required for quadrupole variation method measurements.

At INR RAS linac automatic procedure of emittance measurements was developed and implemented at the exit of accelerator on the base of ionization Beam Cross Section Monitor (BCSM) [2]. This procedure provides disturbing online emittance measurements during routine accelerator operation. Also a program for offline measurements was implemented.

[†] aleksandr.titov@phystech.edu

DESIGN FEATURES

As it was previously mentioned tomography is based on BCSM, which schematic configuration is presented on Fig. 2. Image from its phosphor screen is transferred via catadioptric system and acquired with Basler acA780-75gm camera, which is installed under concrete shielding of accelerator. Camera is connected with computer in the control room via optic fibre.

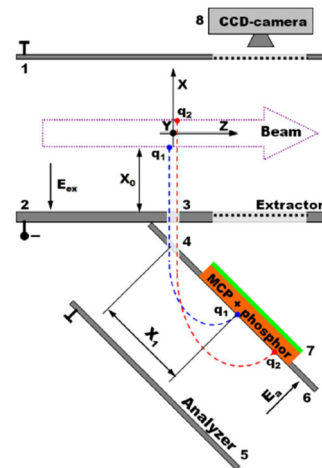


Figure 2: BCSM schematic configuration.

Phase portrait rotation is performed by eight quadrupole doublets, located before BCSM. They are powered by two independent current sources. Transfer matrix method is used for description of focusing structure of accelerator.

SOFTWARE FEATURES

Tomography software at INR is written mostly in LabVIEW [3], tomography kernel is written in Python. Image acquisition and calibration is based on luminescent diagnostics software for INR RAS Proton Irradiation Facility (PIF) and has been described in detail in [4].

Online tomography consists of several steps, which include preplanning of measurements, the measurements of beam profiles and tomographic reconstruction. Preplanning step includes input of currents, which will be set on lenses current sources. After preplanning step user starts up the measurements for tomography.

During the measurement step program changes currents in the sources according to the plan, then the program measures profiles. After making all planned measurements, the program returns initial currents in the sources

DIAMOND BEAM HALO MONITOR*

S. V. Kuzikov[†], S. P. Antipov, P. V. Avrakhov, E. W. Knight, Y. Zhao,
Euclid Techlabs LLC, Bolingbrook, IL, USA
J. G. Power, ANL, Lemont, Illinois, USA

Abstract

Beam halo measurement is important, because novel x-ray free electron lasers like LCLS-II have very high repetition rates, and the average power in the halo can become destructive to a beamline. Diamond quad detectors were previously used for electron beam halo measurements at KEK. Diamond is the radiation hard material which can be used to measure the flux of passing particles based on a particle-induced conductivity effect. However, the quad detectors have metallic contacts for charge collection. Their performance degrades over time due to the deterioration of the contacts under electron impact. We recently demonstrated a diamond electrodeless x-ray flux monitor based on a microwave measurement of the change in the resonator coupling and eigen frequency. We propose similar measurements with a diamond put in a resonator that intercepts the halo. Without electrodes, such a device is more radiation resistant. By measuring the change in RF properties of the resonator, one can infer the beam halo parameters. In a similar manner to traditional beam halo monitors, the diamond plate can be scanned across the beam to map its transverse distribution.

DIAMOND BLADE CONCEPT

Beam halo has a relatively low charge density. However, for high intensity beams, the actual number of particles in the halo is typically quite large. For this reason, the halo is associated with an uncontrolled beam loss, and must be monitored and mitigated [1]. It is difficult to use typical fluorescent screens to monitor beam halo, since the core of the beam will produce a high signal that can leave the halo signal too small to differentiate. The wire scanners allow beam profile characterization its transverse distribution [2]. Even though refractory metals such as tungsten are used for the wires, they must be replaced from time to time due to beam damage. We consider the use of diamond for a sensing material, because of its extraordinary mechanical, electrical, and thermal properties. Large bandgap, radiation hardness, high saturated carrier velocities, and low atomic number make diamond an attractive candidate for the detection of ionizing radiation and charged particles [3]. Diamond quadrant detectors have been successfully used to measure beam halo at KEK [4]. We propose an electrodeless measurement of the charged particle-induced conductivity of the diamond by means of a microwave resonator reflection measurement [5]. A diamond blade will be used to intercept elec-

trons. The blade will be inside a critically coupled resonator, i.e., when fed microwaves at the resonant frequency, there will be no reflection from the resonator. Due to electron interactions with the diamond, the diamond will become weakly conductive. Because of that, the microwave properties of the resonator will change, and it will start to reflect power at the resonant frequency, a signal whose amplitude will be correlated to the intercepted charge from the halo. We propose a reflection-based measurement to detect beam halo (Fig. 1). A diamond blade/wire scans across the beam. The signal recorded is resonator coupling change due to particle-induced conductivity in diamond. The role of charged particles is to promote bound electrons into the conduction band across the band gap.

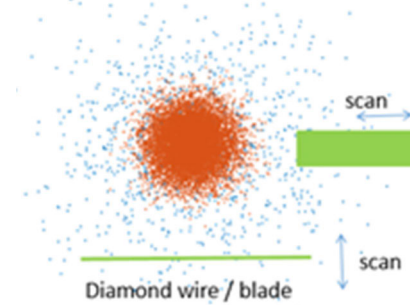


Figure 1: Diamond blade beam halo scanning.

Simulations for Scanning Diamond Blade Scrapper Monitor

To simulate the response of the device to different current densities in the beam halo, we utilized a simple model of a diamond blade positioned between a 100% reflector and a variable reflector (Fig. 2).

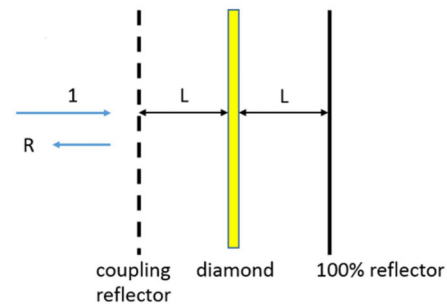


Figure 2: Simulation of resonator S_{11} for beam and no beam for the initial near to critical coupling.

We can adjust the reflectivity of the second reflector to provide critical coupling to this simple resonator. When the coupling is tuned to critical, we can demonstrate a sharp resonance (see Fig. 3). If we change the concentra-

* This work was supported by DoE SBIR grant # DE-SC0019642.

[†] s.kuzikov@euclidtechlabs.com

BEAM COUPLING IMPEDANCE ANALYZE USING BUNCH-BY-BUNCH MEASUREMENT*

X. Y. Xu¹, Shanghai Institute of Applied Physics, CAS, Shanghai, China
Y. B. Leng[†], Shanghai Advanced Research Institute, CAS, Shanghai, China
¹also at University of Chinese Academy of Sciences, Beijing, China

Abstract

Beam coupling impedance is very important parameters for advanced synchrotron radiation facilities. Till now there is no online method to measure beam impedance directly. But some beam parameters such as betatron tune amplitude and frequency, synchrotron phase, bunch lifetime and so on, can be modulated by beam impedance effects. So wake field and beam impedance information could be retrieved by measuring bunch-by-bunch beam 3D positions and analyzing bunch index dependency of above beam parameters. A bunch-by-bunch 3D positions and charge measurement system had been built at SSRF for this purpose and the performance is not good enough for beam impedance analyze due to cross talk between bunches. We upgraded the measurement system to minimize cross talk and improve resolution this year. New beam experiment results and corresponding analyze will be introduced in this paper.

INTRODUCTION

The advanced synchrotron radiation light sources have the following basic characteristics: ultralow beam emittance (few nmrad or even tens of pmrad), ultra-high beam stability (orbital feedback control accuracy is mostly micron or sub-micron level), high average beam current (above 300mA), small-aperture beam vacuum pipe (below 30mm in diameter), a large number of vacuum inserts in , top-up operation mode, small dynamics aperture, with high time resolution experiment ability (time resolution ps order) and so on. The use of small-aperture vacuum pipes and a large number of inserts makes the problem of beam instability caused by the wakefield particularly prominent. Under this condition, the problem of strong beam wakefield (large beam impedance) will become a key issue that limits the further improvement of light facility performance [1]. Correspondingly, how to optimize the beam impedance in the design stage and how to accurately target the source of beam impedance during the commissioning and operation stage to give optimization opinions is the key technical issues that must be resolved when development of the next generation of advanced synchrotron radiation facility.

Under ideal conditions, the particles move steadily in the storage ring. Due to the action of the strong focusing principle and the principle of automatic phase stabilization, the particles make β oscillations around the closed orbit in the

transverse. The synchronous particles in the longitudinal direction make synchronous oscillations. When the oscillation amplitude is small, the transverse oscillation can be considered as simple harmonic vibration. The bunches running in the pipeline will excite the wakefield. If the wakefield decays slowly, it will have an effect on the subsequent bunches. The oscillation amplitude of the bunches under the effect of the wakefield may increase, causing instability. Because its effect is that many bunches are coupled together through the wakefield, it is called coupling instability. The wakefield that can produce coupling instability must not be attenuated before the next bunch arrives. The impedance corresponding to such a wakefield is an impedance with a higher quality factor Q value, or narrow-band impedance. These narrow-band impedances correspond to the higher-order modes of the cavity-like.

At present, the research methods of beam wakefield and impedance mainly include four methods: analytical method, simulation calculation method, emulation test, and beam machine research.

The above methods have their own advantages and limitations in application. The analytical method has the most complete theory, but it can only calculate simple and regular structures, which is not suitable for a new generation of high-performance light sources with many IVU. The simulation calculation method has great application value in the pre-research stage of the accelerator storage ring, but as the structure of the storage ring becomes more and more complex, the device structure cannot be perfectly reconstructed in the software, which has a great influence on the accuracy of the simulation results. In addition, the complicated storage ring structure also brings about the problems that the algorithm cannot converge normally, the calculation time is long, and the resources are occupied. The emulation test method can measure the impedance of some devices in the laboratory. Its disadvantage is that on the one hand, the cold test result in the experiment cannot be completely equal to the result after installation. On the other hand, it is inevitable that the connector will be tightened during the electrical signal input process. The transition section excites a lot of noise signals and causes measurement errors. In order to tighten and straighten the center wire, it is impossible to make it very thin, and there is a certain systematic error. The beam machine research method can directly measure the accelerator beam wakefield, but most of the existing methods require specially designed machine research experiments to measure the wakefield in a special bunch filling mode. The storage ring structure will be adjusted during operation (for example,

* Work supported by National Natural Science Foundation of China (No.11575282) and Ten Thousand Talent Program and Chinese Academy of Sciences Key Technology Talent Program

[†] lengyongbin@sinap.ac.cn

ADVANCED LASER-DRIVEN PLASMA ACCELERATOR ELECTRON-BEAM DIAGNOSTICS WITH COTR-BASED TECHNIQUES*

A. H. Lumpkin[†], Fermi National Accelerator Laboratory, Batavia, IL, USA
M. LaBerge, M. Downer, University of Texas at Austin, Austin, TX, USA
D. W. Rule, Silver Spring, MD, USA
A. Irman, Helmholtz-Zentrum Dresden-Rossendorf, Dresden, Germany

Abstract

A significant advance in laser-driven plasma accelerator (LPA) electron-beam diagnostics has recently been demonstrated based on coherent optical transition radiation (COTR) imaging. We find COTR signal strengths from a microbunched subset of beam exiting the LPA to be several orders of magnitude higher than that of incoherent optical transition radiation (OTR). The transverse sizes are only a few microns as deduced from the point-spread-function-related lobe structure. In addition, the far-field COTR interferometric images obtained on the same shot provide beam-size limits plus divergence and pointing information at the sub-mrad level when compared to a modified analytical model. The integrated image intensities can be used to estimate the microbunching fraction and relatable to the LPA process. Initial results in a collaborative LPA experiment will be reported for electron beam energies of about 215 MeV. A revised configuration is proposed to record energy and energy spread via COTR on the same shot with the interferometer.

INTRODUCTION

The periodic longitudinal density modulation of relativistic electrons at the resonant wavelength (microbunching) is a well-known, fundamental aspect of free-electron lasers (FELs) [1]. In one classic case, microbunching fractions reached 20% at saturation of a self-amplified spontaneous emission (SASE) FEL resulting in gains of 10^6 at 530 nm [2]. In that experiment the concomitant z-dependent gain of coherent optical transition radiation (COTR) was also measured at the $>10^5$ level. Microbunching at visible wavelengths in laser-driven plasma accelerators (LPAs) had been reported previously [3,4], but it has only recently been measured in near-field and far-field images on a single shot for the first time with significant COTR enhancements involved [5-7].

We reintroduce a modified analytical model for COTR interferometry (COTRI) first developed for the SASE-FEL-induced microbunching case [8] to evaluate now the LPA case [7]. The coherence function was treated in this analytical model that addresses both cases and the expected fringe patterns. In the modified model, we consider the increase in the effective beam size in the drift between the foils due to the divergence term [9]. This term has negligible effects for low divergences of the

microbunched electrons.

In the FEL, one identified microbunched transverse cores of 25-100 microns in extent while in the LPA the recently reported transverse sizes at the exit of the LPA were a few microns [5-8]. In the latter case, signal enhancements $>10^5$ and extensive fringes out to 30 mrad in angle space were recorded.

EXPERIMENTAL ASPECTS

The LPA at HZDR

The LPA is based on the DRACO laser with a peak power of 150 TW at a central wavelength 800 nm interacting with a He gas jet (with 3% Nitrogen) at the Helmholtz-Zentrum Dresden-Rossendorf (HZDR) facility [10]. The LPA was operated with a plasma electron density $n_e \sim 3 \times 10^{18} \text{ cm}^{-3}$ in the self-truncated ionization-injection mode. Beam energies of ~ 215 MeV in a quasi-monoenergetic peak were observed in a downstream spectrometer. After the LPA, a 75- μm thin Al foil blocked the laser pulse and was followed by an Al-coated Kapton foil as shown in Fig. 1. The latter's back surface provided the source point of the near field (NF) COTR imaging, and a polished 200- μm thick Si mirror at 45° to the beam direction redirected this light to the microscope objective. The configuration provided a magnification factor of 42 at the camera and a calibration factor of 0.09 $\mu\text{m}/\text{pixel}$. This mirror was located 18.5 mm downstream of the Al-coated Kapton and also generated backward COTR that combined with the first source to provide COTRI in the far-field (FF) imaging camera. The significantly enhanced signal allowed the splitting of the signal into two NF cameras as well as a FF camera with a 633 ± 5 nm bandpass filter (BPF) as shown schematically in Fig. 2.

We propose an extension of the single-shot diagnostics coverage to electron beam energy, energy spread, and optical spectroscopy on the same shot by replacing the thick Si mirror at 45 degrees with a few- μm thin Al/Ti mirror/foil. This is so thin that the energy loss in transit for 215 MeV would be in the 10-4 range so energy spread info is also preserved. Since the scattering is much less than $1/\gamma$ we expect the microbunching fraction to be preserved also. An Al foil at the spectrometer focal plane and narrowband filter in front of the camera would allow the imaging of the COTR for the microbunched electrons.

* This manuscript has been authored by Fermi Research Alliance, LLC under Contract No. DE-AC02-07CH11359 with the U.S. Department of Energy, Office of Science, Office of High Energy Physics.

[†] lumpkin@fnal.gov

FEATURES OF THE METAL MICROSTRIP DETECTORS FOR BEAM PROFILE MONITORING

V. M. Pugatch, D. M. Ramazanov, O. S. Kovalchuk
Institute for Nuclear Research NAN, Kyiv, Ukraine

Abstract

Features of Metal Microstrip Detectors (MMD) are presented for application in beam profile monitoring of charged particles and synchrotron radiation beams. Through an innovative plasmachemistry etching production process, thin metal micro-strips only 1–2 μm thick are aligned. Because of the very thin nature of the strips, the MMD is nearly transparent, and can be used in situ for measuring, tuning and imaging the beam online. Metal structure of sensors guarantees high radiation tolerance (about 100 MGy) providing their stable response to the beam particles (by the secondary electron emission) independent upon the accumulated fluence. The spatial resolution of the MMD is determined by the strips pitch constituting from 5 to 100 μm in currently manufactured samples. The data obtains with MMDs read out by the low noise X-DAS system providing integration time from 1 to 500 ms, and the ability to process signals in real time. The scope of MMD & X-DAS is scientific and applied research using beams: in control systems of accelerators and synchrotron radiation sources. New possibilities are discussed for equipment requiring high spatial resolution and radiation hardness.

INTRODUCTION

Beam diagnostics is an important component of any accelerator. In modern experiments in high-energy physics, particle fluxes reach extremely large values. The increase in intensities and energy leads to an increase in radiation loads on the detector systems. It is known that silicon, scintillation and other detector systems used in most experiments have limited radiation resistance, and at too high radiation fluxes lose their performance. In addition, the main requirement for conducting physical experiments is that the measuring device must not distort the measured value. To date, most detector systems do not meet this statement. In this case, the requirements for detector systems for precision measurements are only increasing. Medical accelerators play a special role in this task, because the life and health of patients depend on the precision of the accuracy and intensity of the beam. A detector system that would independently control the position, size and intensity of the ionizing radiation beam would significantly increase the reliability and safety of irradiation.

This paper describes a detector system that can be used to monitor a beam for various types of radiation therapy, and for accelerators used in high-energy physics experiments. The direction of research is the development of detectors based on the phenomenon of secondary electron emission. Features of secondary electron emission allow to create structurally

simple reliable detector systems for monitoring the flow of charged particles and X-rays. This type of detectors includes metal microstrip detectors presented in this article [1–4].

METAL MICROSTRIP DETECTOR

A distinctive feature of MMD from micro-detectors based on semiconductor or insulating materials, which either completely absorb the investigated beam or significantly deform it, metal sensor is almost ideal operation as a measuring and monitoring device without distorting the characteristics of the investigated particle beam or synchrotron radiation. The MMD sensor is made entirely of metal, making this detector one of the most radiation-resistant.

Principle of Operation

Figure 1 shows the operation principle of an MMD secondary emission monitor grid with ultra-thin wires/strips. One end of each strip is connected to a charge integrator or other measuring system and the other to a stable current source. Incident x-rays on the strips initiate secondary electron emission as they pass through the nearly transparent medium. When this happens, a positive charge appears at the integrator end and is measured.

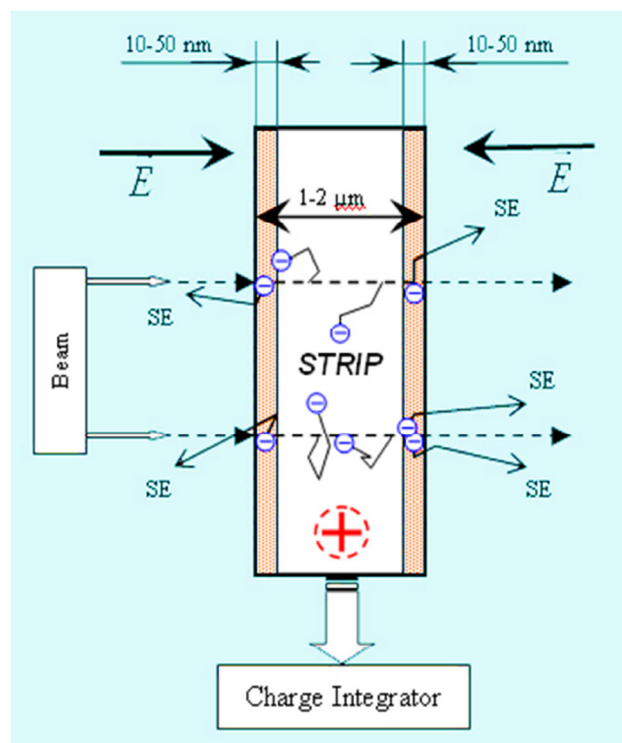


Figure 1: Operation principle of MMD.

TESTBED DEVELOPMENT FOR THE CHARACTERISATION OF AN ASIC FOR BEAM LOSS MEASUREMENT SYSTEMS

F. Martina¹, C. Zamantzas, L. Giangrande, J. Kaplon, P. V. Leitaó, CERN, Geneva, Switzerland
¹also at Dept. of Electrical Engineering and Electronics, University of Liverpool, Liverpool, UK

Abstract

A high-performance, radiation-hardened, application-specific integrated circuit (ASIC) is under development at CERN for digitising signals from beam losses monitoring systems in harsh radiation environments. To fully characterise and validate both the analogue and digital parts of these ASICs, an automated testbed has been developed. Here we report on the components used to build this set-up, its capabilities as well as the methodology of the data analysis. Focus is given to the data collection, the automation and the efficient computation methods developed to extract the merit factors of two different ASIC designs from prototype manufacturing runs.

INTRODUCTION

In view of the HL-LHC upgrade [1], a new version of the Beam Loss Monitoring (BLM) front-end electronics is under development. The BLM system is one of the critical systems for the protection of the particle accelerator against damage (or quenches [2] in the case of the LHC) caused by the energy deposition from lost beam particles and their secondary particle cascades [3].

The new key component of this BLM front-end, as compared to the old system [4-6], is a custom-designed Application Specific Integrated Circuit (ASIC), hereafter referred to as the BLMASIC. The aim of the design is to guarantee high resolution measurements in harsh radiation areas, where off-the-shelf components (COTS) cannot be used. To achieve this, two different BLMASIC architectures have been investigated and designed: one based on current-to-frequency conversion (BLMASIC-CFC, the same concept as the currently operational system); and one implementing a delta-sigma converter (BLMASIC- $\Delta\Sigma$).

The aim of the present research is to measure the ASIC performance and have a first validation of their conformity to the specified requirements for the system. This includes looking at their linearity, their measurement resolution, their temperature stability, their robustness to electrostatic discharge (ESD) at the input, their tolerance to radiation and faults, and their compatibility with the other components required for the BLM system upgrade.

Even though the estimated performance of the device has been simulated using sophisticated tools, tests on the real component are essential to qualify its behaviour after the manufacturing process. There are physical effects not

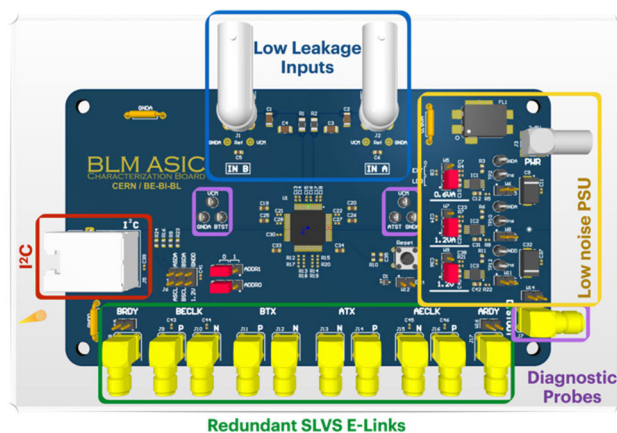


Figure 1: Characterisation Board.

included in the simulations that depend on the fabrication run, and others that are intrinsically too complex to be taken into account. The versatile testbed built should also allow a direct comparison of the two architectures and provide the necessary information to take the decision on which one to select for the final production.

This work focuses on the architecture and assembly of a testbed to perform this testing. It includes the design of a characterisation board, the selection of suitable laboratory instrumentation, the development of the acquisition and configuration firmware, as well as the software for future batch data analysis. An example of noise performance characterisation using this testbed is reported.

TESTBED ARCHITECTURE

In order to validate the performance of the BLMASICs, a multi-layer characterisation PCB has been designed, which provides direct access to the device interfaces, including all the debug features available (Fig. 1). The board is equipped with low leakage BNC inputs for injecting test currents into the device; redundant SLVS lanes to provide the clock and output the digital data stream; an I²C bus to read and configure all the internal registers; three diagnostic probes, which are connected to a programmable multiplexer switching among several internal analogue and digital signals. The final module can either be powered from external power supplies or using the low noise supplies provided by the characterization board. When this last option is chosen, shunt resistors can be used to monitor the current consumption on the power bus.

PROPERTIES OF CHERENKOV DIFFRACTION RADIATION AS PREDICTED BY THE POLARISATION CURRENTS APPROACH FOR BEAM INSTRUMENTATION

D. M. Harryman*, K. V. Fedorov, P. Karataev

JAI, Royal Holloway, University of London, Egham, Surrey, UK

L. Bobb, Diamond Light Source, Oxfordshire, UK

M. Bergamaschi, R. Kieffer, K. Lasocha, T. Lefevre, S. Mazzoni, A. Schloegelhofer
CERN, Geneva, Switzerland

A. P. Potylitsyn, Tomsk Polytechnic University, Tomsk, Russia

Abstract

Cherenkov-Diffraction Radiation (ChDR) appears when a charged particle moves in the vicinity of a dielectric medium with velocity higher than the phase velocity of light inside the medium. As the charged particle does not contact the medium, the emission of ChDR is a phenomenon that can be exploited for a range of non-invasive beam diagnostics. Experimental tests are underway on the Booster To Storage-ring (BTS) test-stand at Diamond Light Source to explore the use of dielectric radiators as Beam Position Monitor (BPM) pickups by measuring the incoherent ChDR emission. In order to compliment the experiments on the BTS test-stand, ChDR simulations have been performed using the Polarisation Currents Approach (PCA) model. This paper explores the PCA simulations for the BTS test-stand, and the application for future diagnostics.

CHERENKOV DIFFRACTION RADIATION

Cherenkov Diffraction Radiation (ChDR) appears when a charged particle moves in the vicinity of a dielectric medium with velocity higher than the phase velocity of light inside the medium [1]. Detecting ChDR in accelerators is being explored in the development of non-invasive beam diagnostics [2]. ChDR appears at the same distinctive angle as Cherenkov radiation that is given by

$$\cos(\theta_{\text{Ch}}) = \frac{1}{\beta n}, \quad (1)$$

where θ_{Ch} is angle of ChDR emission, β is ratio of the particles velocity compared to the vacuum velocity of light, and n is the refractive index of the radiator [3,4]. The emission angle of ChDR allows for a detection system to be designed that can discriminate against noise such as synchrotron radiation. A theoretical model to predict the emission of ChDR has been developed in [5–7], the model developed is called the Polarisation Currents Approach (PCA).

RADIATOR GEOMETRIES

The PCA model can be applied to different radiator geometries where the geometry selected will effect the ChDR

* daniel.harryman.2018@live.rhul.ac.uk

emission [5, 7]. Figure 1 shows a prismatic ChDR radiator where the notation used is as follows; γ is the Lorentz factor β is ratio of the particles velocity compared to the vacuum velocity of light, λ is the wavelength of the radiation, $\varepsilon(\lambda)$ is the wavelength dependant permittivity of the prism, θ_{Ch} is the Cherenkov angle, a is the length of the surface parallel with the electron trajectory, φ is the vertex angle of the prism, δ is $(90^\circ - \varphi)$, b is the impact parameter, h is the angled impact parameter (where $b = h \cos(\delta)$), and ϕ , θ are respectively the azimuthal and polar angles of the emitted radiation [7].

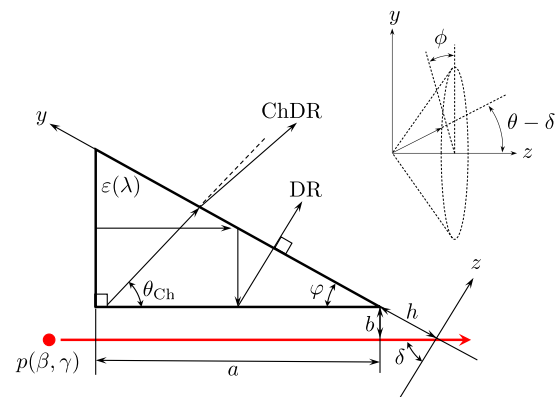


Figure 1: Prismatic Radiator Geometry.

Using a prismatic radiator, the ChDR is generated at the Cherenkov angle which is distinctively different to that of the particle trajectory, once the ChDR reaches the emission surface of the prism it will be emitted at a refracted angle using Snells law [8]. Knowing the index of refraction for the prism, the outside interface, and the Cherenkov angle for that radiator, the vertex angle of the prism is selected for a desired extraction angle. As the ChDR is generated along the entire target length it will be emitted along the majority of the extraction surface.

Extensive work has been done in [7] to obtain the ChDR angular distribution emitted from a prismatic radiator when a charge particle moves parallel to one side (see in Fig. 1). Each polarisation component is then given by Eqs. (2), (3) and (4), where \hbar denotes the reduced Plank constant, α is the fine structure constant, c is the vacuum speed of light, and the notation from Fig. 1 has been used [7].

DEVELOPMENT OF BEAM ABNORMAL STATE MONITORING PROCESSOR ON SSRF STORAGE RING*

L. W. Lai[†], Y. B. Yan, Y. B. Leng

SSRF, Shanghai Advanced Research Institute, Chinese Academy of Sciences, Shanghai, China

Abstract

An abnormal beam state monitoring processor has been developed on SSRF, which is based on the hardware of self-developed digital BPM processor. By applying digital signal processing algorithms in the on-board FPGA, the processor keeps monitoring the beam running state. Once abnormal event is detected, the processor will record the abnormal event type and store the turn-by-turn beam position data before and after the event for later analyzing. The abnormal events including beam loss and beam position jump.

INTRODUCTION

SSRF starts operation since 2009, some unexplained beam loss events occurred on the storage ring during the operation. And the number is rising in this year. BPM data analyzing is one of the effective means to find the possible reason. Libera Electron and Brilliance are deployed on SSRF for BPM signal processing. Libera has a Post mortem input interface. "Post mortem input signal is linked typically with machine protection system. The input signal is usually connected with critical events, such as beam loss. There is a dedicated memory buffer reserved for post mortem data. After Postmortem trigger arrival, the history before the trigger arrival is stored in this buffer. User can access this buffer from the control system. Postmortem buffer contains turn-by-turn data [1]. However, This function relies on the input "Post mortem" signal from interlock system. Sometimes partial beam loss and orbit deviation may not trigger the interlock function, then Libera can't buffer the BPM turn-by-turn data for analyzing.

An in-situ DBPM has been developed in SSRF. Based on the platform, a serial of processors been developed successfully for variety applications over the past few years, including stripline BPM, cavity BPM, BAM, booster BPM, storage ring BPM. The DBPM has been deployed in DCLS, SXFEL, SSRF and Sirius linac in a large scale [2, 3]. Table 1 lists the DBPM specifications and Figure 1 shows the DBPM hardware structure and picture. It consists of an ADC daughter board and a FPGA+ARM mother board.

Compared to the commercial products, DBPM is much more flexible to develop functions for special user applications on the FPGA and ARM. This paper will introduce the development and application of a beam state monitoring processor based on the DBPM. The processor buffers the BPM data when abnormal events are detected by

itself. Abnormal events including user specified beam loss and beam orbit out of range.

Table 1: DBPM Specifications

Parameter	Value
Channels	4
Central Frequency	500MHz
Bandwidth	~20MHz
Dynamic range	31dB
ADC bits	16
Max ADC rate	125MSPS
FPGA	Xilinx xc5vsx50t
CPU	Arm
Clock	Ext./Int.
Trigger	Ext./Self/Period
Software	Arm-Linux/EPICS

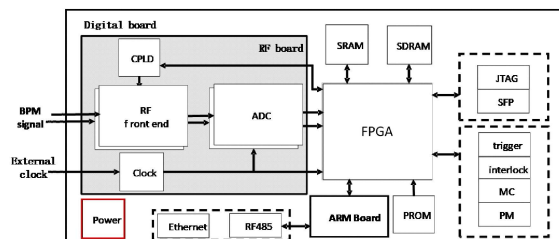


Figure 1: DBPM Processor.

PROCESSOR OVERVIEW

The DBPM in SSRF provides various rate beam position data, including turn-by-turn, 50kHz FA, 10kHz FA and SA. Figure 2 shows the function diagram of the processor.

The processed BPM turn-by-turn data, FA 50kHz data, FA 10kHz data are fed into the function. One of the data is switched by user as the abnormal event detection source, and also fed into a 16384 FIFO. External trigger signal is input to avoid injection events. Then the position data X,Y and sum data S are fed into two different processing channels. The X/Y data are compared to the user configured high limit and low limit respectively. The

*Work supported by Youth Innovation Promotion Association, CAS (Grant No. 2019290); The National Key Research and Development Program of China (Grant No. 2016YFA0401903).

[†] lailongwei@zjlab.org.cn

INFLUENCE OF A BELLOW TO A CAVITY BPM FOR SINBAD

D. Lipka*, DESY, Hamburg, Germany

Abstract

A cavity beam position monitor acts for the detection of the beam location within a pipe with high precision and best resolution. Some of them are used as a fixed point to refer the other parts of the beamline. To be able to fix the monitor against the other vacuum components bellows need to be adapted next to the monitor to relax the other part of the vacuum chamber. The bellow itself can create a resonance which would influence the resonator of the cavity beam position monitor. In this study the influence of the bellow to a cavity beam position monitor is investigated with simulations for a SINBAD project. The result is that the influence to the dipole resonator is below 0.1 %.

INTRODUCTION

SINBAD is a dedicated accelerator R&D facility currently under commissioning at DESY, Hamburg, and will host the ARES linac (Accelerator Research Experiment at SINBAD). It consists of a normal conducting photo-injector and a 100 MeV S-band linear accelerator with beam repetition rates between 10 and 50 Hz for the production of low charge beams (0.5–30 pC) with (sub-) fs duration and excellent arrival time stability [1–4]. For dedicated user experiments bunch charges up to 1000 pC are foreseen. At a bunch compressor a tube diameter of 40.5 mm is requested with high demand on the monitoring of the beam position. Therefore a cavity beam position monitor (CBPM) with best resolution is foreseen as the monitor, the design of the European XFEL will be used [5]. Bellows will be installed before and after the CBPM to relax the vacuum chamber. Such a bellow consists of blades which have a larger diameter of the vacuum tube and will create resonances which could influence the signal of the CBPM. Therefore the influence has to be investigated and if necessary be minimized.

SETUP

Bunch compressors are essential for the generation of short bunches with applications in e.g. colliders, free electron lasers and advanced accelerator concepts. The up-and-coming ARES accelerator located at SINBAD, DESY will support the formation of 100 MeV, pC, sub-fs electron bunches for Laser Wake Field Acceleration research and development [6]. The bunch compressor consists of four dipoles and two collimators. To monitor the beam properties a screen station and a CBPM will be installed. Since the compressor needs to be variable in the beam deflection a relative large beam pipe is requested. One version of the CBPMs of the European XFEL has a beam tube diameter of 40.5 mm which will be used for this bunch compressor at SINBAD too [5].

The CBPM consists of a reference and dipole resonator and is adapted from a design of SACLA [7]. The working resonance frequency of the monopole mode of the reference resonator and the dipole mode of the dipole resonator are tuned to the same value of 3.3 GHz. The first resonator is necessary to measure the amplitude from the monopole mode as a function of charge to normalize the signal from the second resonator and define the beam direction. The second resonator provides a signal generated by the dipole mode proportional to the beam offset; for this the dominant monopole mode of the dipole resonator needs to be reduced. This is done by waveguides or slots [8]. The setup is shown in Fig. 1. Here only the dipole resonator on the left side

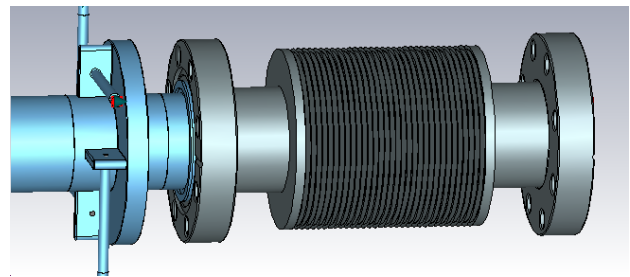


Figure 1: 3-dimensional simulation view of the vacuum part of the dipole resonator on the left in blue with the bellow on the right.

is shown and simulated with the simulation tool CST [9] because the reference resonator provides much higher amplitudes such that an influence from the bellow can be ignored. In Fig. 1 can be seen the dipole resonator vacuum view with slots and feedthroughs for the horizontal and vertical plane; a reversed reality view. The bellow is shown in normal view such that one can see the flanges and blades. Each blade forms a resonator which can induce resonances near the CBPM working frequency due to similar diameters and their amplitude can be enhanced because of the repetitive design. The field of the bellow resonances can be transmitted to the dipole resonator due to the relative large beam tube diameter but will be attenuated due to the distance between resonator and first blade of 73.7 mm.

SIMULATION OF THE INFLUENCE OF THE BELLOW

The tool CST provides beam simulations including wake-field generation which is capable to monitor the fields along the beamline. Resonances due to the beam propagation will be induced into the setup and can be visualized. Here voltage monitors are defined at the end of the feedthroughs from the slots to measure the responds of the beam at the exit of the CBPM. The simulation time of the beam propagation is defined until 18 ns which corresponds to the processing

* Dirk.Lipka@desy.de

STUDY OF MULTI-BLADED PHOTON BPM DESIGNS

Y.-R. E. Tan*, AS - ANSTO, Clayton, Australia

Abstract

New beamlines will be installed in at the AS in the next few years and photon BPMs will be part of the front end design. A theoretical study of the potential benefits of a multi-bladed photon BPM design has been simulated using beam profiles from SPECTRA. The results show that it is possible to remove the gap/field dependence of the photon BPM by a least squares fit of the distribution, in this test case a Gaussian distribution, to the beam profile sampled by the multiple blades.

INTRODUCTION

The majority of photon BPMs (XBPMs) that are located in the front-end of beamlines at light sources use metallic blades as the detector. As synchrotron radiation illuminate the surface of the metallic blades, photo-electrons are ejected (PE effect) and the current is proportional to the photon flux and energy. The drain current at the blade is measured using a picoammeter or equivalent. The strength of such a design is its fairly straight forward design, ability to reach μm resolutions and robustness. The most typical configuration is a pair of blades on either side of the photon beam to measure the vertical displacement. This is typical for dipole and wiggler sources. If transverse directions are required then four blades are used, either arranged in the cardinal directions or rotated by 45° . This is commonly used for undulator sources. There are two well known issues, upstream contamination from other radiation sources and a gain (calibration factor) that depends on the photon distribution, which in turn depends on the insertion device parameter, K_u . This is particularly problematic for APPLEII type insertion devices that have many more degrees of freedom and potential photon distributions. To overcome some of the deficiencies issue other approaches to photon beam detection is being developed such as photoconduction based designs using diamond or SiC based detectors [1], fluorescence based [2] or residual gas [3].

The first issue of upstream photon contamination is difficult to address and is only an issue if the photon flux from the ID at the blade is comparable to the flux from other sources (blades are too far away or $K < 1$) [4]. This report investigates the potential benefits of fitting a Gaussian distribution to the photon distribution sampled at four or more locations. This approach is investigated numerically and compared to traditional methods to show that it has the potential to be more robust against changes to K_u .

* eugene.tan@ansto.gov.au

PHOTON DISTRIBUTION AND BLADE CONFIGURATION

The source radiation will be modelled on a 22 mm period IVU with a K_u between 1.03 and 1.85. Some design parameters include an assumed beamline acceptance of 1.11 mrad by 0.40 mrad and XBPM's located 6.9 m from the source. Assuming the extent of the blade is located at $+0.3$ mrad and maximum beam offsets of ± 1 mm, the minimum observation angle of the blade is approximately 0.2 mrad. In Fig. 1 the energy spectrum at two extreme K_u values has been calculated using SPECTRA [5] showing that above 3 keV the flux peaks have decreased by an order of magnitude. For this study we have limited simulation to an integration of photon distributions calculated at 100 intervals between 100 eV and 3.5 keV. A plot of such a distribution is shown in Fig. 2 for $K_u = 1.03$ along with the blade configuration. A simple blade geometry has been adopted, with a set of 2 mm long vertical blades with a range of horizontal gaps between the blades, $S_x = [0.5, 1.0, 1.5, 2.0, 2.5]$ (mm).

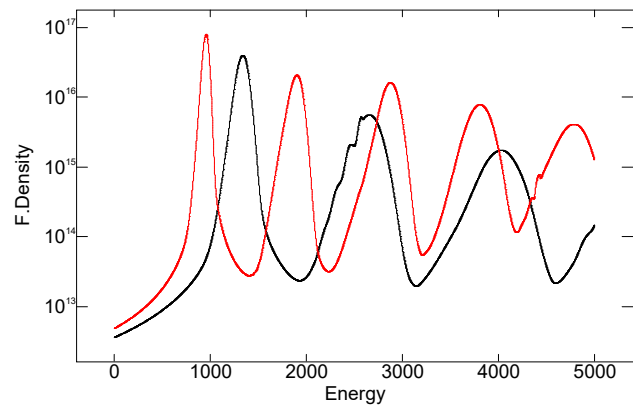


Figure 1: Flux density at an observation angle $\theta_y = 0.2$ mrad for a $K_u = 1.03$ (black) and 1.85 (red).

CENTROID CALCULATIONS

Four methods will be evaluated. The first two are the difference over sum (DS) method given by

$$x^{DS} = K_x^{DS} \frac{[(b_4 + b_9) - (b_2 + b_7)]}{b_2 + b_4 + b_7 + b_9}$$

$$y^{DS} = K_y^{DS} \frac{[(b_2 + b_4) - (b_9 + b_7)]}{b_2 + b_4 + b_7 + b_9}$$

the center of mass (CM) method,

$$x^{CM} = K_x^{CM} \frac{\sum_{n=1}^5 w_n b_n}{\sum_{n=1}^5 b_n}$$

$$y^{CM} = K_y^{CM} \frac{\sum_{n=12,9,4,11} w_n b_n}{\sum_{n=12,9,4,11} b_n}$$

CHARACTERIZATION STUDY OF A BUTTON BPM WITH AN APPROACH TO AUTOMATED MEASUREMENTS

Yogesh Verma*, Indian Institute of Science Education and Research (IISER), Mohali, Punjab, India
Madhuri Aggarwal, Vipul Joshi, Ashish Sharma
Inter University Accelerator Centre (IUAC), New Delhi, India

Abstract

Beam position monitors (BPMs) are one of the very important diagnostic components of any accelerator system giving information about beam position. It is a class of non-intercepting devices which use the coupling of the EM field around a charged particle bunch to some sort of conductor electrodes to recover beam position information from the beam-induced signals. In this paper, a characterization study of an in-house developed Button BPM including sensitivity measurement and transfer impedance studies is presented. Sensitivity measurement was done using the stretched wire method by passing current pulses through the wire of different diameters like 0.5 mm and 1 mm, thus mimicking the behavior of the actual beam. Sensitivity information was then used to reciprocate the 2-D position map of the device. Owing to the time taken for such huge measurements, an automated BPM test bench approach of the whole setup is developed by remote interfacing over LAN. A substantial decrease in measurement time was observed along with a reduction in measurement error.

INTRODUCTION

In particle accelerators, a beam position monitor (BPM) provides crucial information about the beam. A typical button BPM consists of four button-type electrodes mounted inside the surface of cylindrical pipe in vacuum. The main idea is to measure the charges induced by the time varying electric field of the beam particles on an insulated metal plate [1]. By measuring the electrode signal of various electrodes, the relative gains of the electrodes can be calculated. Studies have been performed in calculating the optimal dimension of BPM for maximum gain [2]. Button BPM have been used extensively and deployed at various accelerator systems [3, 4] ranging from ring systems [5] to developing test bench for proton LINAC [6] and with an approach to automation [7].

This paper presents a characterization study of a button BPM with transfer impedance studies and position sensitivity measurements with a development of an automated BPM test bench. Stretched wire method [8] with wire of different diameters 0.5 mm and 1 mm is implemented for sensitivity and mapping measurements to mimic the actual beam. Automated test bench for BPM have been considered an alternative to manual measurements (position mapping, sensitivity etc.) due to consumption of huge amount of time resource. In comparison to a Libera DAQ based automated

test bench [7], the approach presented in this paper is cost effective due to usage of generally available lab equipment's. A comparison of manual measurements vs automated measurements is also been performed to evaluate the performance of automated measurements.

The paper is divided in various sections, first section provides a description of the test setup and device under test. The second section provides the transfer impedance study for both the wires and the third section presents the position sensitivity measurements. Paper is concluded with 2-D position mapping with development and implementation of automated test bench.

TEST BENCH SETUP

Figure 1 shows the automated BPM test bench setup which consists of a function generator, 2 sets of X-Y scanner motor assembly, motion controller, a DSO, Device Under Test (DUT) (BPM) and stretched wire with weights.

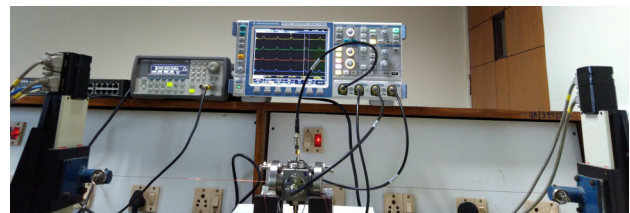


Figure 1: Automated Test bench Setup with Device Under Test (BPM).

Device Under Test

DUT in present case is a cylindrical SS pipe of length 88 mm with DN 63 flange having outer diameter of 63 mm and inner diameter of 35 mm with 4 electrodes (buttons) mounted using vacuum compatible 50 Ω SMA feed-through. Electrodes are of 6mm radius and made of Aluminium.

TRANSFER IMPEDANCE

Transfer impedance relates BPM output signal with the beam current. For measuring the Transfer Impedance of the Button BPM, the modified co-axial cable method [9] is used. In this method the total output voltage for the DUT is given as an infinite summation of the reflected and the transmitted signal converging to a definite value. Schematic setup is shown in Fig. 2. The port-1 node is fixed with the Vector Network Analyzer (VNA) and the port-2 node is varied to all the 4 electrodes to obtain respective transmission coefficients.

* yverma132@gmail.com

SEPTUM ORBIT FEEDFORWARD CORRECTION AT THE AS

C. Lehmann*, University of Queensland, Brisbane, Australia
Y.-R. E. Tan, M. Atkinson, AS - ANSTO, Clayton, Australia

Abstract

The leakage fields generated by the septum in the injection straight perturbs the beam by as much as 130 μm horizontally and 80 μm vertically during injection. Passive shielding with copper collars and Mu metal sheets has reduced the perturbation but not removed them. The remainder of the perturbation will be corrected using an active feedforward system. This report will discuss the design of the system and the effectiveness of the prototype.

INTRODUCTION

The injection scheme in the storage ring is composed of four injection kicker magnets to create a local bump and two horizontal septa (SEP and SEI) to guide the electrons from the injector system into the storage ring. The arrangement of the septa is shown in Fig. 1 and ideally have no influence on the stored beam. As is commonly found, this is not the case due to stray fields and in 2016 we embarked on a project to improve the beam stability by reducing the effect of the two septa on the stored beam. This report will outline the steps taken, both passive and active measures to remove the disturbance.

Passive Shielding

To shield the stored beam from stray fields from SEI, 5 layers of 0.25 mm mu-metal are rolled around the vacuum chamber covering 1100 mm of the storage ring vacuum chamber. The mu-metal was rolled tight to maximise the inter-layer magnetic coupling with kapton tape wrapped around the vacuum chamber to insulate it from the mu-metal. A single layer of omega shaped mu-metal around 90% of the vacuum chamber circumference and loosely coupled to the septa shield plate was installed in one hard to reach section. SEI was run and inspected for arcs and unusual noises, none were found and the mu-metal foil did not appear to vibrate. Two copper boxes were then installed to shield the septa themselves as some parts of the vacuum chamber did not lend themselves to shielding, in particular near the septa ends which appear to have large fringing fields. The copper shield reduced the peak field measured 100 mm from the septa surface by an order of magnitude, it was not possible to measure the shielding effect of the mu metal. Figure 2 shows that these measures reduced the beam disturbance by only 44%. This result indicates that the majority of the disturbance is not due to the stray septum field hence not easily mitigated by shielding. Induced currents up to 30A were observed in the beam pipe and ground circuits, these may have contributed to the disturbance.

To use active compensation to remove the remaining disturbance would require a dipole kick of 10 μrad and 6.5 μrad in the horizontal and vertical planes, with a bandwidth of 2 kHz. This is outside the bandwidth of the Fast Orbit Feedback System [1] at 450 Hz. Therefore a separate feedforward system is required to compensate for this disturbance.

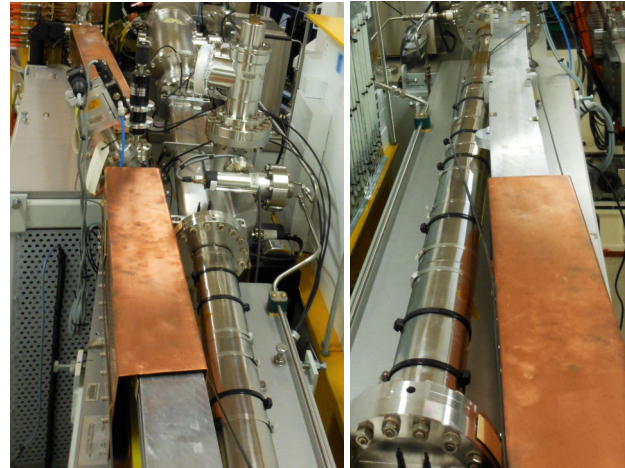


Figure 1: Location of SEP (top of left photo) and SEI (bottom of left photo). Passive shielding using copper sheets around the septa and mu metal sheets around the closest beam chambers (right photo).

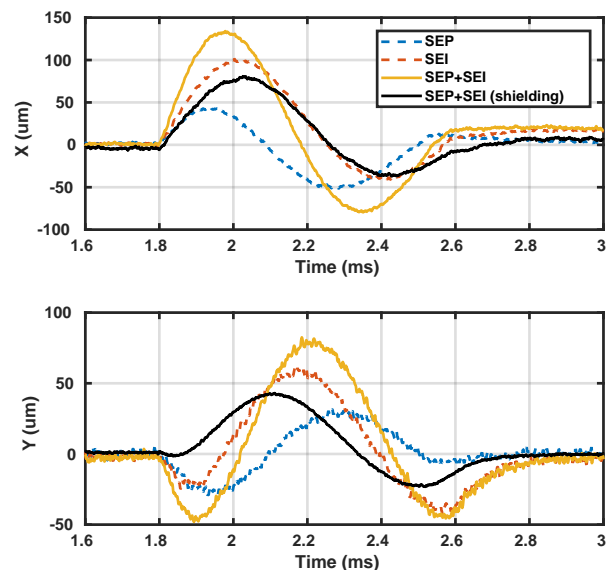


Figure 2: Perturbation from the two septa from turn-by-turn data (1.4 MS/s) and showing the effect of passive shielding that has been installed. Maximum amplitudes reduced from 134.1 μm and 80.5 μm to 80.2 μm and 42.7 μm .

* c.lehmann@uqconnect.edu.au

VIRTUAL SLIT FOR IMPROVED RESOLUTION IN LONGITUDINAL EMITTANCE MEASUREMENT *

K. Ruisard[†], A. Aleksandrov, A. Shishlo
 Oak Ridge National Laboratory, Oak Ridge, TN, USA

Abstract

A technique to reduce point-spread originating from physical slit width in emittance measurements is described. This technique is developed to improve phase resolution in a longitudinal emittance apparatus consisting of a dipole magnet, energy-selecting slit and bunch shape monitor. In this apparatus, the energy and phase resolutions are directly proportional to the width of the slit. The virtual slit method allows sub-slit resolution, with penalty in measurement time and dynamic range. The bunch phase profile is measured at two points in the energy distribution with a separation less than the physical slit width. The difference of these two profiles is used to reconstruct the profile from a virtual slit of width equal to that separation.

INTRODUCTION

Accurate measurement of beam phase space distributions is crucial for verifying correct operation and understanding accelerator dynamics. Phase space measurement can both be the source for simulation bunches and the basis for benchmarks of accelerator models. Longitudinal parameters in particular reflect dynamics within accelerating structures. Work at the Beam Test Facility (BTF) at the Spallation Neutron Source (SNS) has focused on detailed characterization of the beam distribution, including high-dimensional measurements [1] and development of high-dynamic range diagnostics capable of halo measurement [2]. The goal of this work is to obtain loss-level accuracy with particle-in-cell simulation, where the simulation results can be verified down to the halo level.

The phase space measurements use a slit-scan technique, where each dimension is isolated by masking the beam with a thin slits. While the bunch shape monitor (BSM) has sufficient resolution to image the bunch phase distribution, finite slit widths upstream of the BSM cause significant point spread in the BSM. A virtual slit technique is developed to reduce the point spread effect in the phase measurement, significantly improving the resolution of the phase measurement without modifying the existing hardware.

This paper first describes the apparatus for measurement of the longitudinal phase space at the BTF. The virtual slit

* This manuscript has been authored by UT-Battelle, LLC, under Contract No. DE-AC05-00OR22725 with the U.S. Department of Energy. The United States Government retains, and the publisher, by accepting the article for publication, acknowledges that the United States Government retains a non-exclusive, paid-up, irrevocable, world-wide license to publish or reproduce the published form of this manuscript, or allow others to do so, for United States Government purposes. The Department of Energy will provide public access to these results of federally sponsored research in accordance with the DOE Public Access Plan.

[†] ruisardkj@ornl.gov

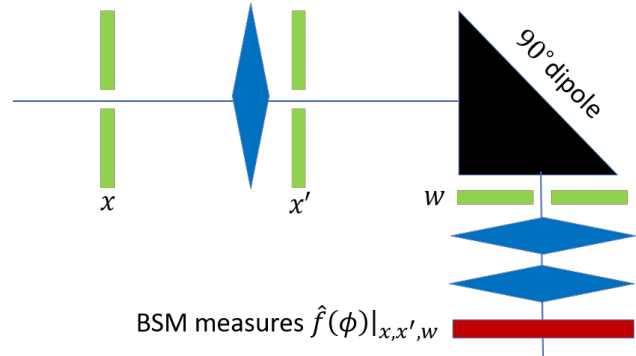


Figure 1: Diagram of longitudinal emittance apparatus. The notation $\hat{f}(\phi)|_{x,x',w}$ is used to indicate that the BSM measures the phase profile for the fraction of the beam that passes through the upstream x , x' and w slits.

technique is introduced for a wide-aperture slit, with an example measurement provided by PIC simulation of the setup. The case of a narrow slit aperture, with reduced but still significant point spread error, is also discussed. The use of a narrow slit complicates the virtual slit approach, but a solution is described. Finally, the data from virtual slit measurements is used to estimate the width of the physical slit aperture.

APPARATUS

The BTF is a test-stand experiment designed as a clone of the SNS front-end, including H^- ion source, LEPT, RFQ and four MEBT quadrupoles, as well as a MEBT extension enabling extensive phase space diagnostics and transport studies. A detailed description of the facility can be found in [3].

The apparatus for measurement of the longitudinal phase space is situated in the 2.5 MeV MEBT. The device consists of a 90° dipole and energy-selecting slit followed by the BSM. The BSM measures the phase profile for the selected energy. The longitudinal phase space $f(\phi, w)$ is measured by scanning the energy selection. Figure 1 shows the geometry of the emittance measurement. Two vertical slits upstream of the dipole are used to create a beam with small horizontal spread at the dipole entrance. In total there are three vertical slits, indicated by green rectangles. Additionally, three quadrupoles (indicated by blue diamonds) are used to control beam size on the energy slit and at the BSM.

At the energy slit location, two different widths are available: 200 μm and 1 mm. In this document, they will be

DESIGN AND DEVELOPMENT OF A NOVEL STRIPLINE FAST FARADAY CUP TO MEASURE ION BEAM PROFILE

A. Sharma^{1†}, R. K. Gangwar, Indian Institute of Technology (ISM), Dhanbad, India
B. K. Sahu, Inter-University Accelerator Centre, New Delhi, India
¹also at Inter-University Accelerator Centre, New Delhi, India

Abstract

Present day heavy ion accelerators use bunched ion beams of sub-nanosecond time scale for beam acceleration. In order to monitor the longitudinal beam bunch profile, Fast Faraday Cups (FFC) are employed. Owing to the advent of microstrip technology and its fabrication process, planar structures have become easier to fabricate. A novel planar design using the same is developed with a special provision for mounting edge launch connectors through a microstripline feed, followed by a microstrip to stripline transition to again a microstrip structure in the beam interaction hole. The entire structure is symmetrical and bidirectional with 50 Ω transmission lines. An experimental study on via placement around central stripline has also been conducted to not only ensure the field containment around the strip but also for bandwidth enhancement. To measure ion beam currents from 10-100 nA and a bunch width of < 1ns, device has a beam interaction hole of around 10mm. 3 dB bandwidth is measured > 6 GHz resulting in a pulse rise time of ~60 ps or less. The proposed device is also provided with a bias ring on the topmost layer of the 3 layer architecture for electron suppression. In this paper, design, fabrication and RF testing of stripline fast faraday cup is presented.

INTRODUCTION

The 15 UD Pelletron and the upcoming High Current Injector produces pulsed ion beam to be further energized by the Superconducting LINAC of IUAC. The bunch length acceptance of the superbuncher cavity of LINAC is ~1-2 ns which further reduce it to 200-500 ps. In order to determine the time and energy structure of the beam bunches, it is essential to measure the longitudinal profile and Time of Flight of the beam. By employing Fast Faraday Cups, longitudinal profile of a beam can be measured. Stripline FFCs are interceptive devices made up of a printed circuit transmission line of 50Ω or any given impedance [1] which can produce picosecond pickup pulse response when ion beam bunches strike on it. Figure 1 shows typical application of FFC device at IUAC where response times of the order of 50-60 ps or > 6 GHz bandwidth are well suited. Aim of this paper is to design such a novel stripline FFC as per IUAC requirement.

The most notable works on stripline FFC design are found in [2-3] which have used multilayer structure with stitching vias to maintain signal integrity, and bandwidth enhancement. While these devices have a small beam

interaction hole and used for very high current, high energy beam species, the proposed design is provided with larger beam interaction hole to cater even for low beam currents produced at IUAC which are of the order to 10-100 nA. Extensive studies on via fencing suggested [4-7] for suppression of spurious modes in stripline geometry using ground-to-ground stitching via filled with copper / metalized rods has been extended for the present case as well.

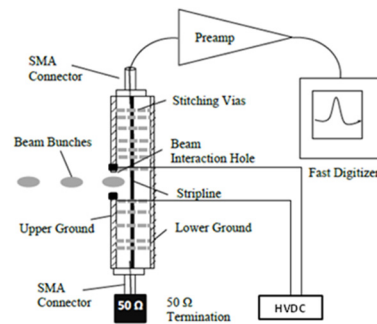


Figure 1: Beamline Test Setup.

Various sections of this paper deals with design equations and novelty implied therein. Emphasis has been given on stitching via placement and its mode suppression-cum-bandwidth extension effects. Paper is concluded by comparison of results of EM simulations done in Ansoft's HFSS with measured results obtained on VNA.

DESIGN DETAILS

The proposed configuration of stripline device is shown in Fig. 2. It is realized as a 3 layer, stacked-up structure of two planar substrates. Upper one has two rectangular notches at both edges so as to connect two SMA edge launch connectors. A beam interaction hole of the order of 10 mm diameter has been made at the center of the device for the beam sizes of the order 3-4 mm in diameter. Lower substrate has a grounded transmission line structure.

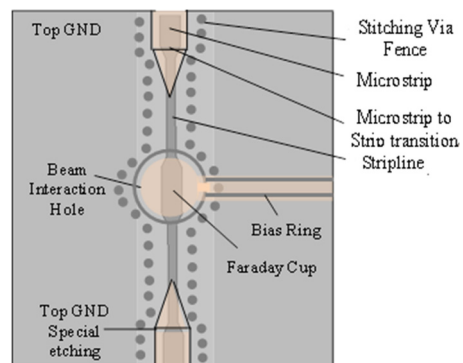


Figure 2: Proposed Stripline FFC Design.

† ashishdelhi.17kt000246@ece.iitism.ac.in

A THz-DRIVEN SPLIT RING RESONATOR FOR TEMPORAL CHARACTERIZATION OF FEMTOSECOND MeV ELECTRON BEAM*

Y. Song[†], K. Fan, Huazhong University of Science and Technology, Wuhan, China

Abstract

The use of THz-driven split ring resonator (SRR) as a streak camera for sub-ps bunch length measurement has been proposed for a few years. Since then, the feasibility of such a method has been experimentally demonstrated for both keV and MeV electron beam. The structural dimensions of SRR has a substantial impact on the resonance frequency, the field enhancement factor and the interaction region of the streaking field, eventually determining the temporal resolution of the bunch length measurement. Here we discuss the quantitative dependence of the streaking field on the structural dimensions of SRR. Combining with an analytical streaking model, we propose a method to optimize the structural dimensions of SRR such that the finest temporal resolution is achieved with given THz pulse.

INTRODUCTION

In the past decade, the femtosecond-level electron beam and its applications have become one of the main interests in the accelerator field. Such an electron beam is essential in many applications, such as ultrafast electron diffraction (UED) [1,2], self-amplified spontaneous emission free-electron laser (FEL) [3] and laser-plasma wakefield accelerators [4].

By using few MeV electron beam and RF compressor, electron bunch with sub-10 fs duration has been achieved [5], which pushes the requirement for the resolution of temporal characterization towards a single fs level. To data, such temporal resolution can be realized via RF deflector [5, 6]. However, the timing jitter between the RF source and laser system is at a few tens fs level which mean the uncertainty between the streak field and arrival time of the electron beam is about few tens fs. This limits the accuracy for time-of-arrival (TOA) characterization, which is very important for experiments like UED.

To provide a sub-10 fs temporal resolution for bunch length measurement and TOA characterization accuracy, a streak camera based on THz-driven split-ring resonator (SRR) is proposed a few years ago [7].

SRR is a sub-wavelength structure that focuses the incident THz radiation into the gap region, and the enhanced streaking field thus emerges in the gap. The streaking field provided by SRR is potentially up to GV/m level [8] and the frequency is about two orders higher than the RF deflector. Moreover, since the THz radiation is originated from the laser system, the streaking field is tightly synchronized to the laser system. Successful temporal characterization experiments have been demonstrated for both keV

[9] and MeV [10-12] electron beam. The experiment results indicate that SRR can provide sub-10 fs temporal resolution for bunch length measurement and sub-fs accuracy for TOA determination.

In this paper, we discuss the optimization of the geometric dimension of a square SRR. The goal of optimization is to obtain the highest streak velocity, and thus the finest temporal resolution. We first present the definition of the temporal resolution and its dependence on the parameters of SRR. Then, we use CST Microwave Studio to calculate the relevant parameters to determine the temporal resolution and therefore perform the optimization.

TEMPORAL RESOLUTION

We first define the passing time $T_p = h/\beta c$ where h is the length of the SRR gap in z-direction (see Fig. 1). β is the normalized velocity, which is about 1 for a few MeV electron beam. ΔT denotes the full-width bunch length of electron beam. The period of the streaking field is defined as T . The resonance frequency of SRR is generally below 1 THz and the electron bunch length we measure is in the fs-level. We can assume that $\Delta T \ll T$.

Consider an electron with longitudinal position ζ where $\zeta=0$ corresponds to the bunch center and $\zeta=\pm\Delta T/2$ the bunch head and tail. The transverse kick of such electron after passing through the SRR gap is

$$\begin{aligned} \Delta P_y(\zeta) &= -e \int_{\zeta-T_p/2}^{\zeta+T_p/2} \bar{E}_y \sin(\omega t + \varphi_0) dt \\ &= \frac{-2e\bar{E}_y}{\omega} \sin\left(\frac{\omega}{2} T_p\right) \sin(\omega\zeta + \varphi_0) \\ &\approx -2e\bar{E}_y \sin\left(\frac{\omega}{2} T_p\right) \left[\frac{1}{\omega} \sin\varphi_0 - \cos\varphi_0 \zeta \right], \end{aligned} \quad (1)$$

where φ_0 is the phase between the electron beam and the streaking field and $\omega = 2\pi f_0$ is the angular resonance frequency. Note that we use the assumption $\Delta T \ll T$. \bar{E}_y is the equivalent streak field whose expression is

$$\bar{E}_y = \frac{\omega}{2} \frac{\int_{-\infty}^{+\infty} A(\beta ct) \cos(\omega t) dt}{\sin(\omega T_p / 2)} E_{\max}, \quad (2)$$

where $A(\beta ct)$ is the normalized profile of the on-axis streaking field (see Fig. 2 for an example) and E_{\max} is the amplitude of the peak streaking field.

The trajectory angle of an electron after the SRR is $\Delta P_y/P$ and thus we define the streaking velocity ω_s is

$$\omega_s = \frac{|\Delta P_y(\Delta T/2) - \Delta P_y(-\Delta T/2)|}{P\Delta T} = \frac{2e\bar{E}_y}{P} \sin\left(\frac{\omega}{2} T_p\right).$$

Therefore, the temporal resolution of the SRR is

$$\tau_s = \frac{\sigma_{y'0}}{\omega_s} = \frac{\sigma_{y'0} P}{2e\bar{E}_y \sin(\omega T_p / 2)}, \quad (3)$$

* Work supported by the National Natural Science Foundation of China (NSFC) 11728508

[†] kjfan@hust.edu.cn

TRACKING FREQUENCY REFERENCE PHASE CHANGES AT POINT OF USE BASED ON BPM MEASUREMENTS

A. Tipper*, M. G. Abbott, G. Rehm†, Diamond Light Source, Oxfordshire, UK

Abstract

Multibunch Feedback systems in Diamond use the RF reference signal to homodyne downconvert the 3rd harmonic of BPM signals and sample the detected output. Uncertain reference phase variations due to upstream adjustments to the RF system previously necessitated regular manual realignment of the reference phase. Implementation of a local carrier recovery and symbol synchronizer at the BPM output by locking the local reference phase to the measured beam phase has been shown to significantly improve the stability and robustness of the system and remove the dependence on absolute RF phase. The system has been successfully deployed on the storage ring at Diamond and has been operating live since October 2019.

INTRODUCTION

The Diamond Multibunch Feedback (MBF) system [1] uses the Libera Bunch by Bunch Front End to provide a 1.5 GHz local oscillator for homodyne detection of the Beam Position Monitor (BPM) signal and a 500 MHz sampling clock as shown in Fig. 1. An IQ mixer is constructed using phase shifters and balanced mixers within the front end to enable measurement of the relative phase of BPM and reference. During operation the adjustment of the RF subsystems cause significant deviations in the measured phase requiring regular manual realignment of the phases within the front end. The variation over 9 months operation is shown in Fig. 2 which shows multiple step changes in the reference phase due to machine adjustments and the subsequent manual realignments. The data indicates a mean time between rephasing of 20 days. To improve this situation a project to investigate beam locked carrier recovery loops at Diamond, internally known as "Doris", was initiated based on Fig. 3 to lock the phase of the MBF clock to the beam.

In order to phase align the 500 MHz reference clock to the clock component in a BPM output a number of possible architectures were examined including

1. Phase locked loop
2. Analogue Delay locked loop
3. Digital IQ Beam locked loop (BLL)

Option (1) adds unwanted phase noise and suffers from nonlinear phase detection issues due to the use of balanced mixers as high frequency phase detectors. Full 360° phase tracking may be difficult to guarantee. Option (2) cannot guarantee continuous phase tracking due to the finite delay achievable whereas option (3) has full 360° linear phase detection and tracking with low additive phase noise. The use of IQ modulators and demodulators for phase detection

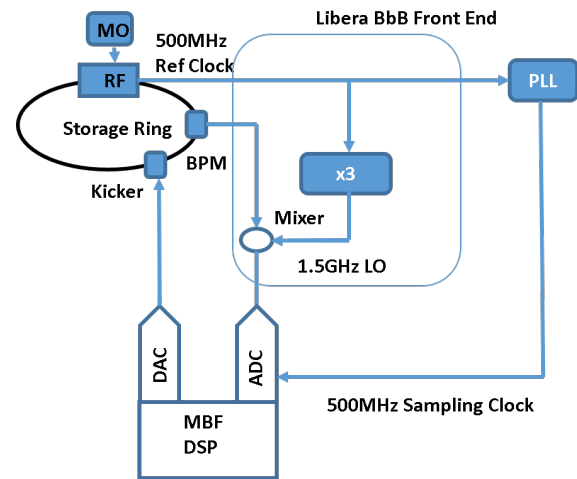


Figure 1: Original architecture.

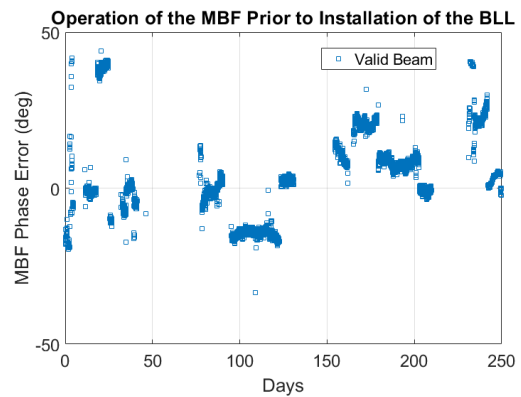


Figure 2: Measured phase variation over 9 months.

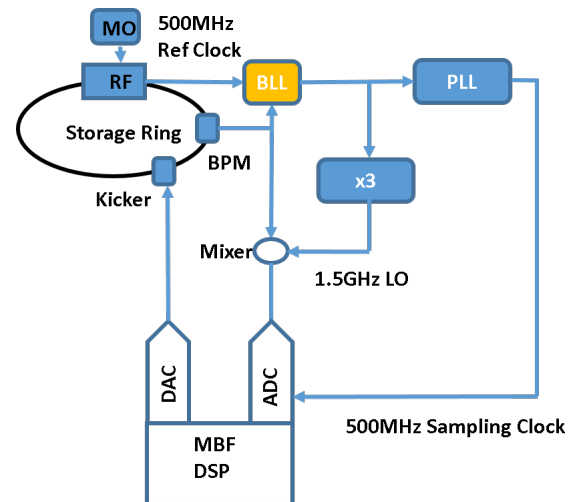


Figure 3: Improved architecture.

* alan.tipper@diamond.ac.uk

† Now at HZB, Berlin, Germany

Content from this work may be used under the terms of the CC BY 3.0 licence (© 2020). Any distribution of this work must maintain attribution to the author(s), title of the work, publisher, and DOI

MEASUREMENTS OF ION INSTABILITY AND EMITTANCE GROWTH FOR THE APS-UPGRADE*

J. Calvey, M. Borland, T. Clute, J. Dooling, L. Emery, J. Gagliano, J. Hoyt, S. Kallakuri, L. Morrison, U. Wienands, Argonne National Laboratory, Lemont, USA

Abstract

Ions are produced in an accelerator when the beam ionizes residual gas inside the vacuum chamber. If the beam is negatively charged, ions can become trapped in the beam's potential, and their density will increase over time. Trapped ions can cause a variety of undesirable effects, including instability and emittance growth. Because of the challenging emittance and stability requirements of the APS-Upgrade storage ring, ion trapping is a serious concern.

To study this effect at the present APS, a gas injection system was installed. A controlled pressure bump of Nitrogen gas was created over a 6 m straight section, and the resulting ion instability was studied using several different detectors. Measurements were taken using a pinhole camera, spectrum analyzer, bunch-by-bunch feedback system, and a gas bremsstrahlung detector. Studies were done under a wide variety of beam conditions, and at different pressure bump amplitudes. In this paper we report on the results of some of these measurements, and discuss the implications for present and future electron storage rings.

INTRODUCTION

The APS-Upgrade is a 4th-generation light source currently under development at Argonne National Laboratory [1], with a design emittance of 42 pm at 6 GeV. In order to make use of this ultra-low emittance, potential instabilities must be anticipated and mitigated.

One particular source of concern is ion instability. Trapped ions can lead to quickly growing transverse (usually vertical) instability, due to coupled motion between the beam and the ions. The strength of the instability is generally proportional to the average beam current, and inversely proportional to the beam size [2]. Thus ions are particularly dangerous for the APS-U, which will have high current and low emittance. Simulations predict a strong coherent instability for 324 bunch mode, which we plan to mitigate with a compensated gap scheme [3]. But even if the coherent instability is damped, incoherent effects such as emittance growth may still be an issue.

To better understand the ion instability and anticipate issues in the APS-U storage ring, we installed a gas injection system in an empty insertion device (ID) straight section of the present APS storage ring. This enabled us to create a controlled and localized pressure bump, and study the resulting instability. This paper will explain the setup and operation of the gas injection system, describe the instruments used

to study the instability, and show the results of some studies we performed.

SYSTEM SETUP

The gas injection system was installed in a spare insertion device straight section in Sector 25 of the APS. Nitrogen gas was chosen for the experiment, for two reasons. First, it was readily available and well understood by vacuum technicians. Second, it is readily pumped by both ion pumps and NEG coating, making the pressure bump easy to localize.

As shown in Fig. 1, the gas injection mechanism was connected to a port on the flange upstream of the spool piece (where the ID would normally be located). The system is operated from the mezzanine above the mechanism. To create a controlled pressure bump, the gas system is first pressurized with ~10 psi of N₂. The leak rate is controlled by two gate valves, operated manually from the mezzanine. Below each gate valve is a pre-set manual leak. Opening valve 5 in Fig. 1 gives a ~100 nTorr bump, while valve 6 gives a ~900 nTorr bump. Using pre-set leaks helps ensure that the amplitude of the pressure bump does not reach the μ Torr scale.

A picture of the gas injection system inside the tunnel is shown in Fig. 2. The trident on the upstream end of the spool piece contains both of the pre-set manual leaks, as well as a cold cathode gauge to monitor the pressure inside the system.

The ion pump located next to the gas injection location is disabled for the study. A cold cathode gauge (SR25:CC1) was installed on the downstream end of the spool piece, to measure the pressure near the peak of the bump. In order to localize the bump, the other ion pumps indicated in the figure are kept on. The activated NEG coating in the chambers upstream and downstream of the gate valves provide additional pumping.

For the 900 nTorr leak, the ion pump downstream of the system (25:2IP1) reads ~200 nTorr, and the next pump downstream (26:3IP1) reads ~40 nTorr. Downstream of this, the ion pump 26:2IP2 reads below 10 nTorr. The same result is seen in the upstream direction: ion pump 25:2IP5 reads a little above 100 nTorr, and 25:2IP4 peaks at ~20 nTorr. Thus the pressure bump is essentially contained in the ~6 m between 25:2IP4 and 26:2IP1.

DIAGNOSTICS

Several diagnostics were employed to study the ion instability- a pinhole camera, spectrum analyzer, feedback system, and gas bremsstrahlung detector. Unless stated oth-

* Work supported by the U.S. Department of Energy, Office of Science, Office of Basic Energy Sciences, under Contract No. DE-AC02-06CH11357.

TRANSVERSE BROAD-BAND IMPEDANCE STUDIES OF THE NEW IN-VACUUM CRYOGENIC UNDULATOR AT BESSY II STORAGE RING

M. Huck*, J. Bahrtdt, H. Huck, A. Meseck, M. Ries

Helmholtz-Zentrum Berlin für Materialien und Energie (HZB), Berlin, Germany

Abstract

The first radiation from the cryogenic permanent magnet undulator (CPMU17) has been observed in December 2018 at BESSY II storage ring at HZB, and since then this device has served as a light source for beamline commissioning. It is the first in-vacuum undulator installed at BESSY II, and a new in-vacuum APPLE undulator (IVUE32) is planned to be installed in near future. Thus, a detailed study of the interactions between such an in-vacuum device and the electron beam is required. Beam-based measurements using orbit-bump and tune-shift methods have been applied to estimate the vertical impedance of CPMU17. For CPMU17 the first results of broad-band impedance studies are presented.

INTRODUCTION

The constantly growing requests of various research fields for synchrotron radiation with higher photon energies demands designing undulators with smaller magnetic periods and gaps. After succeeding in constructing and optimizing small gap in-vacuum undulators (IVUs) in the last two decades, the challenging impacts of such small gaps on beam dynamics can nowadays be estimated and mitigated using modern experimental techniques and high-power numerical calculations. These studies are specially required for complex structures, short bunches and variable polarization IVUs such as CPMU17 and IVUE32. One of the most important related issues is the wake fields effect. Wake fields arise when the relativistic electrons travel inside chambers with nonuniform geometrical cross-section or a resistive wall.

IMPEDANCE BY VARIABLE BEAM OFFSET AND CURRENT

A particle beam that travels off-axis through a vacuum chamber section with a nonzero broad-band transverse impedance will be deflected due to the electromagnetic forces of the wake fields generated by the particle beam itself. In frequency domain and in case of transverse impedance, such a beam-impedance interaction can be represented by a quantity called *transverse kick factor* defined by [1]

$$k_{\perp} = \frac{1}{2\pi} \int_{-\infty}^{\infty} Z_{\perp}(\omega) h(\omega) d\omega, \quad (1)$$

where $Z_{\perp}(\omega)$ is the frequency-dependent *transverse impedance* and $h(\omega) = \lambda(\omega)\lambda^*(\omega)$ is the bunch power spectrum, with $\lambda(\omega)$ the Fourier transform of beam linear density $\lambda(t)$. The kick factors can be calculated for both horizontal and vertical directions. However, in our studies the focus is on the kick in the vertical direction, because a small gap

in-vacuum undulator comprise a flat geometry (two parallel plates), i.e. the width of the structure (46 mm in our case) is larger than its height (half gap of 3 mm-11 mm). And the interaction of the electrons with surrounding structure in the vertical direction is stronger than in the horizontal one. This interaction will cause a linear kick of the beam vertical momentum as follows

$$\Delta y' = eqk_{\perp}y_0/E, \quad (2)$$

where q is the beam charge, y_0 is the beam vertical offset, E is the beam energy, and e is the electron charge. Based on Eq. (2), a method called *orbit bump method* has been developed in 1999 at Budker Institute, Novosibirsk [2] to estimate the transverse kick factor of an individual section. The closed orbit distortion (COD) due to an impedance at a section can be expressed by [1]:

$$\Delta y(s) = \frac{\Delta q}{E/e} k_{\perp} y_0 \frac{\sqrt{\beta(s)\beta(s_0)}}{2\sin\pi Q_y} \cos(|\mu(s) - \mu(s_0)| - \pi Q_y), \quad (3)$$

where Q_y is the vertical betatron tune, $\beta(s)$, $\mu(s)$ and $\beta(s_0)$, $\mu(s_0)$ are respectively the betatron function and phase through the whole ring and at the location of the impedance. y_0 can be varied by introducing a closed-orbit-bump using correction coils. The orbit distortions $\Delta y(s)$ can be measured using beam position monitors (BPMs) at a high and a low beam current with a charge variation of Δq . By measuring and subtracting $\Delta y(s)$ in 4 states i.e. combination of *high-*, *low-current* and *with-*, *no-bump*: $\Delta y(s) = (\Delta y_{wbh} - \Delta y_{nbh}) - (\Delta y_{wbl} - \Delta y_{nbl})$, a COD equal to $\Delta y(s)$ is obtained which is directly proportional to k_{\perp} .

Contributions of dipole and quadrupole components in a wake field expansion have different effects on beam dynamics and can be distinguished by different measurements and models. Due to crossing terms in field expansion in a non-symmetric structure such as an IVU, $k_{\perp}(\omega)$ in Eq. (3) is determined with both dipole and quadrupole terms [1]. However, the quadrupole impedance manifests itself only in multi-bunch interactions [3]. The orbit bump technique is based on the *single-bunch* effect, yielding the contributions from geometric and resistive-wall broad-band dipole impedance. This technique or a variation of it has been implemented at several other institutes such as APS [4], ELETTRA [5], Diamond light source [1], Photon Factory at KEK [6], and ALBA [7].

IN-VACUUM CRYOGENIC UNDULATOR

The new in-vacuum cryogenic permanent magnetic undulator CPMU17 has been installed in summer 2018 at BESSY

* maryam.huck@helmholtz-berlin.de

APPLICATION OF WAVELET ALGORITHM IN TUNE MEASUREMENT*

X. Yang^{1,2}, L. W. Lai[†], F. Z. Chen,

SSRF, Shanghai Advanced Research Institute, Chinese Academy of Sciences, Shanghai, China

¹also at University of Chinese Academy of Sciences, Beijing, China

²also at Shanghai Institute of Applied Physics, Chinese Academy of Sciences, Shanghai, China

Abstract

Tune is a very important parameter for storage ring of advanced synchrotron radiation facilities. At present, fast Fourier transform (FFT) is the core algorithm of the beam spectrum analysis used in tune measurement. Taking into account the nonlinear effect in the accelerator, tune changes during the process of storage ring injection and booster energy upgrading. However, the Fourier method is used to analyse the global sampling point, and the ability to distinguish the local variation of the tune in the sampling time is poor. This paper leads wavelet analysis method as the core algorithm into beam spectrum analysis method, further analyses the change of the tune with beam amplitude in sampling time, and compares this new algorithm with the traditional Fourier method. New experimental results and corresponding analysis for the data from SSRF will be introduced in this paper.

INTRODUCTION

Tune measurement is very important for a storage ring. Some key accelerator parameters are calculated by measuring the tune value, including beta function, chromaticity, impedance, etc [1]. SSRF starts top-up operation since 2012. Injection introduced beam oscillation can be used to measure real-time tune value on storage ring during user operation [2, 3]. Fast Fourier transform (FFT) is the most commonly used algorithm in the tune calculation, which frequency resolution is determined by the number of sampling points N , that is $1/N$. The tune accuracy and tune drift measurement in the injection process is limited by the short oscillation damping time (about 10,000 turns).

As for the booster ring, the tune drift during ramping reflects the real-time operating status of the booster. The short-time Fourier transform (STFT) is used to calculate the tune drift [4]. However, the short ramping time (about 20,000 turns) during booster top-up injection makes the accurate tune drift measurement with STFT difficult.

Wavelet transform is a commonly used time-varying frequency analysis algorithm. There already have some related researches on beam analysing using Wavelet. The signal is analysed by selecting an appropriate base function with limited energy on the time axis. The continuous wavelet transform is defined as following quotation.

$$WT(a, \tau) = \frac{1}{\sqrt{a}} \int_{-\infty}^{\infty} f(t) * \psi\left(\frac{t-\tau}{a}\right) dt$$

where ψ is the mother wavelet, τ is the delay coefficient, and a is the scale coefficient which can be converted to corresponding frequency. The final result is a two-dimensional array of coefficients (a, τ) [5, 6].

This article uses Morlet wavelet as the mother wavelet to analyse the turn-by-turn data from storage ring and booster of SSRF during injection. Morlet wavelet is a complex wavelet whose envelope is the Gauss function. Its analytical formula is:

$$m(t) = e^{j\omega_0 t} e^{-t^2/2}$$

The real part image of the function is shown in the Figure 1.

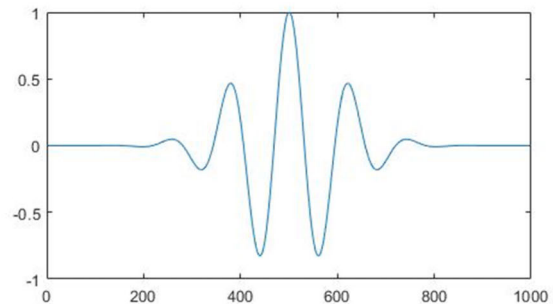


Figure 1: Morlet Wavelet.

ALGORITHM EVALUATION

Before use this new algorithm, we must test this wavelet method with Monte Carlo method. We established some test signals to simulate the real sampling.

It can be seen that FFT is restricted by the number of sampling points, and the frequency resolution is always in a relatively poor range in the Fig. 2. It cannot capture the subtle changes of tune. However, the morlet wavelet method has a relatively high value when the number of points is relatively small. The resolution is concentrated in the vicinity of the true frequency, and there is a lot of jitter when the SNR is low. As the number of sampling points increases, the stability of the morlet wavelet method is greatly improved, but the resolution of the FFT does not change significantly.

There is a special parameter in morlet wavelet analysis called analysis length, which affects the degree of time-frequency emphasis of wavelet analysis. The larger the analysis length, the higher the frequency resolution and the lower the time resolution, and vice versa. Use the simulation signal to analyse, get Fig. 3.

*Work supported by Youth Innovation Promotion Association, CAS (Grant No. 2019290);

[†] lailongwei@zjlab.org.cn

SIMULATION METHODS FOR TRANSVERSE BEAM SIZE MEASUREMENTS USING THE HETERODYNE NEAR FIELD SPECKLES OF HARD X-RAYS

A. Goetz*, D. Butti, S. Mazzoni, G. Trad, CERN, Geneva, Switzerland

U. Iriso, A. A. Nosych, L. Torino, ALBA-CELLS, Cerdanyola Del Vallés, Spain

B. Paroli, M. A. C. Potenza, M. Siano, L. Teruzzi, Università degli Studi di Milan, Milano, Italy

Abstract

Heterodyne Near Field Speckles (HNFS) is a special type of interferometry technique where radiation is scattered by nanoparticles suspended in a medium. The weak scattered waves and the intense transmitted beam form an interference pattern, which is modulated by the spatial coherence of the radiation and by the scattering properties of the nanoparticles. The random superposition of many such interference patterns results in a speckle field from which the spatial coherence of the radiation, thus the transverse beam profile, can be determined. In this contribution we present approaches for simulating the HNFS patterns from hard X-ray radiation and compare then with data from experiments at the ALBA synchrotron.

INTRODUCTION

With photon beam energies of up to 100 keV in combination with an unprecedented brightness and manifold focusing possibilities, third-generation light sources have become an indispensable tool for modern nanoscale science [1]. Precise knowledge about the coherence properties of the synchrotron radiation offers a wide range of technical applications. It is at the basis of many coherence-based techniques [2], and can also give insights into the transverse particle beam distribution. As such, coherence measurements are currently studied in the context of a non-invasive transverse beam profile monitor for the Future Circular Collider, FCC-ee [3].

In this framework, the Heterodyne Near Field Speckle method is particularly appealing since it allows to access the 2D transverse coherence properties of an X-ray beam without the need of any dedicated X-ray optics. Originally introduced in the optical domain as a particle-sizing technique by Giglio et al. [4], it has been recently extended by Alaimo et al. in 2009 to the characterization of the spatial coherence properties of undulator X-ray beams [5]. An extensive study on the application of the HNFS method to spatial and temporal coherence measurements of visible synchrotron radiation has been reported in 2016 by Siano et al. [6].

In spite of its experimental success, the method still lacks robust simulations that take into account the peculiar features of undulator radiation and the optical properties of the scattering particles. In this contribution we aim to compare two different approaches of simulating X-ray Heterodyne Near Field Speckles.

* alexander.goetz@cern.ch

THEORY OF THE HNFS

As far as transverse coherence is concerned, the radiation emitted by a single electron moving through an undulator is fully coherent. A statistical ensemble of electrons, with a Gaussian shaped profile with horizontal size σ_x and vertical size σ_y , gives rise to coherence areas of size $\sigma_{vcz,x/y}$ at a distance z from the undulator center. These coherence areas follow the Van Cittert and Zernike theorem [7, 8]:

$$\sigma_{vcz,x/y} = \frac{\lambda z}{2\pi \sigma_{x/y}} \quad (1)$$

where $\sigma_{vcz,x/y}$ is the transverse coherence length along the x/y direction, λ is the radiation wavelength, z is the distance from the center of the undulator and $\sigma_{x/y}$ is the rms size of the electron beam along the corresponding direction. When such a partially coherent wavefront impinges onto a suspension of particles with diameter d (a colloidal suspension), the synchrotron radiation is scattered. The weakly scattered spherical waves interfere with the intense trans-illuminating beam to generate Heterodyne Near Field Speckles [6]. The near field conditions, which are eponymous to this technique, require to measure the resulting interference pattern at distances z_2 downstream the scattering plane fulfilling

$$z_2 < \frac{\sigma_{vcz,x/y}^2}{\lambda} \quad (2)$$

Let us write the field of the synchrotron radiation produced by a given electron with index l as $E_l(\mathbf{x})$, the positions of the colloids with index j as \mathbf{x}_j and their scattering amplitude function as $S(\mathbf{x})$. The interference image is then given by

$$I(\mathbf{x}) = \sum_l \left| \sum_j E_l(\mathbf{x}) + E_l(\mathbf{x}_j) \cdot S(\mathbf{x} - \mathbf{x}_j) \right|^2 \quad (3)$$

The individual electrons are assumed to be uncorrelated, which is why they are summed outside of the absolute square. The intensity captured by a sensor is then Fourier transformed and the corresponding power spectrum $I(\mathbf{q})$ is computed with a spatial frequency variable \mathbf{q} . The power spectrum shows fringes that decay due to the scattering amplitude function (the particle form factor) $S(\mathbf{q})$, the spatial coherence of the radiation $C(\mathbf{q})$ and the optical transfer function $H(\mathbf{q})$. It is additionally shaped by the Talbot oscillations $T(\mathbf{q})$ and exhibits a noise pedestal $P(\mathbf{q})$ [6]:

$$I(\mathbf{q}) = S(\mathbf{q}) \cdot T(\mathbf{q}) \cdot C(\mathbf{q}) \cdot H(\mathbf{q}) + P(\mathbf{q}) \quad (4)$$

CALIBRATION AND IMAGE RESTORATION FOR THE BEAM PROFILE MEASUREMENT SYSTEM*

L. X. Hu¹, Y. T. Song[†], K. Z. Ding,
 Institute of Plasma Physics, Chinese Academy of Sciences, Hefei, China
 Y. C. Wu, Hefei CAS Ion Medical and Technical Devices Co., Ltd, Hefei, China
¹also at University of Science and Technology of China, Hefei, China

Abstract

The transverse beam profile parameters are closely related to the beam tuning and optimization of the cyclotron. In order to improve the precision and efficiency of beam profile measurement system, A calibration method has been implemented for the calibration of the imaging system. Moreover, a new image noise reduction algorithm has been developed to improve the image quality, and then to improve the measurement accuracy of the beam profile parameters. In addition, two image restoration algorithms have also been adopted to eliminate the effects of defocusing blur. The experiment results show that the calibration of the imaging system enable the system to provide quantitative information for beam diagnosis. The image noise reduction and restoration algorithm greatly improve the measurement accuracy of beam profile parameters.

INTRODUCTION

The beam profile parameters are one of the important parameters, which represent the beam quality [1]. The performance of the accelerator and the safe and stable operation are closely related to the transverse beam distribution [2]. The measurement of beam profile parameters can provide an important basis for the debugging and commissioning of the accelerator and the improvement of beam quality [3]. The most commonly used beam profile measurement instruments include: Scintillator detector [4], OTR target [5], synchronized light imaging [6] and wire scanning [7].

Due to the limitation of the imaging system and the influence of the imaging and signal transmission environment, there will inevitably be distortion and deviation between the observed image and the actual image, which is called image degradation [8]. The main factors leading to the image degradation of the scintillator detector include:

- The image distortion caused by the aberration and nonlinear distortion of the imaging system;
- Various noises introduced by the imaging system and image transmission process;
- Defocus blur caused by inaccurate focus of the camera.

The phenomenon of image degradation has a significant impact on the image measurement and analysis.

Work supported by grants 1604b0602005 and 1503062029.
 email address: hulx@ipp.ac.cn

IMAGING SYSTEM CALIBRATION

Basis of Coordinate Transformation

The conversion relationship between the pixel coordinate system and the world coordinate system is given by

$$z_c \cdot \begin{bmatrix} u \\ v \\ 1 \end{bmatrix} = \begin{bmatrix} f_x & 0 & u_0 & 0 \\ 0 & f_y & v_0 & 0 \\ 0 & 0 & 1 & 0 \end{bmatrix} \cdot \begin{bmatrix} \mathbf{R}_{3 \times 3} & \mathbf{T}_{3 \times 1} \\ \mathbf{0} & 1 \end{bmatrix} \cdot \begin{bmatrix} x_w \\ y_w \\ z_w \\ 1 \end{bmatrix} = \mathbf{M}_1 \mathbf{M}_2 \mathbf{X}_w \quad (1)$$

where $[u \ v]$ is the coordinates in the pixel coordinate system, u_0 and v_0 denote the translation amount of the image coordinate system relative to the pixel coordinate system, f is the focal length of the camera, $\mathbf{R}_{3 \times 3}$ represents the rotation matrix, $\mathbf{T}_{3 \times 1}$ represents the translation matrix, $[x_w \ y_w \ z_w]$ is the coordinates in the world coordinate system. \mathbf{M}_1 is called the internal parameter matrix. \mathbf{M}_2 is called the external parameter matrix.

Camera Distortion

The image distortion of the visual system occurs in the process of imaging. The radial and tangential distortion have great influences on the image. Radial distortion occurs when light rays bend more near the edges of a lens than they do at its optical center. Tangential distortion occurs when the lens and the image plane are not parallel.

The radial distortion is corrected by the Taylor series expansion shown in Eq. (2) and (3):

$$x_c = x(1 + k_1 r^2 + k_2 r^4 + k_3 r^6), \quad (2)$$

$$y_c = y(1 + k_1 r^2 + k_2 r^4 + k_3 r^6), \quad (3)$$

where k_1 , k_2 and k_3 are radial distortion coefficients, r represents the distance from the imaging center, (x, y) and (x_c, y_c) are the undistorted and the distorted points.

The tangential distortion is corrected by the following formulas:

$$x'_c = x + [2p_1 y + p_2 (r^2 + 2x^2)], \quad (4)$$

$$y'_c = y + [2p_2 x + p_1 (r^2 + 2y^2)], \quad (5)$$

where p_1 and p_2 are tangential distortion coefficients of the lens.

Camera Calibration

For stereo applications, these distortions need to be corrected first. To find the internal and external parameters and camera distortion parameters, what we have to do is to provide some sample images of a well-defined pattern (e.g. chess board). Important input data needed for camera

LENS CALIBRATION FOR BEAM SIZE MONITORS AT ThomX

S. D. Williams, G. N. Taylor, The University of Melbourne, Melbourne, Australia
I. Chaikovska, N. Delerue, V. Kubytskyi, H. Monard,
A. Moutardier, A. Gonnin, Université Paris-Saclay, Orsay, France

Abstract

ThomX is a novel compact X-ray light source, utilising a laser and 50 MeV electron storage ring to produce X-ray photons via Compton scattering. Screens, observed by zoom lenses and optical cameras, can be used to monitor the transverse beam profile at various points.

An issue with the implementation of this system is that after adjusting the zoom one needs to recalibrate the the optical system, measuring the resolution of the optical system and deducing the transformation from pixel space observed on the camera to geometrical space in the laboratory.

To calibrate and measure the resolution limit of the cameras a USAF 1951 resolution chart that can be moved into or out of the screen position is used.

We will report on and demonstrate the use of open source computer vision libraries to compute this calibration, and the affine transformation between the camera image plane and the screens can be deduced. We will also comment on how consumer available Canon EF mount lenses may be used as a remote controllable optical system.

INTRODUCTION

Beam size measurement is one of the important diagnostic measurements performed at the ThomX light source, and is measured at three stations of the injection line and at two stations just before the two beam dumps.

At each diagnostic station along the beamline a YAG screen, USAF1951 microscope resolution target, and blank screen are mounted on rails driven by a stepper motor. These can be moved in or out of position, in or out of the trajectory of the beam, and are observed by the optical system mounted underneath. The optical system consists of a Tamron B028 18–400mm F/3.5–6.3 telephoto lens and digital camera which is mounted underneath the station. To focus the optical system the internal motors of the lens are used, and to control the zoom level an external belt and motor system is being developed, with the aim that once position at the monitoring station the optical system can be completely controlled from the control room.

We note that the camera and lens image plane is not parallel to the plane of the screens or microscope target, but at roughly forty-five degrees. More information, including descriptions and images of the diagnostic stations, can be found in the ThomX TDR [1].

The work discussed in this publication deals with the calibration of the camera and optical systems used to observe the YAG screens, and the repurposing of Tamron EF lenses for effective remote focus control.

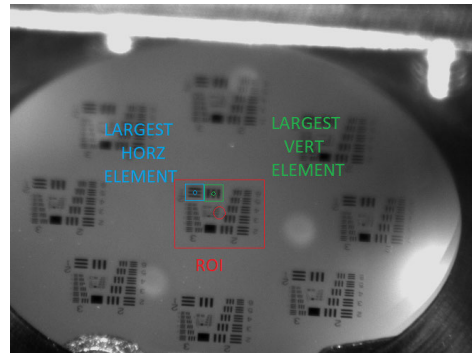


Figure 1: Highlighting a detected region of interest, and the largest horizontal and vertical elements detected.

NOMENCLATURE AND DEFINITIONS

We shall define the following terms now to simplify the reading of this document. Firstly, the entire glass slide is referred to as a USAF1951 test chart. There are nine targets on each USAF1951 test chart, as seen in Fig. 1. Each target is made up of differently but precisely proportioned bar patterns, and we refer to a set of three bars in the same orientation as an element, a set of three elements as a group.

The USAF1951 test chart is a somewhat common calibration chart, and more detail is easily found via an internet search.

OPERATION OF OPTICAL SYSTEM

During the commissioning and later operation of ThomX, the ideal operator workflow is that the operator should be able to adjust the camera zoom to be able to view the entire YAG screen, then zoom in as appropriate to clearly view the beam spot. This means imaging an area of roughly 23 mm by 23 mm to 4 mm by 4 mm at either extreme, and recalibrating the cameras each time the cameras are moved. Recalibrating the cameras, and checking the transverse beam size is expected to occur at least daily, if not more often, and if this were to require manual experienced operator supervision or take too long to run operational run times could be affected. Thus, the process should be nearly entirely automatic, and finished in a reasonable length of time.

The objective of the system calibration is to ascertain the resolution of the system and the appropriate coordinate transform from image pixels to laboratory distances. In this context the resolution refers to the resolving power of the entire optical and camera system, in terms of the size of the smallest details that can be reasonably distinguished.

PROTOTYPE DESIGN OF WIRE SCANNER FOR SHINE*

J. Wan, Shanghai Institute of Applied Physics, Chinese Academy of Science, 202009 Shanghai, China also at University of the Chinese Academy of Science, 100049 Beijing, China

Y.B. Leng[†], K.R. Ye, W.M. Zhou, L.Y. Yu, Jie. Chen, B. Gao, F.Z. Chen

Shanghai Advanced Research Institute, CAS, Shanghai, China

Abstract

SHINE is a high repetition rate XFEL facility, based on an 8 GeV CW SCRF linac, under development in Shanghai. In order to meet the requirements of measuring the beam profile of shine in real time and without obstruction, a new diagnostic instrument, wire scanner has been designed. This paper mainly describes the design of wire scanner in shine, and some simulation results are also shown and discussed.

INTRODUCTION

SHINE [1] has 3 undulator lines that consist of FEL-I, FEL-II and FEL-III and 10 experimental stations in phase-I, it can provide the XFEL radiation in the photon energy range of 0.4 -25 keV. In SHINE, wire scanners will be used to monitor the transverse profile of a 10-300 pC electron beam with a final energy of 8GeV and repetition of 0-1MHz. Providing a high resolution measurement of electron beam profile averaged over many shots is the primary purpose of the wire scanner (WSC). Profile measurements can also be used to determine transverse beam emittance and twiss parameters without changing the magnet settings [2]. Compared to view screens, WSC offer a non-destructive monitoring of the beam transverse profile, and avoiding secondary particle damage to superconducting cavity. At present, the preliminary design scheme WSC in SHINE has been completed. The specific equipment parameters, such as the material, diameter, scanning speed, scanning mode need to be determined according to simulation and performance. Now simulation based on MATLAB has obtained some results.

OVERVIEW

At SHINE, design of WSC includes wire scanner detector, PMT detector, data acquisition electronics, data processing module, and remote monitoring. General block diagram of the WSC is shown in Fig. 1.

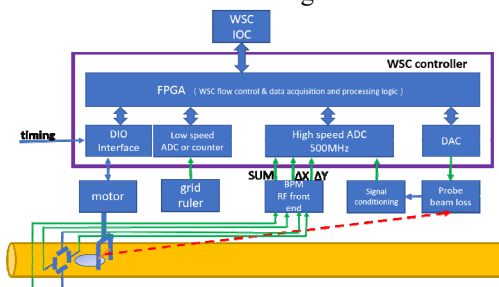


Figure 1: General block diagram of the system.

Wires in wire scanner detector driven by linac motor interacting with electron beam generates γ rays which are received by the PMT detector. Data acquisition electronics is to collect the PMT beam loss signal, wire position back-reading and BPM output. Data processing module is responsible for information extraction and Gaussian fitting, and remote monitor implements user interface and terminal control of WSC.

For reason of high repetition rate, slow scanning mode with step by step is more likely to cause damage to wire than fast mode. Therefore SHINE's WSC will apply fast scanning mode, in which wires will be swept fastly and smoothly through the beam pipe at one time to prevent large vibrations.

At present, WSC of SHINE is still in simulation of actual parameters and development of key technologies, and the hardware parts have not been assembled and coordinated to realize functions. Unsolved problems include heating damage of tungsten wire under high repetition rate beam [3], vibration of tungsten wire in fast scanning mode [4] which Influences system resolution, selection of PMT probe position which influences beam loss signal quality, unknown SNR of PMT beam loss signal which also influences system resolution, and optimization of data processing algorithm which influences on system precision and speed. In future, according to the theoretical analysis and simulation results, wire scanner device parameter will be configured which includes wire diameter, scanning speed, PMT requirements, ADC requirements, etc, and beam experiments will be carried out to observe its working state to evaluate the performance of wire scanner.

Wire Scanner Detector

The wire scanner detector will be installed along the beam line. When it needs to be used, commands generated by upper software is sent to control the motor to drive the wires to sweep through the beam. After the measurement, the wires will be moved out of the beam channel to avoid blocking the beam. Wire scanner detector is driven by linear motor, and encoder is used to feedback position. The motion of the wire scanner detector has high reliability, and there is no movement stuck fault, and repetition accuracy of the motion is better than 20 μm . The wire scanner detector mainly includes a vacuum chamber with flange, flexure, linear motor and magnetic grid ruler, 45 degree mounting seat, and independent adjustable supporting base as shown in Fig. 2. We use 10 μm and 20 μm tungsten wires for test recently.

*Work supported by The National Key Research and Development Program of China (Grant No. 2016YFA0401903, 2016YFA0401900)

[†]lengyongbin@sinap.ac.cn

DIRECT DIGITIZATION AND ADC PARAMETER TRADE-OFF FOR BUNCH-BY-BUNCH SIGNAL PROCESSING*

I. Degl'Innocenti^{†1}, A. Boccardi, M. Wendt, CERN, Geneva, Switzerland
 L. Fanucci, Department of Information Engineering, Università di Pisa, Pisa, Italy
¹also at Department of Information Engineering, Università di Pisa, Pisa, Italy

Abstract

With the technology improvements of analog-to-digital converters in terms of sampling rate and achievable resolution, direct digitization of beam signals is of growing interest in the field of beam diagnostics. The selection of a state-of-the-art analog-to-digital converter for such a task imposes a trade-off between sampling frequency and resolution. Understanding the dependency of the system performance on these features is fundamental. This paper presents an analysis and design methodology for such architectures. Analytical tools are used to guide the designer and to estimate the system performance as a function of the analog-to-digital converter performance. These estimations are then validated by Monte-Carlo simulations. As an example of this methodology an analysis for the next-generation electronics of the Large Hadron Collider beam position monitoring system is presented. The analytical model and the results obtained are discussed, along with comparisons to beam measurements obtained at the Large Hadron Collider.

INTRODUCTION

Beam instrumentation and diagnostics are fundamental in the operation and control of particle accelerators. An instrument for beam diagnostics purposes must process the signal generated by the sensor interacting with the beam, to provide measured values about the beam parameter under consideration, and deliver the information in a digital format with the required performance, typically accuracy, resolution and processing time or bandwidth. The read-out electronics extracts this information from the beam sensor by utilizing a combination of analogue signal conditioning and digital signal processing techniques, with a digitization stage in between.

We define *direct digitization* to mean that the digitization is performed at an early stage in the processing chain, using minimal analog signal conditioning hardware.

Direct digitization has several advantages and limits the total number of hardware components required for the processing electronics. Fewer electronics components typically means less spread in board to board parameters, fewer drift effects and less uncontrolled parasitics, thus improving the general system performance and robustness with respect to environmental changes. In addition, such systems profit from the advantages to process the data in the digital domain. For example, the system can rely on the flexibility of re-programmable algorithms and the possibility to imple-

ment complex digital filters that are impossible to build in the analog domain.

On the other hand, a direct digitization based architecture usually imposes higher requirements on the digitization stage, in terms of sampling rate and resolution. Analog-to-digital converters (ADC) with sufficiently high sampling rate and analog bandwidth are needed to digitize bunched beam pulsed signals without loss of information, and to acquire single-shot signal events. ADCs with sufficiently high effective quantization resolution are necessary to obtain high precision measurements covering a large dynamic range. In practice however, the technology imposes a trade-off between the ADC's maximum sampling rate and its effective resolution.

The ADC Performance Trade-off

In characterizing and comparing ADCs a widely used figure of merit is the *performance P*, which is defined as product between the effective number of logical levels (effective number of bits, ENOB) and the maximum sampling rate:

$$P = 2^{ENOB} \cdot f_s \quad (1)$$

In his paper [1] Walden produced an overview of ADC performance trends up to 1997, concluding that *P* has remained relatively steady. Already in 2005 Bin Le et al. [2] had observed that technology advancement brought a general improvement in measurement performance, even though not uniformly achieved over a wide range of sampling rates and resolutions. Nevertheless, it is undeniable that higher sampling rates come at the cost of resolution and the parameter *P* helps to describe the performance boundary of converters with similar characteristics and technology (see Fig. 1).

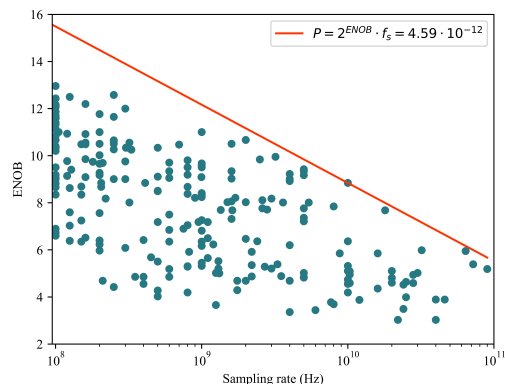


Figure 1: Performance distribution of ADC components in the years 1997 to 2020, showing the resolution in *effective number of bits* versus the maximum sampling rate. The red line represents the performance *P* boundary, as set by the best ADCs in terms of *P*. The data are taken from the online database [3].

* Work supported by CERN, Beams Department, Beam Instrumentation Group

[†] irene.degl'innocenti@cern.ch

COMMISSIONING OF THE BEAM ENERGY POSITION MONITORING SYSTEM FOR THE SUPERCONDUCTING RIKEN HEAVY-ION LINAC

T. Watanabe*, N. Fukunishi, H. Imao, O. Kamigaito, T. Nishi, K. Ozeki,
N. Sakamoto, A. Uchiyama, Y. Watanabe, K. Yamada, RIKEN, Wako, Japan
T. Toyama, KEK/J-PARC, Tokai, Japan
A. Kamoshida, National Instruments Japan Corporation, Tokyo, Japan
K. Hanamura, Mitsubishi Electric System & Service Co., Ltd., Tokai, Japan
R. Koyama, SHI Accelerator Service Ltd., Wako, Japan

Abstract

Beam commissioning for the RIKEN Heavy-ion Linac (RILAC) upgrade, including the new Superconducting Linac (SRILAC), has been successfully completed. The RILAC upgrade aims at promoting super-heavy element searches and radioactive isotope production for medical use. When the SRILAC beam is accelerated, the beam loss must be reduced to under 1 W/m. To continuously monitor the beam nondestructively, we have developed a new beam energy position monitoring (BEPM) system capable of simultaneously measuring the beam position and energy by measuring the time-of-flight. A great advantage of this system is that it can handle a time-chopped beam by synchronizing the measurement system with the beam-chopping signal. At the start of commissioning, the beam was chopped to 3% duty cycle to protect the SRILAC cavity from beam loss. Even though the beam intensity was 20 enA, we measured the beam position and energy to accuracies of ± 0.1 mm and several 10^{-4} precision, respectively. Here, we present details concerning the BEPM system and commissioning results.

INTRODUCTION

Nihonium (Nh) is a synthetic super-heavy (SH) element with atomic number 113 and is the first element ever discovered in Asia [1]. It's name comes from the word "Nihon", which means "Japan" in Japanese. To promote the research for even heavier synthetic elements and to enhance the production capability of the short-lived radio isotope ^{211}At , which is expected to be useful in cancer therapy [2], an upgrade project of the RIKEN Heavy-ion Linac (RILAC) [3] has begun called the RI Beam Factory (RIBF) project [4,5]. The project aims to increase the intensities and energies of the heavy ion beams by introducing a superconducting electron cyclotron resonance (ECR) ion source [6] and a superconducting booster named the Superconducting RILAC (SRILAC) [7].

In this scheme, it is crucial to monitor a beam to accelerate it stably. Destructive monitors generate outgassing; if they are used, it becomes difficult to maintain the Q value and surface resistance of the superconducting radio frequency (SRF) cavities over a long period of time. For this reason, we have developed a new beam energy and position monitoring (BEPM) system to continuously monitor the beam nondestructively.

* wtamaki@riken.jp

BEPM SYSTEM FOR THE SRILAC

RILAC and SRILAC

The newly constructed beam transport lines and the SRILAC were installed in February 2020. The existing RILAC and the upgraded facilities are shown in Fig 1. The SRILAC consists of three cryomodules (CM1, CM2, and CM3). CM1 and CM2 each contain four quarter-wavelength resonators (QWR) at 73 MHz and CM3 contains two QWRs. The total acceleration voltage is designed to produce 18 MW with a Q value of 1×10^9 . To maintain the ultra-high vacuum ($< 10^{-8}$ Pa) and particulate-free conditions, a non-evaporable getter-based differential pumping system was developed and installed upstream and down-stream of the SRILAC [8].

Heavy-ion beams accelerated by the SRILAC are used by the GAs-filled Recoil Ion Separator (GARIS) III to search for SH elements and to produce radioisotopes (RI) for medical use. If further acceleration is necessary in the future, the beams are to be transported to the rear stage Riken Ring Cyclotron (RRC).

Three Types of BEPMs

Depending on the installation location, 3 types of BEPM (Types I, II, and III) were designed and 11 BEPMs were fabricated [9] by Toyama Co., Ltd. [10]. BEPMs are installed in the centers of the quadrupole magnets (Fig. 1) that are located between the SRF cavities. Photographs of the 3 types

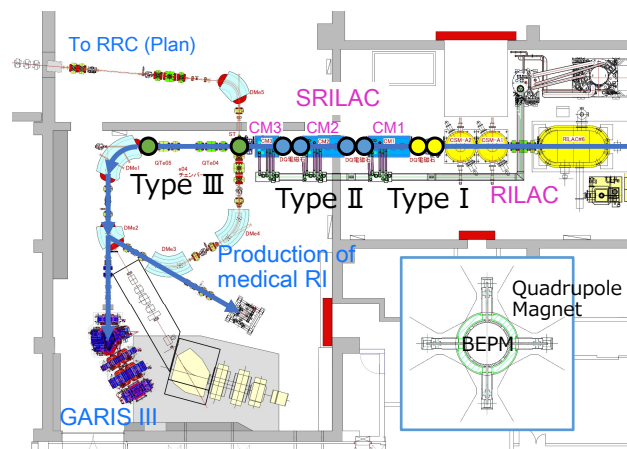


Figure 1: Schematic drawing of the RIKEN Heavy-ion Linac (RILAC), the upgraded Superconducting Linac (SRILAC), and the installation locations of the 3 types of BEPM.

